PARTIAL MELTING RELATIONSHIPS OF THREE GRANITIC ROCKS

by

JAMES A. WHITNEY

SUBMITTED IN PARTIAL FULFILLMENT

OF THE REQUIREMENTS FOR THE

DEGREES OF BACHELOR OF

SCIENCE

AND

MASTER OF SCIENCE

at the

MASSACHUSETTS INSTITUTE OF

TECHNOLOGY

January, 1969

Signature of Author _____
Department of Geology and Geophysics,
January 20, 1969

Certified by _____
Thesis Supervisor

Accepted by _____
Chairman, Departmental Committee
on Graduate Students

PARTIAL MELTING RELATIONSHIPS OF THREE GRANITIC ROCKS

by

JAMES A. WHITNEY

SUBMITTED IN PARTIAL FULFILLMENT
OF THE REQUIREMENTS FOR THE
DEGREES OF BACHELOR OF
SCIENCE
AND
MASTER OF SCIENCE

The melting relations of 3 granitic rocks have been studied using sealed capsule techniques in the saturated and undersaturated cases. All experiments were conducted at 2 kb total pressure and temperatures between 650 and 800°C.

Reactions involving accessory minerals agree with experimental data on synthetic systems. Feldspars tend to remain in low to intermediate structural states and conform to a ternary solvus that is in agreement with recent synthetically determined metastable low structural state solvi on the albite-orthoclase sideline.

The composition of the liquid in equilibrium with feldspar and quartz moves from the saturated minimum at 690°C ($Q_{34}Or_{26}Ab_{40}$) to a point at about $Q_{35}Or_{28.5}Ab_{36.5}$ at 740°C due to the effects of anorthite. Subsequent migration due to undersaturation caues the liquid to move to a point at $Q_{30}Or_{36.5}Ab_{33.5}$ by 800°C with f_{H_2O} about that corresponding to one kilobar water pressure.

This study suggests that melting relationships of granitic rocks may be represented in the system $CaAl_2Si_2O_8$-$NaAlSi_3O_8$-$KAlSi_3O_8$-SiO_2-H_2O if water as a component and water as a pressure medium are considered separately.

These trends in liquid composition, in conjunction with phase relations among the accessory minerals, may be used to make semi-quantitative estimations of pressure, temperature, water fugacity, and oxygen fugacity for the origin and crystallization of granitic assemblages and associations.

In light of these trends, the Westerly Granite of Rhode Island may have been formed at several kilobars pressure under water undersaturated conditions and was subsequently intruded at pressures of one to two kilobars and water pressures approximately equal to load pressures. The Cape Ann and related alkali rocks of the Boston Area may represent crystallization of a common undersaturated magma from depths under different total pressures. The Mount Airy leucogranodiorite of North Carolina may have originated under 5 to 10 kilobars of load pressure with slightly lower water pressure, and was intruded under a fairly high pressure indicating deep depths.

Thesis Supervisor: David R. Wones
Title: Associate Professor of Geology

TABLE OF CONTENTS

LIST OF ILLUSTRATIONS

LIST OF TABLES

LIST OF ABBREVIATIONS

Phases

Or	Potassium Feldspar (When used as a component, $KAlSi_3O_8$)
Sa	Sanidine ($KAlSi_3O_8$)
Pl	Plagioclase
Ab	Albite ($NaAlSi_3O_8$)
An	Anorthite ($CaAl_2Si_2O_8$)
Q	Quartz
Bi	Biotite
Ann	Annite ($KFe^{+2}_3AlSi_3O_{10}(OH)_2$)
Ha	Hastingsitic Amphibole (End Member $NaCa_2Fe^{+2}_4Fe^{+3}Si_6Al_2O_{22}(OH)_2$)
Ac	Acmite
Ae	Aegirine-Augite (Aegirine End Member $NaFe^{+3}Si_2O_6$)
Py	Augitic Pyroxene
He	Hedenbergite
Fa	Fayalite ($Fe^{+2}_2SiO_4$)
Mu	Muscovite
Ep	Epidote
Zo	Zoisite
Cz	Clinozoisite
Gr	Grosslarite
Zi	Zircon
H	Hematite
Mg	Magnetite
W	Wustite

Fe	Elemenatal Iron
L	Silicate rich Fluid Phase (Liquid)
V	Aqueous Fluid Phase (Vapor)

Symbols used in tables of experimental runs

( )	Metastable Persistant
?	Phase whose stability (or presence) is in doubt. Usually used with vapor phase.

Thermodynamic Quantities

$Wt\%H_2O$	Water Content, by Weight, in Original Charge.
f_{O_2}	Fugacity of Oxygen
f_{H_2O}	Fugacity of Water
γ_{H_2O}	Fugacity Coefficient of Water, Defined by the Relationship $f_{H_2O} = \gamma_{H_2O} P_{H_2O}$
P_{H_2O}	Vapor Pressure of Water, or Effective Vapor Pressure of Water as Defined by the Fugacity and Fugacity Coefficient.
P_{Total}	Total Pressure on Charge
W_{H_2O}	Total Mass of Water Present in Closed System
W_L	Total Mass of Silicate Liquid in the Charge.
W_{ch}	Total Mass of Charge, Including Water
$Y^L_{H_2O}$	Mass Fraction of Water in Silicate Melt
X_{H_2O}	Mole Fraction of Water in Silicate Melt
ρ_L	Density of Silicate Melt
ρ_{ch}	Average Density of Charge, Including Water
V_L	Volume of Silicate Melt Present in Charge
V_{ch}	Volume of Charge
$V\%_L$	Percent of Volume of Charge Which is Silicate Melt
W_i	Mass of Phase i that is Present

u_{H_2O}	Chemical Potential of Water
u_o	Chemical Potential of Water Vapor at Temperature T and 1 At. Water Pressure
u^*	Chemical Potential of Water in Silicate Melt at Temperature T and 1 At. Water Pressure
a_{H_2O}	Chemical Activity of Water
a_{Phase}	Chemical Activity of Given Phase
α_{H_2O}	Activity Coefficient of Water in Silicate Melt at a Given Point T. Defined by the Relationship $a_{H_2O} = \alpha_{H_2O} X_{H_2O}$
K	Equilibrium Constant in Heterogeneous Equilibrium
$\Delta\bar{G}$	Change in Mass Reduced Gibbs Free Energy During a Reaction
$\Delta\bar{V}$	Change in Mass Reduced Volume During a Reaction
$\Delta\bar{S}$	Change in Mass Reduced Entropy During a Reaction
$\frac{\partial\bar{G}}{\partial p}$	Change in Mass Reduced Gibbs Free Energy with Pressure

INTRODUCTION

The increasing amount of information developed on synthetic systems and stability fields for synthetic minerals is being used more and more effectively to interpret the origin and history of naturally occurring assemblages. In most work on synthetic systems one of three assumptions is often built into the nature of the experiments:

1. Generally, there is a free aqueous vapor phase present so that $P_{H_2O} = P_{Total}$;
2. The behavior of complex natural systems with regard to temperature and pressure may be modeled by a simpler synthetic system, both qualitatively and quantitatively;
3. The stability of single minerals within a complex assemblage may be studied effectively by considering it as a subsystem of the original assemblage.

This study was set up to examine one very important system, the system SiO_2-$KAlSi_3O_8$-$NaAlSi_3O_8$-H_2O, in both the saturated and undersaturated region using chemically complex natural materials. At the same time the reactions involving the minor phases were studied 1) to see how they compared with synthetic studies, and 2) to outline important possibilities for future research.

To study the effects of undersaturation, water content was determined by controlling the amount of water initially present in the system. Another interesting way would have

been to control the water fugacity by exterior means as described by Shaw (1967) and Eugster and Skippen (1968).

EXPERIMENTAL PROCEDURE

STARTING MATERIALS

For these experiments three granitic rocks of differing chemistry were chosen. These were the Westerly Granite (quartz monzonite), the Cape Ann Granite and the Mount Airy leucogranodiorite. Powders were prepared by grinding first in a plattner mortar and then in an agate mortar. Average grain size was about 0.05 mm, but the powders were not sieved since such a process would have removed much of the biotite and muscovite. Chemical analyses of these rocks are summarized in Table 1. Modal analyses of both thin sections and powders used in this study, along with those from previous work are summarized in Table 2. For the prupose of calculation and plotting, the compositions in the system $KAlSi_3O_8$-$NaAlSi_3O_8$-$CaAl_2Si_2O_8$-SiO_2 were calculated and are presented in Table 3.

WATER CONTENT OF CHARGE

The water content was measured by carefully weighing the water added to a dried and dessicated charge. Water content is believed to be accurate to between 0.1 and 0.05 milligrams. Thus, in a 50 mg sample water content is believed to be accurate to better than 0.2% by weight. At each temperature capsules containing approximately 1, 2, 3, 5, and 10% water by weight were used for each anhydrous material.

TABLE 1. CHEMICAL ANALYSES

Oxide	1	2	3	4	5	6	7	8	9	10	11
SiO_2	72.34	72.27	72.41	77.61	72.26	71.90	71.19	70.70	67.33	69.08	71.03
Al_2O_3	14.34	14.32	14.27	11.94	13.18	12.98	12.21	16.50	18.51	18.15	16.52
Fe_2O_3	0.68	0.95	0.87	0.55	0.24	0.81	1.94	2.34	1.78	1.21	1.94
FeO	1.13	1.01	0.98	0.87	2.77	2.85	3.71	----	----	----	----
MgO	0.37	0.28	0.41	Trace	0.20	0.02	0.19	0.29	0.41	0.14	----
MnO	0.02	0.03	0.03	----	0.10	0.08	0.10	----	----	----	----
CaO	1.52	1.39	1.39	0.31	1.10	1.04	1.19	2.96	2.63	1.95	1.93
Na_2O	3.37	3.79	3.32	3.80	3.99	4.19	3.67	4.56	3.60	5.30	5.53
K_2O	5.97	5.48	5.45	4.98	5.01	5.60	5.08	2.45	3.96	3.44	3.71
H_2O^-	0.06	0.11	0.06	Trace	0.08	----	----	----	1.20	----	0.19
H_2O^+	0.30	0.39	0.34	0.23	0.20	0.20	0.11				
TiO_2	0.26	0.26	0.26	0.25	0.36	0.34	0.33	----	0.38	0.43	----
P_2O_5	----	0.11	0.09	----	0.07	----	----	----	----	0.05	----
ZrO_2	----	0.03	----	----	----	0.12	0.34	----	----	----	----
CO_2	----	Trace	0.08	----	0.04	----	----	----	----	----	----
Total	99.86	100.87	99.96	100.54	99.60	100.13	100.06	99.80	99.80	99.70	100.85

1. Westerly Granite, Tuttle and Bowen, 1958.
2. Westerly Granite, Schlect and Stevens, 1951. Also contains; BaO, 0.13; SrO, 0.04; Li_2O, 0.006; Cr_2O_3, 0.009; V_2O_5, 0.04; and S, 0.01. Average of 34 analyses.
3. Westerly Granite, Stevens and Niles, 1960. Average of 61 analyses.
4. Cape Ann Granite, from Rockport, Washington, 1917.
5. So called 'Quincy' of Tuttle and Bowen, 1958. Sample from Peabody Granite according to Toulmin, 1964.
6. Peabody Granite, Old Quarry, South Lynnfield, Clapp, 1921.
7. Peabody Granite, Toulmin, 1964. Calculated from modal analysis.
8-10. Chemical analyses I,II, and III of Dietrich, 1961 wherein the original sources may be found. Average density calculated from analyses 8-10, 2.68. Actual density 2.648+.001.
11. Chemical composition calculated from the modal analyses of Dietrich, 1961. Average density calculated from chemical analysis 11, 2.65. Actual density 2.648+.001.

TABLE 2. MODAL ANALYSES

	1	2	3	4	5	6	7	8	9	10	11	12
Quartz	26.8	26.4	27.4	32.06	30.54	34.0	35.5	26.8	----	19.8	17.8	20.6
Perthite	----	----	----	58.58	54.15	60.0	60.7	63.9	88.5	----	----	----
Microcline	33.3	33.0	32.0	29.90*	27.60*	26.9**	28.2	30.9**	32.3**	21.9	22.3	19.6
Plagioclase	33.9	33.6	33.4	29.92*	26.48*	33.1**	32.5	32.9**	55.8**	50.6	51.3	55.2
Biotite	3.9	4.8	3.8	2.46	3.02	----	----	0.3	3.0	4.3	5.1	2.5
Muscovite	1.2	1.4	2.3	----	----	----	----	----	----	1.5	1.7	----
Ferrohornblende....	----	----	----	4.02	8.14	4.0	2.0	6.2	2.8	----	----	----
Riebeckite	----	----	----	0.51	1.00	----	----	0.1	----	----	----	----
Pyroxene	----	----	----	0.05	0.50	2.5	----	0.2	5.5	----	----	----
Epidote	----	----	----	----	----	----	----	----	----	1.1	1.0	----
Accesories	0.7	0.8	1.2	2.32	2.65	----	0.5	1.1	2.2	1.8	0.7	3.0+
Total	99.8	100,0	100.1	100.00	100.00	100.5	98.7	98.6	102.0	100.1	99.9	100.9

1. Westerly Granite, thin section analysis, average of two. Total number of points, 2127.
2. Westerly Granite, analysis on powder. Total number of points, 2249.
3. Westerly Granite, from Chayes, 1952. Average of analyses on 13 samples.
4. Cape Ann Granite, thin section analysis. Total number of points, 2240.
5. Cape Ann Granite, analysis on powder. Total number of points, 2050.
6. Cape Ann Granite, average of modal analysis given by Toulmin, 1964.
7. Cape Ann Granite, modal analysis of Washington, 1917.
8. Peabody Granite, average of modal analyses given by Toulmin, 1964.
9. Massive Beverly Syenite, average of modal analyses given by Toulmin, 1964.
10. Mount Airy leucogranodiorite, thin section analysis. Total number of points, 2273.
11. Mount Airy leucogranodiorite, analysis on powder. Total number of points, 2232.
12. Mount Airy leucogranodiorite, modal analysis of Dietrich, 1961.

* Calculated from composition of perthite as described in the text.

** Calculated from composition of perthite as given by Toulmin, 1964.

+ This figure includes muscovite and epidote in Dietrich's analysis.

TABLE 3. COMPOSITIONS EXPRESSED IN THE SYSTEM SiO_2-$KAlSi_3O_8$-$NaAlSi_3O_8$-$CaAl_2Si_2O_8$

	SiO_2	$KAlSi_3O_8$	$NaAlSi_3O_8$	$CaAl_2Si_2O_8$
1†.....	28.8	34.5	29.3	7.3
2†.....	28.3	34.7	29.6	7.4
3†.....	29.84	33.66	29.20	7.30
4.....	27.6	34.5	30.3	7.6
5.....	30.15	34.28	29.34	6.23
6††.....	35.85	32.75	30.15	1.25
7††.....	36.8	32.4	29.8	1.3
8††.....	36.5	29.0	33.0	0.5
9.....	36.3	30.2	32.7	0.85
10††.....	36.6	29.0	35.5	
11††.....	29.6	34.1	35.8	0.55
12.....	27.6	34.5	30.3	7.6
13††.....	----	36.7	60.5	2.8
14†.....	21.6	23.1	47.0	8.3
15†.....	19.6	23.9	48.0	8.5
16†.....	21.2	22.0	47.2	9.6
17.....	29.2	15.1	40.5	15.3
18.....	27.3	25.4	33.1	14.3
19.....	21.1	21.1	47.3	10.1

1. Westerly Granite. Calculated from modal analysis on thin section.
2. Westerly Granite. Calculated from modal analysis on powder.
3. Westerly Granite. Calculated from modal analysis of Chayes, 1952.
4. Westerly Granite. From C.I.P.W. norm of Tuttle and Bowen, 1958.
5. Westerly Granite. Average of 34 C.I.P.W. norms of Schlect and Stevens, 1952.
6. Cape Ann Granite. Calculated from modal analysis on thin section.
7. Cape Ann Granite, Calculated from modal analysis on powder.
8. Cape Ann Granite. Calculated from modal analysis of Washington, 1917.
9. Cape Ann Granite. From normative analysis of Washington, 1917.
10. Cape Ann Granite. Calculated from average mode given by Toulmin, 1964.
11. Peabody Granite. Calculated from average mode given by Toulmin, 1964.
12. Peabody Granite. Calculated from norm of Tuttle and Bowen, 1958.
13. Massive Beverly Syenite. Calculated from average mode given by Toulmin, 1964.
14. Mount Airy leucogranodiorite. Calculated from modal analysis on thin sections.
15. Mount Airy leucogranodiorite. Calculated from modal analysis on powder.
16. Mount Airy leucogranodiorite. Calculated from modal analysis of Dietrich, 1961.
17-18. Mount Airy leucogranodiorite. From chemical analyses I, II, and III of Dietrich, 1961.

* Calculated using ρ_Q= 2.65; ρ_{Mi}= 2.56; ρ_{Pl}= 2.66; and plagioclase of An_{20}.

** Calculated using ρ_Q= 2.65; ρ_{Perth}= 2.58; and composition of the feldspar as $Or_{51}Ab_{47}An_2$.

† Calculated using ρ_Q= 2.65; ρ_{Mi}= 2.56; ρ_{Pl}= 2.65, and a plagioclase of An_{15}

Capsules were carefully weighed before and after sealing to assure against loss of water during welding. Each series of five capsules were sealed in a single stellite cold seal vessel (Tuttle, 1949).

PRESSURE CONTROL

In all runs the pressure medium was water at a run pressure of two kilobars. Pressure was measured on a gauge calibrated in turn against a seven kilobar Heise gauge. During each run, the pressure was monitored on a smaller gauge roughly calibrated against the master gauge, and was periodically checked against the original gauge. During any run the pressure did not vary by more than about ± 50 bars.

TEMPERATURE CONTROL

Temperatures were measured with unsheathed chromel-alumel thermocouples made from matched wire. To keep down the affects of deterioration over long periods of time at high temperatures a new thermocouple was employed for each series of runs. These thermocouples were calibrated in place in the thermocouple well against the alpha-beta quartz transition and the melting point of sodium chloride using D.T.A. methods, and also against the melting point of sodium chloride using sealed evacuated capsules. Temperature gradients were also measured over the first inch and a half of

the vessel and were found to be less than ± 1°C. During a run, temperature was continuously monitored on an Esterline Angus twenty-four channel recorder, and were measured at least twice a day against a potentiometer. The temperature variation during a run, after the initial setting, did not vary by more than ± 2°C. Therefore, temperatures are believed to be known to about ± 3°C. Runs were made at 650°C and at 20° intervals between 680° and 800°C.

OXYGEN FUGACITY

Most runs were conducted in thin walled gold capsules with no attempt to control oxygen fugacity. In the Westerly, both hematite and magnetite crystallized from decomposition of the biotite at temperatures up through 800°C. This suggests that f_{O_2} was buffered along the hematite-magnetite curve by the oxidation state of the charge itself. Due to the absence of hematite and fayalite in the Cape Ann and Mount Airy runs the f_{O_2} can be assumed to be between the hematite-magnetite and quartz-magnetite-fayalite buffer curves, but it cannot be assumed that they are on the nickel-nickel oxide buffer curve, as suggested by Eugster and Wones (1962) for unbuffered experiments in platinum capsules.

Upon removal, capsules were weighed to assure against leakage and the crystalline phases identified by optical and X-ray techniques.

WATER CONTENT OF LIQUID PHASE

To determine the water content of the silicate melt, two parameters are readily available in this study, the initial water content of the charge, and the volume percent of glass formed. The latter was determined by point counts on the run products. Generally 200 points in groups of 50 were used, and variation between groups was usually less than ± 5% glass.

To relate these parameters to water content of the liquid phase, consider the formation of a liquid in an undersaturated region where no significant amount of vapor phase will be formed. Then, if the liquid phase is the only phase absorbing significant water;

$$W_{H_2O} = Y^{L}_{H_2O} W_L$$

where W_{H_2O} is the weight of water present in the system, $Y^{L}_{H_2O}$ is the weight fraction of water in the liquid phase, and W_L is the weight of the liquid formed. This equation may be rewritten in terms of the volume of the liquid;

$$W_{H_2O} = Y^{L}_{H_2O} V_L \rho_L$$

where ρ_L is the density of the liquid. Then dividing by by the weight of the charge and subsitiuting the equality;

$$W_{ch} = V_{ch} \rho_{ch}$$

we can obtain;

$$\frac{W_{H_2O}}{W_{ch}} = Y^{L}_{H_2O} \frac{\rho_L}{\rho_{ch}} \frac{V_L}{V_{ch}} \quad .$$

Or, substituting weight and volume percents;

$$Wt\%_{H_2O} = Y^{L}_{H_2O} \frac{\rho_L}{\rho_{ch}} V\%_L \quad .$$

Using average values for the densities of the starting granites and natural obsidians the densities of the charge and liquid may be calculated for different amounts of original water and ratio tabulated (Table 4). Thus, for runs in which no significant vapor phase is present, if the volume percent of glass is known, and the original amount of water is known, the weight percent of water in the glass can theoretically be calculated by the relationship;

$$Y^{L}_{H_2O} = \frac{Wt\%_{H_2O}}{Vol\%_L \; \rho_L/\rho_{ch}} \quad .$$

When some other phase, such as a vapor phase is present, this simple analysis breaks down, for the first equation becomes;

$$W_{H_2O} = \Sigma Y^{i}_{H_2O} \; W_i$$

where this sum is taken over all water bearing phases into which the water is going. It can be seen that when an aqueous vapor phase with Y_{H_2O} approximately equal to one forms, a significant amount of water goes into the vapor. The reaction of water bearing phases may be accommodated into the same formula with negative W_i. Since all of the hydrated phases,

TABLE 4.

DENSITY RATIOS FOR WEIGHT FRACTION CALCULATIONS

$Wt.\%_{H_2O}$	1	2	3	5	10
ρ_{ch}*	2.64	2.63	2.61	2.57	2.49
ρ_L/ρ_{ch}**	0.898	0.903	0.908	0.923	0.953

* Calculated by the formula $\rho_{ch} = \rho_{granite} \times Wt.Frac_{Gr} + \rho_{H_2O} \times Wt.Frac_{H_2O}$ using the average density of granite given by Daly et.al. (1966). (2.667)

** Calculated using the average density of rhyolitic obsidians given by Daly et.al., (1966). (2.370)

such as biotite, are present in small amounts and have a fairly small Y_{H_2O}, their contribution will be negligible.

It can also be seen from this presentation that as long as the liquid is the only major water bearing phase, and the $Y^{L}_{H_2O}$ varies only slightly, a plot of $Vol\%_L$ vs. $Wt\%_{H_2O}$, or $Vol\%_{H_2O} \frac{\rho_L}{\rho_{ch}}$ vs. $Wt\%_{H_2O}$ will be almost linear, with a slight increase in slope with increasing $Wt\%_{H_2O}$. When a vapor phase forms, a great deal of the water will go into the vapor and the curve will steepen markedly, becoming vertical. There will obviously be scatter, but the general trend should become apparent in the plots. Several plots for the several granites at different temperatures are shown in the following sections.

WESTERLY GRANITE; EXPERIMENTAL RESULTS

PETROGRAPHIC DESCRIPTION

The Westerly Granite is better described as a metaaluminous quartz monzonite. It is composed of a little over a third oligoclase (An_{20}), one third microcline and a quarter quartz, with greenish biotite, some minor muscovite, and magnetite. Accessories include allanite, apatite, sphene, zircon, and secondary epidote. It is a fine grained, light gray, massive equigranular rock that is quite uniform over most exposures.

The best detailed petrographic study has been made by Chayes (1950). He has presented a table of 13 modal analyses, the average of which is presented on Table 2. The particular sample used in the present study came from the Bradford quarry, the site of the G-1 sample commonly used as a chemical standard (Fairbairn et. al., 1951). A large number of chemical analyses have been done on this sample and are reported by Fairbairn et. al. (1951), Stevens and Niles (1960), Fleischer and Stevens (1962) and Fleischer (1965).

In connection with the present work, modal analyses were done on two thin sections taken from immediately adjacent to the powdered sample, as well as an analyses on the actual powder used (Table 2). These two analyses gave practically identical results. The amount of biotite determined from the powder is slightly higher due to the tendency for biotite

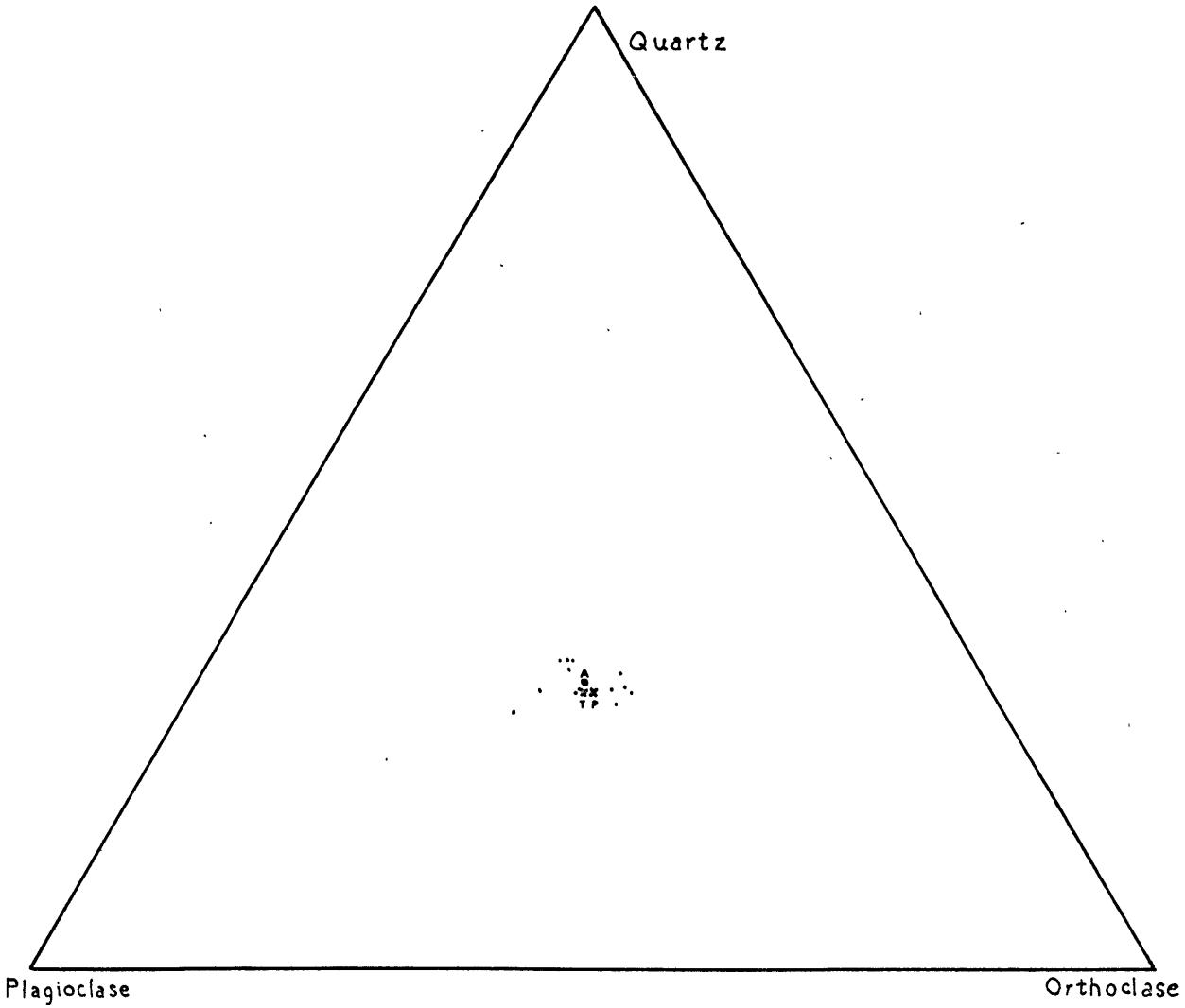
Quartz
Plagioclase
Orthoclase

to lie flat in oil mounts. The modal analyses are compared with the 13 of Chayes in Figure 1, and may be seen to agree well with his data for a number of samples. The composition from these modal analyses expressed in the system $KAlSi_3O_8$-$NaAlSi_3O_8$-$CaAl_2Si_2O_8$-SiO_2 agree well with the analyses of Schlecht and Stevens (1951) and Stevens and Niles (1960) (Table 3).

This sample appears to be just slightly less silica rich than the average analyses of the G-1 sample, but is well within the scatter in the various chemical analyses.

MELTING RELATIONSHIPS

Experimental results on the Westerly Granites are summarized in Table 5.

The glass in the Westerly runs appears to be light brown to clear with a refractive index of 1.486 to 1.490, and often quite variable. Traces of glass were noted in saturated runs at 700°C, but no significant melting was observed until 720°C, at which time it was present in all runs. The persistent condensed assemblage in all runs through 740°C was Pl,Or,Q,L. By 760° the saturated run appears to have passed into the liquid-vapor field, with only small amounts of badly corroded orthoclase. The 5% water run does not pass into the liquid field until around 780-800°C. Even at 800°C the 1, 2, and 3% samples contain orthoclase, plagioclase, quartz and glass, although in the 3% run the orthoclase content is

TABLE 5.

RESULTS OF EXPERIMENTS ON WESTERLY

Run No.	Wt.% H_2O	Temp.(°C)	Time(hrs)	Vol.% Glass	R.I. Glass	Phases Observed
W 101	9.61	650	1533	----	-----	Or,Pl,Q,Bi,H,Mg,Mu?,V
W 54	0.99	680	725	----	-----	Or,Pl,Q,Bi,H,Mg,Mu?,V
W 55	2.91	680	725	----	-----	Or,Pl,Q,Bi,H,Mg,Mu?,V
W 56	4.98	680	725	----	-----	Or,Pl,Q,Bi,H,Mg,Mu?,V
W 57	10.00	680	725	----	-----	Or,Pl,Q,Bi,H,Mg,Mu?,V
WR 19-1	1.00	700	746	Trace	-----	Or,Pl,Q,Bi,H,Mg,Mu?,(L),V?
W 20	2.04	700	791	Trace	-----	Or,Pl,Q,Bi,H,Mg,Mu?,(L),V
W 21	2.95	700	791	Trace	-----	Or,Pl,Q,Bi,H,Mg,Mu?,(L),V
W 22	5.00	700	791	Trace	-----	Or,Pl,Q,Bi,H,Mg,Mu?,(L),V
W 23	9.40	700	791	Trace	1.486	Or,Pl,Q,Bi,H,Mg,Mu?,(L),V
W 24	1.04	720	767	----	1.486	Or,Pl,Q,Bi,H,Mg,L,V?
W 25	1.83	720	767	----	1.486	Or,Pl,Q,Bi,H,Mg,L,V?
W 26	3.02	720	767	----	1.485	Or,Pl,Q,Bi,H,Mg,L,V
WR 27-1	4.99	720	725	45	1.485	Or,Pl,Q,Bi,H,Mg,L,V
W 28	10.19	720	767	58	1.486	Or,Pl,Q,Bi,H,Mg,L,V

TABLE 5. (Cont.)

Run No.	Wt.% H_2O	Temp. (°C)	Time (hrs)	Vol.% Glass	R.I. Glass	Phases Observed
W 49	0.99	740	766	----	-----	Or,Pl,Q,Bi,H,Mg,L
W 50	1.99	740	766	----	-----	Or,Pl,Q,Bi,H,Mg,L
W 51	2.97	740	766	----	-----	Or,Pl,Q,Bi,H,Mg,L,V?
W 52	4.99	740	766	----	-----	Or,Pl,Q,Bi,H,Mg,Px,L,V
W 53	9.93	740	766	70	1.487	Or,Q,Bi,H,Mg,Px,L,V,Pl?
W 34	1.00	760	744	20	1.498	Or,Pl,Q,Bi,H,Mg,Px,L
W 35	1.93	760	744	37	1.493	Or,Pl,Q,Bi,H,Mg,Px,L
W 36	2.94	760	744	52.5	1.492	Or,Pl,Q,Bi,H,Mg,Px,L
WR 37-2	5.00	760	897	77	1.490	Or,Bi,H,Mg,Px,L,(Q),(Pl)
W 38	10.85	760	744	81	1.490	Bi,H,Mg,Px,L,V,Or?,(Pl),(Q)
WR 39-1	1.00	780	897	21	1.500	Or,Pl,Q,Bi,H,Mg,Px,L
W 40	1.98	780	779	41.5	1.490	Or,Pl,Q,Bi,H,Mg,Px,L
W 41	3.00	780	779	61	1.487	Or,Pl,Q,Bi,H,Mg,Px,L
W 42	5.12	780	779	82	1.486	Or,Bi,H,Mg,Px,L,(Pl),(Q)
W 43	9.89	780	779	90	1.492	Bi,H,Mg,Px,L,V,(Or),(Q)

TABLE 5. (Cont.)

Run No.	Wt.% H_2O	Temp.(°C)	Time(hrs)	Vol.% Glass	R.I. Glass	Phases Observed
W 44	1.00	800	766	38.5	1.502	Or,Pl,Q,Bi,H,Mg,Px,L
W 45	1.88	800	766	62	1.486	Or,Pl,Q,Bi,H,Mg,Px,L
W 46	3.07	800	766	82	1.486	Or,Pl,Q,Bi,H,Mg,Px,L
W 47	4.97	800	766	91	1.484	Bi,H,Mg,Px,L,(Or),(Pl)
WR 48-1	9.94	800	897	97	1.490	Bi,H,Mg,Px,L,V

very small, and crystalline phases composed only 18% of the charge.

The persistence of a two feldspar assemblage at all temperatures is surprising considering the fact that the sanidine-high albite alkali feldspar solvus is considerably below the temperatures of these experiments. (Luth and Tuttle, 1966, Orville, 1963). Much more will be said about the composition and state of these feldspars later on, but it may be mentioned here that the effects of structural state and anorthite content are of critical importance.

Biotite

The biotites in the Westerly were seen to react to form more magnesium rich members, but good pale green biotite persisted up through 800°C. The decomposition of the iron end member was not a simple reaction though. The large flakes were characteristically darker brown with larger 2V then previously seen with erratic refractive indices that were generally higher than that of the original biotite or the fine-grained biotite in the run products. This was interpreted as metastable oxybiotite formed by the oxidation of part of the iron end member in the biotite solid solution series (Wones and Eugster, 1965):

$$KFe^{+2}_3AlSi_3O_{10}(OH)_2 + \tfrac{1}{2}O_2 \rightarrow KFe^{+2}Fe^{+3}_2AlSi_3O_{10}(O)_2 + H_2O.$$

Given time this product would then break down to sanidine plus a mixture of magnetite and hematite by the reactions:

$$KFe^{+2}Fe_2^{+3}AlSi_3O_{10}(O)_2 \rightarrow KAlSi_3O_8 + Fe_3O_4$$

$$KFe^{+2}Fe_2^{+3}AlSi_3O_{10}(O)_2 + \tfrac{1}{4}O_2 \rightarrow KAlSi_3O_8 + 3/2Fe_2O_3$$

In the fine grained biotite no such behavior was seen. Refractive indices were measured for these finer grained material and the 'apparent' annite concentrations tabulated from the data of Wones (1963) (Table 6). In the biotite series, titanium tends to raise the refractive index while fluorine tends to lower it (Hall, 1941). Thus, the presence of titanium tends to make estimates of the annite component too large, so that the composition determined is only an 'apparent' one.

When the 'apparent' annite contents were plotted against temperature (Fig. 2) and compared with the curve for biotite in equilibrium with sanidine, magnetite, and water vapor found by Wones and Eugster (1965), the compositions followed the curve fairly well, but was displaced to the high annite side by about 15% annite. This is probably due to the presence of titanium. On the graph, if the experimental curve found in the present work is extrapolated back a short distance it will cross the original apparent composition at a temperature of about 650°C. At this temperature, a biotite in equilibrium with magnetite, hematite, potassium feldspar, and water vapor at about 2 kilobars has an effective annite composition from the curve of Wones and Eugster (1965) of about 29% annite. Thus, the annite component of the original biotite, at least that effectively shown by this extrapolation, should be about 29%. This value

TABLE 6.

COMPOSITION OF BIOTITE IN THE WESTERLY

RUN NO.	TEMP. (°C)	%H_2O	γ	2V	Apparent % Annite
W 0	---	--	1.655	<10°	57
W 101	650	10	1.651	<10°	55
W 54	680	1	1.650	<15°	54
W 55	680	3	1.649	<10°	52.5
W 56	680	5	1.646	<15°	51
W 57	680	10	1.646	<10°	50
WR 19-1	700	1	1.644	--	48.5
W 21	700	3	1.642	<10°	47.5
W 22	700	5	1.639	--	44.5
W 23	700	10	1.638	<10°	43
W 24	720	1	1.639	<10°	44.5
W 26	720	3	1.637	--	42
WR 27-1	720	5	1.636	--	41.5
W 28	720	10	1.634	--	40
W 49	740	1	1.634	--	40
W 51	740	3	1.632	--	39
W 52	740	5	1.631	--	39
W 53	740	10	1.629	--	38
W 34	760	1	1.630	--	38
W 36	760	3	1.628	<15°	36
WR 37-2	760	5	1.626	--	34
W 38	760	10	1.624	--	32

TABLE 6. (Cont.)

RUN NO.	TEMP. (°C)	%H_2O	γ	2V	Apparent % Annite
WR 39-1	780	1	1.625	--	33
W 40	780	2	1.623	--	32
W 41	780	3	1.623	--	32
W 42	780	5	1.622	--	31
W 43	780	10	1.622	--	31
W 44	800	1	1.622	--	31
W 45	800	2	1.621	--	30.5
W 46	800	3	1.620	--	30.5
W 47	800	5	1.620	--	30.5
W 48	800	10	1.620	--	30

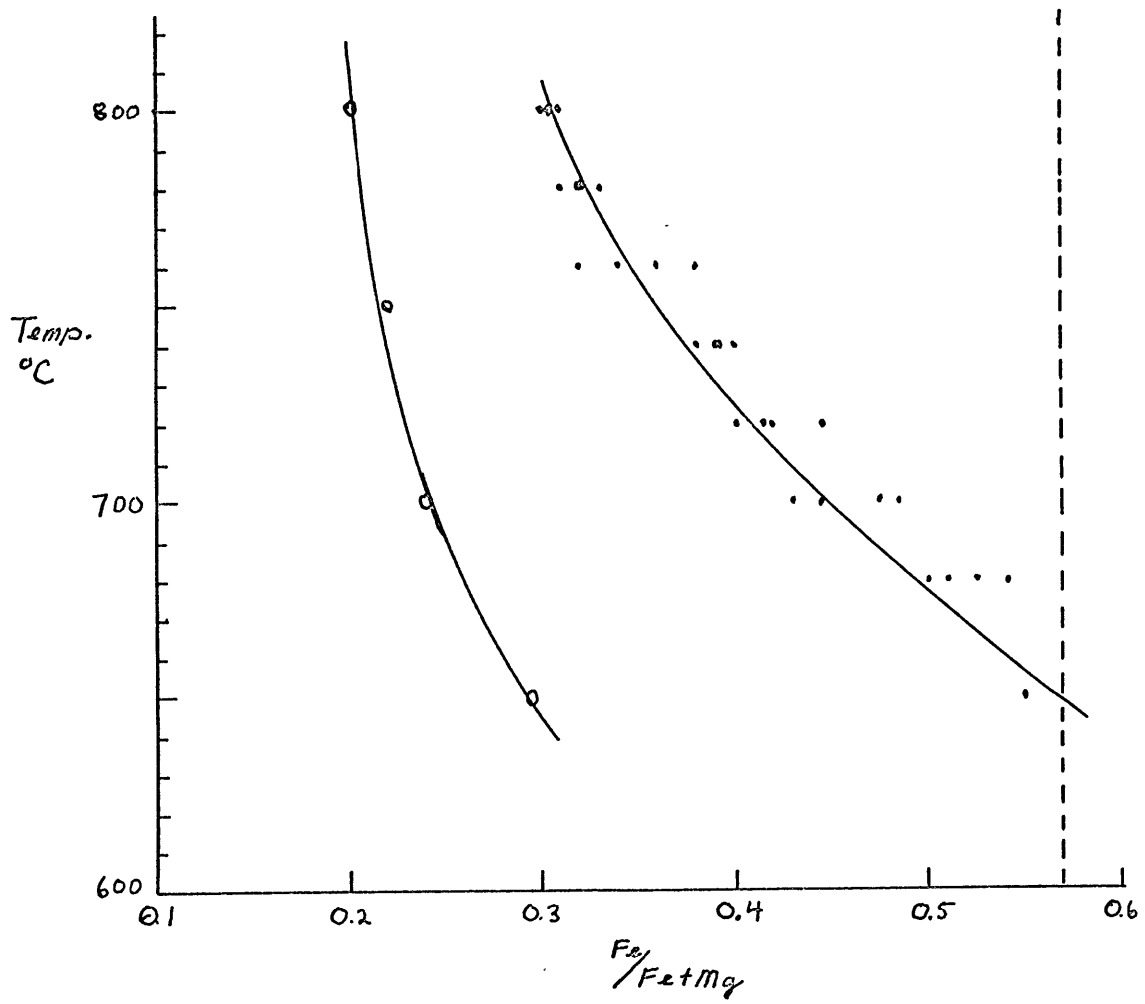

Figure 2. Variation in Biotite Composition with Temperature On Westerly Granite.

Points mark the 'apparent' Fe/Fe+Mg ratio determined from the γ index by comparison with the data of Wones,1963.

Open circles represent the data of Wones and Eugster, 1965,along the Hematite-Magnetite buffer curve.

The dashed line represents the 'apparent' ratio of the original material from the Westerly.

may be used in the formula for water fugacity in equilibrium with magnetite, potassium feldspar, and a biotite of a given composition as given by Wones and Eugster to calculate an approximate water fugacity for crystallization of the Westerly.

$$\mathrm{Log}_{10} f_{H_2O} = \frac{3428 - 4218(1-x_1)^2}{T} + \tfrac{1}{2}\mathrm{Log}_{10} f_{O_2} + \mathrm{Log}_{10} x_1 + 8.23$$

To do this an assumption as to the fugacity of oxygen present must be made. In the rock there is no apparent hematite, and no apparent fayalite of a primary nature, so that the original oxygen fugacity probably was between these two buffer curves. For purposes of calculation the Ni-NiO curve was used. Using these values the curve seen on Figure 3 was calculated. This may be displaced toward lower temperatures by increasing oxygen fugacity or to higher temperatures by lowering it. This curve crosses the beginning of melting in the saturated system $KAlSi_3O_8$, $NaAlSi_3O_8$, SiO_2 as determined by Tuttle and Bowen as shown. This suggests that the fugacity of water was at least somewhat above 1000 bars. This is only an estimate since a change in f_{O_2} or a lower activity of potassium feldspar would displace the biotite curve to higher temperatures, while the effects of calcium or undersaturation would displace the granite curve to higher temperatures. In general it appears that the water fugacity was probably above 1000 bars.

Muscovite

Within the Westerly, the muscovite could be either primary or secondary. Certainly there is secondary sericite in

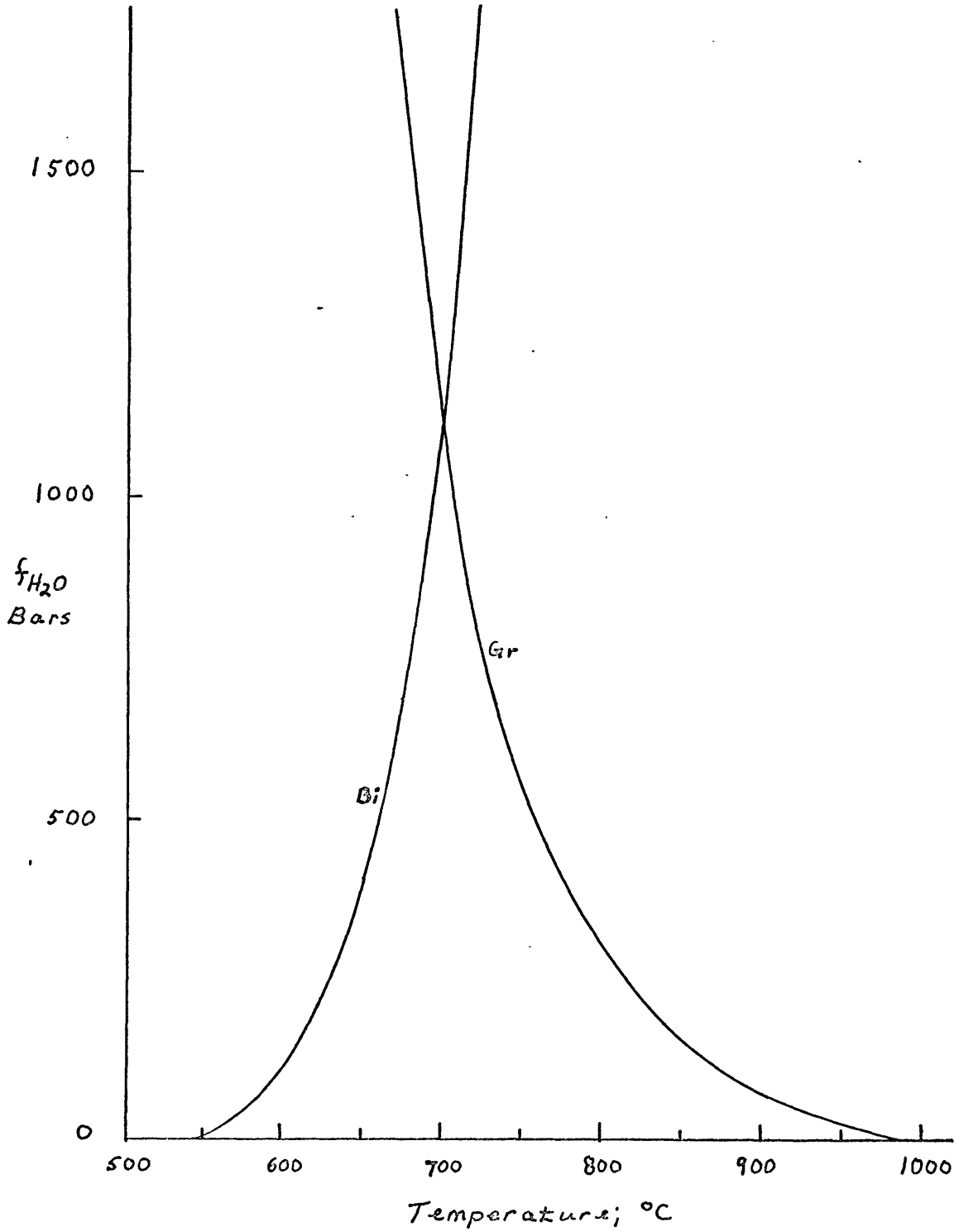

Figure 3. f_{H_2O} vs. T for Formation of the Westerly Granite.

The curve 'Gr represents the minimum melting in the saturated granite system from Tuttle and Bowen, 1958. The Curve 'Bi' represents the decomposition of the biotite in the Westerly along the Ni-NiO buffer, using $X_1 = 0.29$.

much of the feldspars. It is possible that some of the coarser material could be primary.

In this study large flakes of muscovite were observed up to 720°C, after beginning of melting.

The work of Evans(1965) is probably the best data available on the stability of muscovite and muscovite plus quartz. Other stability work on muscovite has been done by Yoder and Eugster (1955), Crowley and Roy (1964), and Velde (1966). The data of Evans indicates that muscovite should react at a water pressure of two kilobars at a temperature of about 680°C, whereas muscovite plus quartz should react well below this temperature. Of all experimental work only that of Yoder and Eugster comes anywhere near a temperature of 720°C for the stability of even pure muscovite.

Upon careful examination it was noted that only coarse flakes of muscovite were present in the runs above about 650°C. Some small masses of finely crystalline material were observed that appeared as if they might have been sanidine and an aluminosilicate after muscovite. Considering the metastability observed in the coarse biotites it appears likely that the coarse muscovite observed represents metastable persistance, continuing until the reaction rate becomes sufficiently rapid for large grains to react within the time span of the experiment. Probably the occurrence of an abundant liquid phase speeded the decomposition of the muscovite.

Pyroxene

At temperatures above 760°C small amounts of a pale green pyroxene were observed. These were studied optically (Table 7) and appear to be an augite. This mafic mineral never became very plentiful, although small amounts could be found in almost every run, and biotite continued to be the dominant mafic phase.

TABLE 7.

OPTICAL PROPERTIES OF PYROXENE IN HYDROTHERMAL RUNS ON WESTERLY

Run and Optic Direction	n	Color	Orientation	2V
W 42				
X	1.686±.001	Pale Green	X'∧c*= 53-54°	
Y	1.695±.001	Pale Brown	= b	50-55°
Z	1.705±.005	Pale Brown to Green	Z'∧c = 36-37°	
W 43				
X	1.682±.001	Pal3 Green	X'∧c = 54°	
Y	1.692±.001	Pale Brown	= b	50°
Z	1.700±.005	Pale Brown to Green	Z'∧c = 36°	
W 47				
X	1.680±.001	Pale Green	X'∧c = 54°	
Y	----------	Pale Brown	= b	---
Z	1.700±.005	Pale Brown to Green	Z'∧c = 36°	

* All primes refer to values measured on the (110) cleavage fragement.

CAPE ANN GRANITE; EXPERIMENTAL RESULTS

PETROGRAPHIC DESCRIPTION

The Cape Ann Granite is a alkali rich granite, very similar to the 'Quincy' used by Tuttle and Bowen (1958). It has long been quarried at Rockport, Massachusetts for building stone. The Cape Ann forms a large part of the bed rock in the 15 minute quadrangle of Gloucester, and the two $7\frac{1}{2}$ minute quadrangles of Essex and Marlboro North in the county of Essex, Massachusetts (Clapp, 1921; Emerson, 1917). The western part of the body extends into the quadrangles of Salem and Georgetown. This formation has been described by Warren and McKinstry (1924), Clapp (1921), and Washington (1898, 1899, 1917). Recent work on the Salem quadrangle by Toulmin (1964) also discusses part of the Cape Ann and related bodies. Originally the Cape Ann, Peabody, Quincy, and other smaller alkalic granitic bodies in this part of Massachusetts were mapped as 'Quincy" (Clapp, 1921; Emerson, 1917). Although these bodies are very similar, there are differences in chemistry and mineralogy and they are now referred to as different bodies. The actual sample used by Tuttle and Bowen (1958) and called by them 'Quincy' is reported by Toulmin (1964) to have come from the Peabody body.

Mineralogically, this rock is composed dominantly of a microcline perthite with low albite lamellae and smokey quartz with small amounts of green amphibole, magnetite, and biotite.

The feldspar often forms large poikilitic crystals enclosing minor amounts of mafic minerals. The quartz content is quite variable from sample to sample. In general the Cape Ann body is more quartz rich than the other alkalic granitic rocks from this area which were observed during this study.

These rocks are in general coarse grained with a hypidiomorphic to allotrimorphic-granular texture with occassional large poikilitic feldspars. The dominant mafic mineral is a green amphibole similiar to that described by Toulmin (1964), but having smaller extincting angles and higher indices (Table 8). An analysis of the amphibole of the Peabody (Toulmin, 1964) shows it to be dominantly a hastingsite with some arfvedsonite component (Table 9). The dominant amphibole in the Cape Ann is probably a slightly more iron rich variety of the same series (Deer et. al., vol. 2, 1963).

There is a second blue, sodium rich amphibole present that appears to be riebeckite (Table 8) although it may have substantial arfvedsonite component. This occurs in a variety of textures. It is occassionally found in round, radial aggregates sometimes about a core of pale green material of high relief and moderate interference colors that appears to be an aegerine augite. It also seems to form homoaxial intergrowths with the green amphibole, often associated in this relationship with brown biotite and magnetite.

Most of the mafics are in interstitial aggregates with an Fe^{+3}rich biotite. It is this iron rich biotite that was originally called 'annite' by Dana (1898). Analysis has

TABLE 8.

OPTICAL PROPERTIES OF THE AMPHIBOLES

IN THE CAPE ANN AND RELATED ROCKS

Sample and Direction	n	Color	Orientation	$2V_x$
Green Amphibole Cape Ann				
X	1.686±.002	Pale Greenish Grey		
Y	1.710±.005	Deep Greenish Grey	= b	25-30°
Z	1.720±.005	Dark Bluish Green	Z∧c = 5°. On (110 cleavage fragments, Z' c = 12°	
Green Amphibole, Peabody Granite*				
X	1.709±.002	Tan		
Y	----------	Deep Green	= b	40-1°
Z	1.715±.002	Dark, Brownish green.	Z∧c = 7°, On (110), Z'∧c = 12°	
Blue Amphibole, Cape Ann				
X	1.696±.002	Clear	X∧c = 5.8°	
Y	1.699±.002	Medium Blue to Violet	= b	Large
Z	1.705±.005	Deep Bluish Purple		

* From Toulmin, 1964. See chemical analysis, Table9.

TABLE 9.

CHEMICAL COMPOSITION OF THE AMPHIBOLE FROM THE PEABODY GRANITE*

Oxide	Analysis	Corr.For Impurities	Metal Atoms Per 23 Oxygen	Metal Atoms In Structure
SiO_2	40.06	39.01	6.730	8.000
Al_2O_3	7.34	6.91	1.270	
			0.138	
Fe_2O_3	5.45	5.45	0.704	
FeO	28.40	26.34	3.800	5.191
MgO	1.83	1.80	0.466	
TiO_2	1.89	0.63	0.083	
MnO	0.92	0.92	0.135	
CaO	9.04	9.04	1.667	2.000
Na_2O	2.71	2.71	0.198	
			0.713	0.920
K_2O	1.18	0.94	0.207	
H_2O^+	1.09	1.00	1.160	1.160
H_2O^-	0.52	----	-----	
F	0.1	----	-----	
ZrO_2	None	----	-----	
V_2O_5	Trace	----	-----	
TOTAL	100.43	94.75	-----	-----

* From Toulmin,1964. Impurities included 2.7% biotite,1.7% ilmenite, and 0.3% quartz from modal analysis.

shown that a good deal of the iron is in the ferric state, (Cook, 1867, Foster 1960). At times it appears as if some of the biotite is sheathing the green amphibole, however small amounts of biotite are found independent of other mafic minerals and sometimes is found included in quartz or feldspar.

Occassionally there are patches of yellow, almost isotropic material described by Toulmin (1964) and Warren and McKinstry (1924) as being an alteration product after fayalite. In the samples studied here only one piece of fayalite in the center of this material was seen. Zircons are quite common in all sections.

The amount of quartz varies from sample to sample and commonly appears in large aggregates, and sometimes as more interstitial material. The overall composition of the alkali feldspar was determined by homogenizing at 950°C for several days, and subsequent measurement of the $\bar{2}01$ reflection using spinel as an internal standard (Table 10). This gave an overall orthoclase content of 51% by weight from the data of Orville (1967) as presented by Wright (1968). The plagioclase part of the perthite is almost pure albite, with an apparent anorthite component of up to about 4% (Table 11). Point counts were done on both thin sections and powder used (Table 2). For plotting and calculations the composition with respect to $KAlSi_3O_8$, $NaAlSi_3O_8$, $CaAl_2Si_2O_8$, and SiO_2 were calculated from these modal analyses using a composition of the plagioclase of An_4 (Table 3). For comparison, chemical an-

TABLE 10.

ORTHOCLASE CONTENT OF CAPE ANN PERTHITE*

	$2\theta_{,,\bar{2}01}$**	Wt.% Or†
1.	21.45°	51
2.	21.46°	52
3.	21.44°	50
4,	21.45°	51
	Average	51

* Sample homogenized at 950°C for one week.

** From four separate scans at 1/2° 2 /min., using spinel as an internal standard.

† From data of Orville,1967, as presented by Wright, 1968

TABLE 11.

ANORTHITE CONTENT OF PLAGIOCLASE IN CAPE ANN PERTHITE

α	β	γ	2V*
1.530±.002	1.534±.002	1.540±.002	80±1°

Composition: An_4†

Each value represents average of at least 10 measurements.

* Measured from thin sections using universal stage.

† From diagrams given by Deer et.al., Vol. 4, 1963.

alyses given by Washington (1917) and analyses on related rocks given by Toulmin (1964) are listed (Table 2, 3).

MELTING RELATIONSHIPS

Experimental results on the Cape Ann Granite are summarized in Table 12.

Of all three rocks, the Cape Ann was the first to melt. Small amounts of glass in the form of small rims were seen at 680°C, in most runs, but by 700°C large amounts of glass had formed in all runs. By 720°C orthoclase and plagioclase had become very scarce in the saturated sample and by 740°C only quartz was left and this was badly rounded and corroded. By 760°C the stable assemblage in the saturated case was liquid and vapor. By 760°C only the 1 and 2% water runs still had plagioclase, orthoclase, and quartz present while the 3% run contained quartz and orthoclase with a very little badly corroded plagioclase, while the 5% run contained only quartz and glass. At 780°C assemblages were similiar except that no plagioclase could be found in the 3% run. By 800°C the orthoclase departed from the 3% run and quartz disappeared from the 5% run, leaving only magnetite and pyroxene in the 5 and 10% runs. Only 1 and 2% runs contained good orthoclase and plagioclase, and both contained a fair amount of both.

TABLE 12.

RESULTS OF EXPERIMENTS ON CAPE ANN

Run No.	Wt.%H_2O	Temp.(°C)	Time(hrs)	Vol.% Glass	R.I. Glass	Phases Observed
Q 101	961	650	1.533	----	-----	Q,Or,Pl,Bi,Mg,Ac,V
Q 31	1.00	680	725	----	-----	Q,Or,Pl,Bi,Mg,Ac,V
Q 32	3.04	680	725	Trace	-----	Q,Or,Pl,Bi,Mg,Ac,V,L?
Q 33	4.75	680	725	Trace	-----	Q,Or,Pl,Bi,Mg,Ac,V,L?
Q 34	9.96	680	725	Trace	1.488	Q,Or,Pl,Bi,Mg,Ac,V,L?
QR 1-1	1.00	700	746	2-5	-----	Q,Or,Pl,Mg,Ac,L,V,Bi?
Q 2	1.77	700	862	16	1.488	Q,Or,Pl,Mg,Ac,L,V,Bi?
Q 3	2.85	700	862	26	1.488	Q,Or,Pl,Mg,Ac,L,V,Bi?
Q 4	5.65	700	862	56	1.486	Q,Or,Pl,Mg,Ac,L,V,Bi?
Q 5	11.91	700	862	67	1.488	Q,Or,Pl,Mg,Ac,L,V,Bi?
Q 6	0.89	720	767	13	1.488	Q,Or,Pl,Mg,Ac,L,V?
Q 7	1.94	720	767	26.4	1.488	Q,Or,Pl,Mg,Ac,L,V?
Q 8	2.98	720	767	42	1.488	Q,Or,Pl,Mg,Ac,L,V
Q 9	4.86	720	767	71	1.490	Q,Or,Pl,Mg,Ac,L,V
Q 10	9.97	720	767	95	1.488	Q,Mg,Ac,L,V,Or?,Pl?(Bi)

TABLE 12. (Cont.)

Run No.	Wt.% H_2O	Temp. (°C)	Time (hrs)	Vol.% Glass	R.I. Glass	Phases Observed
Q 11	1.02	740	742	19	1.490	Q,Or,Pl,Mg,Ac,L
QR 12-1	2.00	740	725	37	1.490	Q,Or,Pl,Mg,Ac,L
Q 13	2.95	740	742	56.7	1.486	Q,Or,Pl,Mg,Ac,L
Q 14	4.94	740	742	82	1.488	Q,Or,Pl,Mg,Ac,L
QR 15-1	10.07	740	725	96	1.490	Q,Mg,Ac,L,V,Or?
QR 16-1	1.00	760	897	20	1.490	Q,Or,Pl,Mg,Ac,L
Q 17	1.97	760	744	42	1.490	Q,Or,Pl,Mg,Ac,L
Q 18	2.97	760	744	60	1.489	Q,Or,Mg,Ac,L,Pl?
QR 19-1	5.01	760	897	85	1.489	Q,Mg,Ac,L,(Or),(Pl)
Q 20	9.72	760	744	96	1.488	Mg,Ac,L,V,(Q)
Q 21	1.00	780	778	26	1.492	Q,Or,Pl,Mg,Ac,L
Q 22	2.00	780	778	45	1.487	Q,Or,Pl,Mg,Ac,L
Q 23	2.92	780	778	70	1.487	Q,Or,Mg,Ac,L,Pl?
Q 24	4.96	780	778	89	1.487	Q,Mg,Ac,L
QR 25-1	9.91	780	897	97	1.489	Mg,Ac,L,V,(Q)
Q 26	0.99	800	756	50	1.486	Q,Or,Pl,Mg,Ac,L

TABLE 12. (Cont.)

RunNo.	Wt.%$_{H_2O}$	Temp.(°C)	Time(hrs)	Vol.% Glass	R.I. Glass	Phases Observed
Q 27	1.99	800	756	50	1.486	Q,Or,Pl,Mg,Ac,L
Q 28	2.99	800	756	76	1.487	Q,Mg,Ac,L,(Q)
Q 29	4.84	800	756	92	1.487	Mg,Ac,L,(Q)
Q 30	10.00	800	756	99	1.489	Mg,Ac,L,V

BUFFERED RUNS

Run No.	Wt.%$_{H_2O}$	Temp.(°C)	Time(hrs)	f_{O_2} Buffer	Phases Observed
QB 1	~10.00	650	672	Hem-Mag	Q,Or,Pl,Mg,Ac,V
QB 2	~10.00	680	672	Hem-Mag	Q,Or,Pl,Mg,Ac,V,L?
QB 3	~10.00	650	672	Q-Mag-Fay	Q,Or,Pl,Mg,Ac,Ha?,V
QB 4	~10.00	680	672	Q-Mag-Fay	Q,Or,Pl,Mg,Ac,V,L?

ACCESSORY MINERALS

In addition to the unbuffered runs, some saturated runs were made using hematite-magnetite and quartz-magnetite-fayalite buffers to better determine the stability of the amphiboles. The results of these runs are listed on Table 12 along with the unbuffered runs.

Amphibole

The amphibole decomposed early in the experimental runs. In the unbuffered runs no hastingsitic nor riebeckitic amphibole was seen. Large clots of greenish pyroxene, identified as aegerine-augite (Table 13), and magnetite were observed that were probably formed by decomposition of the amphiboles. Often, there were bits of moderate relief material observed within these clots. These appeared as if they might be a plagioclase, moderately rich in anorthite, but the crystals were too small and always buried within these mafic aggregates so that no positive identification could be made. A probably idealized reaction for the iron end member of the hastingsite series might be written as:

$$NaCa_2Fe^{+2}_4Fe^{+3}Si_6Al_2O_{22}(OH)_2 + \tfrac{1}{2}O_2 \rightarrow$$

$$2(Ca_{0.5},Na_{0.5})(Fe^{+2}_{0.5},Fe^{+3}_{0.5})Si_2O_6 + CaAl_2Si_2O_8 + Fe_3O_4 + H_2O$$

The oxygen fugacity in these unbuffered runs must have been somewhere between the buffer curves for hematite-magnetite, and that for the reaction of quartz and magnetite to form

fayalite, due to the lack of hematite or fayalite in the runs and the abundance of magnetite and quartz.

In the buffered runs using quartz, fayalite, and magnetite as a buffer the hastingsite had not completely reacted. There appeared to be cores of amphibole still present. As will be seen, little can be said about the ultimate stability of these amphiboles since the rock contained both quartz and potassium feldspar.

No sodium amphibole was seen in any of the runs. This is not conclusive however for the sodium amphibole was scarce in the original material and small amounts could still be present and not have been observed. The decomposition would be consistant with the high temperature stability data of Ernst (1962) on riebeckite-arfvedsonite solutions. Even with oxygen buffered by the quartz-magnetite-fayalite assemblage Ernst found the amphibole to decompose before 650°C at two kilobars P_{H_2O}.

Pyroxene

In all runs up through 800°C, the dominant mafic phases were magnetite and aegerine-augite. The biotite decomposed fairly early, at about 720°C. At temperatures between 700 and 760°C good aegerine and magnetite could be seen to be crystallizing in euhedral forms within the glass. At temperatures of 780 and 800°C the aegerine did not appear to be crystallizing from the glass and some of it appeared to be slowly dissolving. Due to the small size of the crystals

TABLE 13.

OPTICAL PROPERTIES OF PYROXENE IN

EXPERIMENTAL RUNS ON THE CAPE ANN

Run No. and Direction	n	Color	Orientation
Q 5			
X	1.765±.005	Green	
Y	1.790±.005	Light Green	= b
Z	>1.800	Light Yellow to Green	$Z \wedge c = 65\text{-}66^{\circ}$
Q 10			
X	1.763±.003	Green	
Y	----------	Light Green	= b
Z	>1.800	Light Yellow to Green	$Z \wedge c = 55\text{-}60^{\circ}$
Q 21 (Yellowish Green Variety)			
X	1.760±.005	Green	
Y	1.785±005	Light Green	= b
Z	>1.800	Light Yellow to Green	$Z \wedge C = 60^{\circ}$
Q 21 (Pale Green Variety in Glass)			
X		Pale Green	
Y		Pale Green to Tan	= b
Z		Clear	$Z \wedge c = 37^{\circ}$
Q 22 (Pale Green Variety in Glass)			
X		Pale Green	
Y		Tan to Clear	= b
Z		Clear	$Z \wedge c = 36^{\circ}$

and their association with glass it was not possible to determine changes in retractive indices of the pyroxene accurately, but the extinction angles appeared to increase and the color decrease. The α index appeared to decrease. This would tend to indicate that the pyroxene was becoming more augite rich. In one run at 780°C (Q 21) two distinct pyroxenes were seen. The first was similiar to the aegerine-augite in other runs, and the second was growing in the glass and was much paler with larger extinction angles and somewhat brighter interferance colors than the material in mafic clots with magnetite (Table 13). It thus appears that at temperatures in the neighborhood of 780 or 800°C with oxygen fugacities lying between the hematite-magnetite and magnetite-quartz-fayalite buffer curves the aegerine-augite reacts with the granitic melt to form a more augite-like pyroxene.

Stability of Hastingsite

From the experimental runs presented here, it appears as if the hastingitic amphibole is decomposing directly at temperatures above 650°C with oxygen fugacities at or above the quartz-magnetite-fayalite buffer. If we draw an f_{O_2} versus T diagram for this reaction, we can draw a schematic stability diagram for hastingsite at two kilobars P_{H_2O} (Figures 4, 5). When the reaction stated before for the breakdown of hastingsite crosses the Q-Mg-Fa buffer curve, an invariant point at this P_{H_2O} is generated, and from this point comes the reaction:

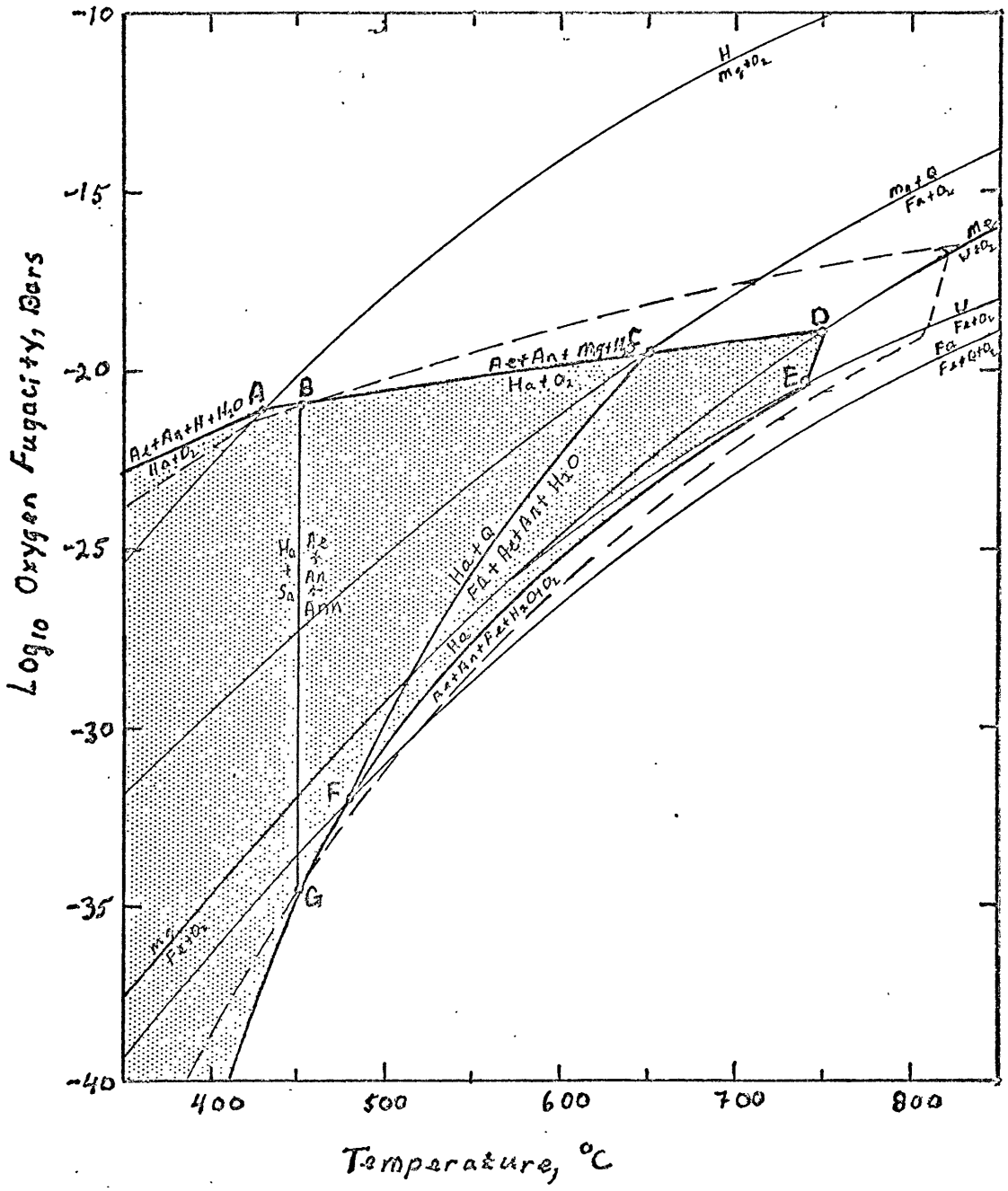

Figure 4. Schematic Diagram for Stability Field of Hastingsit. At 2 Kilobars Water Pressure.

Lettered points are shown in detail in Figure 5.

Figure 5. Specific Points for Stability Field of Hastingsite.

Dashed lines represent oxygen absent reactions that do not appear on the f_{O_2}-T diagram, Figure 4, due to the nature of the plot.

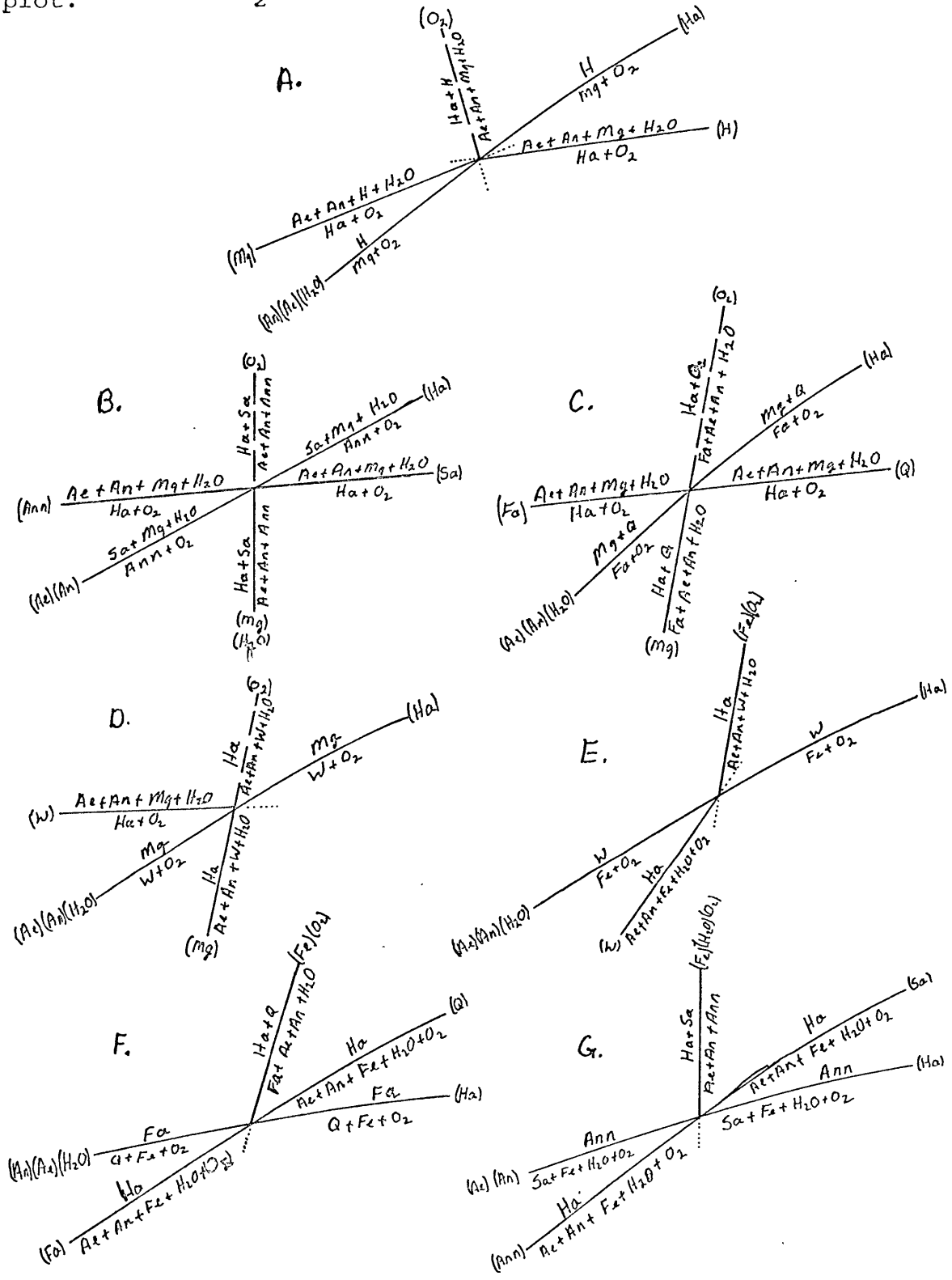

$$NaCa_2Fe^{+2}_4Fe^{+3}Al_2Si_6O_{22}(OH)_2 + 3/2\ SiO_2 \rightarrow$$

$$2(Ca_{0.5},Na_{0.5})(Fe^{+2}_{0.5},Fe^{+3}_{0.5})Si_2O_6 + CaAl_2Si_2O_8 + 3/2\ Fe_2SiO_4 + H_2O$$

Hastingsite + 3/2Quartz → 2Aegerine-Augite + Anorthite + 3/2Fayalite + Water

This reaction will be independent of oxygen fugacity but will depend on f_{H_2O} and total pressure. From the schematic f_{O_2} - T diagram (Figure 5) it can be seen that for oxygen fugacities above the Q-Mg-Fa buffer curve the hastingsite and hastingsite plus quartz stability fields overlap, so that only when f_{O_2} is less than that for the Q-Mg-Fa buffer can the presence of excess quartz decrease the stability of hastingsite.

A second interesting reaction occurs if the stability field of hastingsite crosses the stability curve of annite as determined by Eugster and Wones (1962). Here another invariant point will occur in the f_{O_2} - T diagram and out of this will come a reaction between hastingsite and potassium feldspar.

$$NaCa_2Fe^{+2}_4Fe^{+3}Si_6Al_2O_{22}(OH)_2 + KAlSi_3O_8 \rightarrow KFe^{+2}_3AlSi_3O_{10}(OH)_2 +$$

$$2(Na_{0.5},Ca_{0.5})(Fe^{+3}_{0.5},Fe^{+2}_{0.5})Si_2O_6 + CaSl_2Si_2O_8$$

Hastingsite + Sanidine → Annite + Aegerine-Augite + Anorthite

This reaction is independent of both oxygen fugacity and water fugacity and is only dependent on total pressure. If the stability field of hastingsite does not cross the boundary of the annite field, then the assemblage hastingsite plus sanidine will never be stable.

If we consider the equilibrium constant K for this last reaction we have:

$$K = \frac{(a_{Ann})(a_{Ae.A})^2(a_{An})}{(a_{Ha})(a_{Sa})}$$

Or, rewriting the pyroxene in terms of hedenbergite and aegerine we would have

$$K = \frac{(a_{Ann})(a_{He})(a_{Ae})(a_{An})}{(a_{Ha})(a_{Sa})}$$

It can now be seen that the activity of sanidine in the alkali feldspar is a critical factor in the stability of hastingsite in a granitic rock. It is significant that in most alkalic rocks containing a hastingsitic amphibole the dominant feldspar is often a perthite, in which the activity of sanidine was lowered due to dilution and changes in structural state.

If K for this reaction could be estimated from the assemblage in the rock, and if reasonable thermodynamic properties of volume and entropy where known for these materials, then a relationship between temperature and pressure could be derived from the relationships:

$$\ln(K) = -\frac{\Delta\overline{G}}{RT}$$

$$\Delta\overline{G} = P\Delta\overline{V} - T\Delta\overline{S}$$

$$P_{Tot} = -\frac{RT}{\Delta\overline{V}}\ln(K) + T\frac{\Delta\overline{S}}{\Delta\overline{V}}$$

If this is done, using thermodynamic data for tremolite and diopside in the absence of other data, and attempting to maximize K so as to minimize P, pressures in the neighborhood

of 25 kilobars are obtained. Due to the extreme extrapolation involved in the thermodynamic data, and because values for tremolite and diopside must be used for the amphibole and pyroxene properties, this can only be interpreted as not being opposed to a high pressure for the origin of this assemblage.

For future work, this type of reaction, along with the earlier reaction between hastingsite and quartz might be very powerful tools in determining the conditions of P_{Tot} and f_{H_2O} for the formation of alkalic rock series. It is also clear that the activity of potassium feldspar in a crystallizing magma may be of critical importance as to whether an amphibole or a biotite is formed.

MOUNT AIRY; EXPERIMENTAL RESULTS

PETROGRAPHIC DESCRIPTION

The Mount Airy 'granite' is actually best described as a peraluminous leucogranodiorite. It is best exposed in a quarry of the North Carolina Granite Corporation near Mount Airy, North Carolina. The petrology and occurrence are well described by Dietrich (1961), and were briefly mentioned by Watson (1910). The rock is foliated to nonfoliated, hypidiomorphic, medium-grained, with white feldspars, slightly smokey quartz, biotite and accesories. Plagioclase composes over half of the rock and is both progressively and oscillatorally zoned from An_{20} to An_{12}. The great bulk of the plagioclase is around An_{15}, although cores up to An_{24}, and rims, especially near microcline, may be as low as An_5. Good crosshatched microcline composes about 20% of the rock and quartz another 20% with some perthite and myrmekite. The microcline is often poikilitic including plagioclase, some quartz and mafic accessory minerals. The quartz often occurs in irregular blebs of coarse crystals. The biotite is greenish black and composes about 2% of the rock. Accessory minerals include green epidote, orange-brown monazite, and muscovite, all of which are often closely associated with biotite. There are very few opaques although there appears to be a little magnetite. The muscovite often occurs as idiomorphic crystals sometimes intergrown with biotite, and occasionally bent about

contacts with other minerals. The epidote is classified by Dietrich as being pistacite with about 12 to 25% of the iron end member. Optical properties of the sample used in this study agree with this identification (Table 14). The epidote is commonly idiomorphic often being inclosed within biotite with sharp crystal faces and angles. Much of this euhedral epidote gives every appearance of being a primary phase. The biotite and other accessory minerals often form small clots of mafic material. Excellent serrate borders are observed where quartz grains cut across twin planes in the plagioclase. For a more thorough description of textures and relationships, the reader is referred to Dietrich.

In this study, modal analyses were done on both thin sections and powder of the material used. These are listed in Table 2 along with the analyses of Dietrich. Several chemical analyses were presented by Dietrich, but unfortunately these are of unknown value due to lack of information as to analytic technique. Table 1 lists these analyses along with the analyses calculated from the modal analyses of Dietrich and those done in connection with the present study. The specific gravity calculated from the chemical analyses (average 2.68) do not correlate with the average density reported by Dietrich of 2.648 ± .001. For the present study the chemical composition was determined from the modal analyses on the powdered sample using An_{15} for an average composition of the plagioclase (Table 3). One of

TABLE 14.

OPTICAL PROPERTIES OF EPIDOTE FROM

MOUNT AIRY

Direction	n	Color	Orientation
X	1.726±.004	Pale Green to Yellowish	$X \wedge c = 40 \pm 1^{\circ}$
Y	1.746±.004	Green	= b
Z	1.762±.004	Yellowish Green	$Z \wedge a = 29 \pm 1^{\circ}$

Optically negative with large 2V of aroung $70\text{-}80^{\circ}$.

the thin sections used in the analyses appear to have an anomalously high quartz content and this accounts for most of the difference between the powder and thin section analyses.

MELTING RELATIONSHIPS

The experimental runs and their results are listed in Table 15.

Melting in the Mount Airy started at somewhat lower temperature than the Westerly. Small amounts of glass were present in all runs at 700°C, but much less glass was found than was seen in the Cape Ann. The glass was usually clear with little coloration. The refractive index was always between 1.486 and 1.490 and was fairly constant. Between 720 and 740°C the saturated Mount Airy composition passed out of the assemblage Q-Or-Pl-L-V into the Pl-Q-L-V field. By 780°C all but the 1 and 2% water runs had passed out of the Q-Pl-Or-L field into the Pl-Q-L or Pl-Q-L-V fields. At 780°C the orthoclase in the 2% run was also becoming scarce. By 800°C the saturated run has passed into the L-V field while all the runs except the 1% run has lost all orthoclase.

Again the two feldspars persisted to high temperatures within those runs that were in the appropriate composition fields, and no trace of an intermediate composition was seen.

The Mount Airy did not pass into the liquid-vapor field until about 800°C, some 30 to 40°C higher than predicted by Tuttle and Bowen (1958). This is probably caused by the anorthite component in the plagioclase.

TABLE 15.

RESULTS OF EXPERIMENTS ON MOUNT AIRY

Run No.	Wt.% H_2O	Temp.(°C)	Time(hrs)	Vol.% Glass	R.I. Glass	Phases Observed
MA 101	9.21	650	1533	----	-----	Pl,Or,Q,Bi,H,Mg,Zi,V,Mu?,Ep?
Ma 31	0.99	680	725	----	-----	Pl,Or,Q,Bi,H,Mg,V,Mu?,Ep?
Ma 32	2.96	680	725	----	-----	Pl,Or,Q,Bi,H,Mg,V,Mu?
MA 33	5.02	680	725	----	-----	Pl,Or,Q,Bi,H,Mg,Zi,V,Mu?
MAR 34-1	10.23	680	893	----	-----	Pl,Or,Q,Bi,Mg,Zi,V,Mu?
MA 1	0.81	700	766	2-5	-----	Pl,Or,Q,Bi,Mg,L,V,Mu?
MA 2	1.76	700	766	10	1.489	Pl,Or,Q,Bi,Mg,L,V,Mu?,Ep?
MA 3	3.24	700	766	20	1.488	Pl,Or,Q,Bi,Mg,L,V,Mu?
MA 4	5.02	700	766	29	1.488	Pl,Or,Q,Bi,Mg,L,V,Mu?
MA 5	9.37	700	766	38	1.488	Pl,Or,Q,Bi,Mg,L,V
MA 6	0.99	720	809	12	1.490	Pl,Or,Q,Bi,Mg,L,V,Mu?
MAR 7-2	1.97	720	725	22	1.488	Pl,Or,Q,Bi,Mg,L,V,Ep?
MA 8	3.04	720	809	36	1.487	Pl,Or,Q,Bi,Mg,L,V
MA 9	4.96	720	809	64	1.487	Pl,Or,Q,Bi,Mg,L,V
MA 10	9.84	720	809	70	1.486	Pl,Q,Bi,Mg,L,V,Or?,Ep?

TABLE 15. (Cont.)

Run No.	Wt.% H_2O	Temp.(°C)	Time(hrs)	Vol.% Glass	R.I. Glass	Phases Observed
MAR 11-1	0.94	740	725	17	1.490	Pl,Or,Q,Bi,Mg,L,Ep?
MA 12	1.97	740	742	32	1.490	Pl,Or,Q,Bi,Mg,L
MA 13	2.98	740	742	48	1.489	Pl,Or,Q,Bi,Mg,L,Ep?
MA 14	4.94	740	742	62	1.487	Pl,Q,Bi,Mg,L,V,Or?
MA 15	9.74	740	742	78	1.488	Pl,Q,Bi,Mg,Zi,L,V
MA 35	1.00	760	893	20	1.487	Pl,Or,Q,Bi,Mg,L
MA 36	2.01	760	893	49	1.487	Pl,Or,Q,Bi,Mg,L
MA 37	2.99	760	893	65	1.487	Pl,Q,Bi,Mg,L,Ep?
MA 38	4.99	760	893	76	1.487	Pl,Q,Bi,Mg,L,V
MA 39	9.89	760	893	84	1.487	Pl,Q,Bi,Mg,L,V
MA 21	0.98	780	771	23	1.489	Pl,Or,Q,Bi,Mg,L
MA 22	1.99	780	771	50	1.487	Pl,Q,Bi,Mg,L,Or?,Ep?
MA 23	2.99	780	771	67	1.487	Pl,Q,Bi,Mg,L,(Or)
MA 24	4.94	780	771	83	1.487	Pl,Q,Bi,Mg,L
MA 25	9.51	780	771	90	1.487	Pl,Q,Bi,Mg,L,V
MA 26	0.99	800	756	27	1.487	Pl,Or,Q,Bi,Mg,L

TABLE 15. (Cont.)

Run No.	Wt.% H_2O	Temp. (°C)	Time (hrs)	Vol.% Glass	R.I. Glass	Phases Observed
MA 27	1.99	800	756	55	1.487	Pl,Q,Bi,Mg,L,Ep?
MA 28	3.00	800	756	73	1.487	Pl,Q,Bi,Mg,L,Ep?
MA 29	4.96	800	756	89	1.487	Pl,Bi,Mg,L,Ep?
MA 30	9.97	800	756	95	1.488	Bi,Mg,L,V,(Pl)

ACCESSORY MINERALS

Biotites

The biotite continued to be present up through 800°C. No significant change in the optical properties were seen in the finer grained biotites up through this temperature. Again some oxybiotite was seen to occur in some runs, but was much less conspicuous than in the Westerly. This lack of variation with temperature is in good agreement with the data of Wones and Eugster for oxygen fugacities lying between the hematite-magnetite and Ni-NiO buffer curves. Since the content of titanium and its effect on refractive index, nor the effective annite component can be determined to any degree of accuracy, an argument similiar to the previous one used for Westerly to estimate f_{H_2O} for the formation of the granite cannot be made. Also the scarcity of magnetite in the rock makes it possible that the biotite was not in equilibrium with magnetite at the time of its formation.

Muscovite

Muscovite was again observed up to temperatures above 700°C. In the Mount Airy though it appeared to react much faster than in the Westerly and it was more scarce in all runs. It may be that a reaction between it and epidote might be important in this disappearance. The following reaction may be written for idealized end members.

$$KAl_2AlSi_3O_{10}(OH)_2 + Ca_2Al_2Fe^{+3}Si_3O_{12}(OH)_2 \rightarrow 2CaAl_2Si_2O_8 + KAlSi_3O_8 + 1/3Fe_3O_4 + 2H_2O + 1/3O_2$$

Muscovite + Epidote → 2Anorthite + Kspar + 1/3Hematite + 2 water + 1/3 oxygen

For more aluminous epidote an aluminosilicate might be formed. Again no small flakes of muscovite were seen at temperatures above 650°C and it is believed that its persistence to temperatures above the stability of quartz and muscovite determined by work such as that of Evans is metastable persistence.

If part of the muscovite in the Mount Airy is primary, which it gives every appearance of being, then the water pressure must have been greater than two kilobars during its crystallization. From the data of Evans, it would appear that it would probably have had to have been at least three kilobars or perhaps greater for muscovite and quartz to be stable at melting temperatures.

Epidote

The epidote appears to be unstable at all temperatures observed in this study. In a number of runs dark mafic clots with cores of epidote were seen. This reaction rim was fine grained and mostly opaque. At least part of it was probable magnetite. Also present was a material of moderate relief that may have been an anorthite rich plagioclase. A number of mafic aggregates resembling these reaction rims, but with no epidote left in the center were also seen. This suggests

that most of the epidote was completely reacted. Whether this means that the epidote is outside of its stability field or just reacting with some other phase cannot be determined, but it does not appear to be stable at the solidus at two kilobars P_{H_2O} and an oxygen fugacity somewhere between the hematite-magnetite and quartz-magnetite-fayalite buffers.

Merrin (1960) determined a point on the epidote stability curve at 650±10°C and 4 kilobars P_{H_2O}. This curve is said to have a positive slope of 17.8±2.8 bars/°C. Fyfe (1960) has also synthesized epidote minerals by seeding at two kilobars at temperatures between 505 and 630°C. He further states that the epidote minerals are probably stable to about 650°C at two kilobars, but by 700°C the stable phases would be anorthite, garnet, and magnetite.

$$Ca_2Al_2Fe^{+3}Si_3O_{12}(OH)_2 \rightarrow \tfrac{1}{2}Ca_3Al_2Si_3O_{12} + \tfrac{1}{2}CaAl_2Si_2O_8 + 1/3Fe_3O_4 + \tfrac{1}{2}SiO_2 + H_2O + 1/3O_2$$

Newton (1966) gives the reaction

$$Zo + Q \rightarrow An + Gr + V:$$

as occurring at 500°C at 2 kb and about 650°C at 5.5 kb.

Holdaway (1966) studied the stability of clinozoisite plus quartz between two and four kilobars using a rate technique similar to that used by Evans (1965). Holdaway gives the reaction;

$$Cz + Q \rightarrow Ep + An + Gr$$

as occurring at 600°C at 2 kb and 660°C at 4 kb. The final stability of epidote and quartz is located at a minimum of 650°C at 2 kb and 700°C at 4 kb. This reaction is:

$$Ep + Q \rightarrow An + Gr \pm H_2O$$

This is in good agreement with the experimental results seen here. There could easily be fine grained garnet in the reaction rims along with anorthite and magnetite. Clearly, from what scanty data as is available on the epidotes it can only be said that if the epidote seen in the Mount Airy is primary, then crystallization must have taken place at water pressures above about 4 kilobars. Consideration of possible reactions between epidote and other minerals might raise this estimate even higher.

FELDSPAR RELATIONSHIPS

COMPOSITION OF COEXISTING FELDSPARS

In most runs on all three granitic rocks, two feldspars were observed to exist at the end of the run. The potassium feldspar component was determined from the $\bar{2}01$ reflection by two methods simultaneously; 1) The distance between the $\bar{2}01$ of the feldspar and the $10\bar{1}0$ of quartz was measured and compared with the data of Tuttle and Bowen (1958). 2) The value of 2θ was measured using spinel (a=8.0833Å) as an internal standard and compared against the data of Orville (1967) as presented by Wright (1968). These compositions have been tabulated (Tables 16-18) and the second series have been plotted versus temperature for each of the rocks (Figures 6-8).

A number of solvi for the feldspar polymorphs have been presented by Tuttle and Bowen (1958), Orville (1963), Luth and Tuttle (1966), and Bachinski and Orville (1968). Among the factors affecting the solvus are; 1) structural state of the feldspar, 2) calcium content, and 3) non-stoichiometry of alkalies and aluminum in the crystallization environment. The solvi for the feldspars in this study all fall well above solvi for the disordered feldspars (Tuttle and Bowen, 1958; Luth and Tuttle, 1966; Orville, 1963), even that for the Cape Ann where there is very little calcium to affect the

TABLE 16.

$\bar{2}01$ REFLECTIONS AND OR CONTENT

OF FELDSPARS FROM EXPERIMENTS ON WESTERLY

Run No.	Temp. (°C)	Wt.% H_2O	2θ, $\bar{2}01$ (K-spar)	Wt.%Or_1	Wt.%Or_2	2θ, $\bar{2}01$ (Na-spar)	Wt.%Or_1	Wt.%Or_2
W 0	---	---	----	--	---	22.02	0	0
W 101	650	10	21.10	82	80.5	22.00	0	1
W 102	650	10	21.07	84	83.5	21.97	3	5
W 54	680	1	21.04	90	86	21.97	3	5
W 55	680	3	21.10	82	80.5	21.94	3	8
W 56	680	5	21.12	80	78	21.96	6	6
W 57	680	10	21.13	79	77	21.97	4	5
WR 19-1	700	1	21.13	80	77	21.97	3	5
W 20	700	2	21.12	81	78	21.97	3	5
W 21	700	3	21.14	77	76	21.96	3	6
W 22	700	5	21.15	76	75.5	21.99	4	2
W 23	700	10	21.15	76	75.5	21.97	3	5
W 24	720	1	21.17	75	73.5	21.99	0	2
W 25	720	2	21.15	76	75.5	21.97	3	5
W 26	720	3	21.15	76	75.5	21.96	4	6

TABLE 16.. (Cont.)

Run No.	Temp. (°C)	Wt.% H_2O	$2\theta,\bar{2}01$ (K-spar)	Wt.%Or_1	Wt.%Or_2	$2\theta,\bar{2}01$ (Na-spar)	Wt.%Or_1	Wt.%Or_2
WR 27-1	720	5	----	---	---	21.95	5	7
W 28	720	10	21.14	77	76	21.98	2	4
W 49	740	1	21.15	76	75.5	21.94	6	8
W 50	740	2	21.16	75	74.5	21.97	3	5
W 51	740	3	21.15	76	75.5	21.99	0	2
W 52	740	5	21.12	81	78	21.93	6	8
W 53	740	1o	21.11	82	79.5	21.94	6	8
W 34	760	1	21.18	71	72.5	21.94	6	8
W 35	760	2	21.20	71	70	21.94	6	8
W 36	760	3	21.19	72	72	21.97	3	5
WR 37-2	760	5	-----	---	---	-----	--	--
W 38	760	10	-----	---	---	-----	--	--
WR 39-1	780	1	21.23	68	68	21.93	7	8
W 40	780	2	21.19	72	72	21.94	6	8
W 41	780	3	21.16	75	74.5	21.91	8	10
W 42	780	5	-----	---	---	-----	--	--

TABLE 16. (Cont.)

Run No.	Temp. (°C)	Wt.% H_2O	2θ,$\bar{2}$01 (K-spar)	Wt.%Or_1	Wt.%Or_2	2θ,$\bar{2}$01 (Na-spar)	Wt.%Or_1	Wt.%Or_2
W 43	780	10	-----	---	---	-----	--	--
W 44	800	1	21.20	71	71.5	21.90	10	11
W 45	800	2	21.22	70	69	21.93	7	8
W 46	800	3	21.23	68	68	21.95	4	7
W 47	800	5	-----	---	---	-----	--	--
WR 48-1	800	10	-----	---	---	-----	--	--

All 2θ values for $\bar{2}$01 reflections were measured using $Cu_{k_{\alpha 1}}$ radiation with spinel as an internal standard as described in the text.

1. All compositions in the columns labeled with a one were determined measuring the angle between the $\bar{2}$01 of feldspar and $10\bar{1}0$ of quartz and comparing with the data of Tuttle and Bowen, 1958.
2. All compositions in the columns labeled with a two were determined by comparing their 2θ values with the data of Orville, 1967, as presented by Wright, 1968.

TABLE 17.

$\bar{2}01$ REFLECTIONS AND OR CONTENT

OF FELDSPARS FROM EXPERIMENTS ON CAPE ANN

Run No.	Temp. (°C)	Wt.% H_2O	$2\theta, \bar{2}01$ (Kspar)	Wt.% Or_1	Wt.% Or_2	$2\theta, \bar{2}01$ (Na-spar)	Wt.% Or_1	Wt.% Or_2
Q 0	---	--	-----	-----	---	22.04	0	0
Q 101	650	10	21.21	70	70	22.02	0	4
Q 102	650	10	21.20	71	71.5	22.03	0	3
Q 31	680	1	21.18	74	72.4	22.03	0	3
Q 32	680	3	21.21	70	70	22.02	0	4
Q 33	680	5	21.20	71	71	22.01	0	5.5
Q 34	680	10	21.19	73	72	22.03	0	3
QR 1-1	700	1	21.23	69	68	21.99	0	6.5
Q 2	700	2	21.23	69	68	21.99	0	7
Q 3	700	3	21.24	68	66.5	22.02	0	4
Q 4	700	5	21.28	64	62.5	21.96	3	9
Q 5	700	10	21.27	65	64	22.00	0	6.5
Q 6	720	1	21.30	62	61	21.99	0	7
Q 7	720	2	21.33	59	59.5	21.95	4	10

TABLE 17. (Cont.)

Run No.	Temp. (°C)	Wt.% H_2O	$2\theta, \bar{2}01$ (K-spar)	Wt.% Or_1	Wt.% Or_2	$2\theta, \bar{2}01$ (Na-spar)	Wt.% Or_1	Wt.% Or_2
Q 8	720	3	21.35	58	58	21.95	4	10
Q 9	720	5	21.38	56	56	21.93	5	12
Q 10	720	10	21.40	53	53.5	-----	--	--
Q 11	740	1	21.38	56	56	21.98	1	8
QR 12-1	740	2	21.27	65	63	-----	--	--
Q 13	740	3	-----	--	--	-----	--	--
Q 14	740	5	-----	--	--	-----	--	--
QR 15-1	740	10	-----	--	--	-----	--	--
QR 16-1	760	1	21.39	54	55.5	21.99	0	7
Q 17	760	2	21.41	52	53	21.98	1	8
Q 18	760	3	21.39	57	55.5	21.99	0	7
Q 19	760	5	-----	--	--	-----	--	--
Q 20	760	10	-----	--	--	-----	--	--
Q 21	780	1	21.41	52	53	21.93	5	12
Q 22	780	2	21.35	57	58	21.98	1	8
Q 23	780	3	-----	--	--	-----	--	--

TABLE 17. (Cont.)

Run No.	Temp. (°C)	Wt.% H_2O	2θ, $\bar{2}01$ (K-spar)	Wt.%Or_1	Wt.%Or_2	2θ, $\bar{2}01$ (Na-Spar)	Wt.%Or_1	Wt.%Or_2
Q 24	780	5	-----	--	--	-----	--	--
QR 25-1	780	10	-----	--	--	-----	--	--
Q 26	800	1	21.42	52	52	21.89	9	15
Q 27	800	2	21.49	46	46	21.89	10	15
Q 28	800	3	-----	--	--	-----	--	--
Q 29	800	5	-----	--	--	-----	--	--
Q 30	800	10	-----	--	--	-----	--	--

All 2θ values for $\bar{2}01$ reflections were measured using $Cu_{k_{\alpha 1}}$ radiation with spinel as an internal standard as described in the text.

1. All compositions in the columns labeled with a one were determined by measuring the angle between the $\bar{2}01$ of feldspar and the $10\bar{1}0$ of quartz and comparing with the data of Tuttle and Bowen, 1958.
2. All compositions in the columns labeled with a two were determined by comparing their 2θ values with the data of Orville, 1967, as presented by Wright, 1968.

TABLE 18.

$\bar{2}01$ REFLECTIONS AND OR CONTENT

OF FELDSPARS FROM EXPERIMENTS ON MOUNT AIRY

Run No.	Temp. (°C)	Wt.% H_2O	$2\theta,\bar{2}01$ (K-spar)	Wt.% Or_1	Wt.% Or_2	$2\theta,\bar{2}01$ (Na-spar)	Wt.% Or_1	Wt.% Or_2
MA 0	---	--	-----	--	--	22.01	0	1
MA 101	650	10	21.10	84	80.5	21.99	0	2
MA 31	680	1	21.14	78	76	21.98	1	4
MA 32	680	3	21.11	80	79.5	21.98	1	4
MA 33	680	5	21.13	79	77	21.97	3	5
MAR 34-1	680	10	-----	--	--	-----	--	--
MA 1	700	1	21.22	70	69	21.95	5	7
MA 2	700	2	21.23	69	68	21.96	4	6
MA 3	700	3	21.22	70	69	21.98	1	4
MA 4	700	5	21.23	68	68	21.96	4	6
MA 5	700	10	21.19	72	72	21.93	6	8
MA 6	720	1	21.24	69	66.5	21.96	4	6
MAR 7-2	720	2	21.76	76	74.5	21.96	4	6
MA 8	720	3	-----	--	--	21.95	5	7
MA 9	720	5	21.15	76	75.5	21.95	5	7

TABLE 18. (Cont.)

Run No.	Temp. (°C)	Wt.% H_2O	20,$\bar{2}$01 (K-spar)	Wt.%Or_1	Wt.%Or_2	20,$\bar{2}$01 (Na-spar)	Wt.%Or_1	Wt.%Or_2
MA 10	720	10	-----	--	--	21.96	4	6
MAR 11-1	740	1	21.20	75	71.5	21.95	5	7
MA 12	740	2	21.17	74	73.5	21.94	6	8
MA 13	740	3	21.24	69	66.5	21.90	9	10
MA 14	740	5	-----	--	--	21.92	8	9
MA 15	740	10	-----	--	--	21.92	8	9
MA 35	760	1	-----	--	--	21.96	--	6
MA 36	760	2	-----	--	--	21.95	--	7
MA 37	760	3	-----	--	--	21.96	--	6
MA 38	760	5	-----	--	--	21.93	--	8
MA 39	760	10	-----	--	--	21.92	--	9
MA 21	780	1	21.24	69	66.5	21.96	4	6
MA 22	780	2	-----	--	--	21.93	7	8
MA 23	780	3	21.19	72	72	21.95	0	7
MA 24	780	5	-----	--	--	21.90	9	11
MA 25	780	10	-----	--	--	21.95	5	7

TABLE 18. (Cont.)

Run No.	Temp. (°C)	Wt.% H_2O	2θ, $\bar{2}01$ (K-spar)	Wt.%Or_1	Wt.%Or_2	2θ, $\bar{2}01$ (Na-spar)	Wt.%Or_1	Wt.%Or_2
MA 26	800	1	-----	--	--	21.92	8	9
MA 27	800	2	-----	--	--	21.92	8	9
MA 28	800	3	-----	--	--	21.92	8	9
MA 29	800	5	-----	--	--	21.93	6	8
MA 30	800	10	-----	--	--	21.90	9	11

All 2θ values for $\bar{2}01$ reflections were measured using $Cu_{k_{\alpha 1}}$ radiation with spinel as an an internal standard as described in the text.

1. All compositions in the columns labeled with a one were determined by measuring the angle between the $\bar{2}01$ of feldspar and the $10\bar{1}0$ of quartz and comparing with the data of Tuttle and Bowen, 1958.
2. All compositions in the columns labeled with a two were determined by comparing thier 2θ values with the data of Orville, 1967, as presented by Wright, 1968.

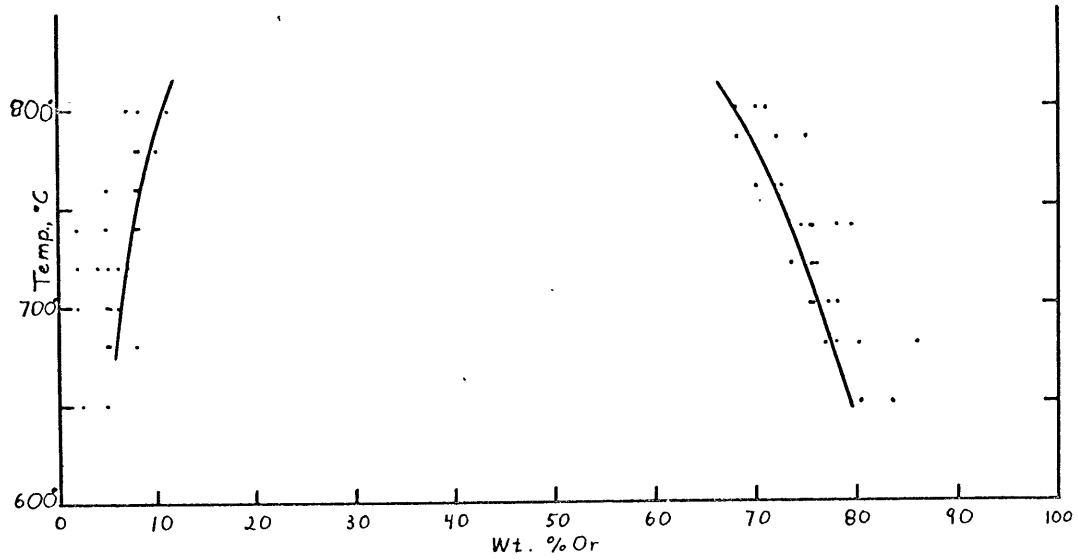

Figure 6. Or. Content of Feldspars in Experiments on Westerly.

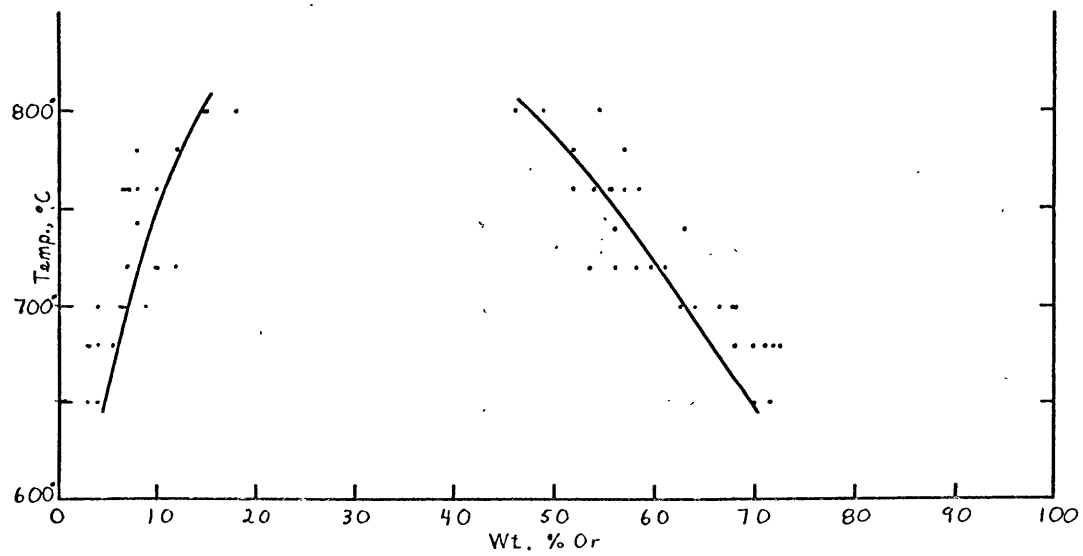

Figure 7. Or. Content of Feldspars in Experiments on Cape Ann.

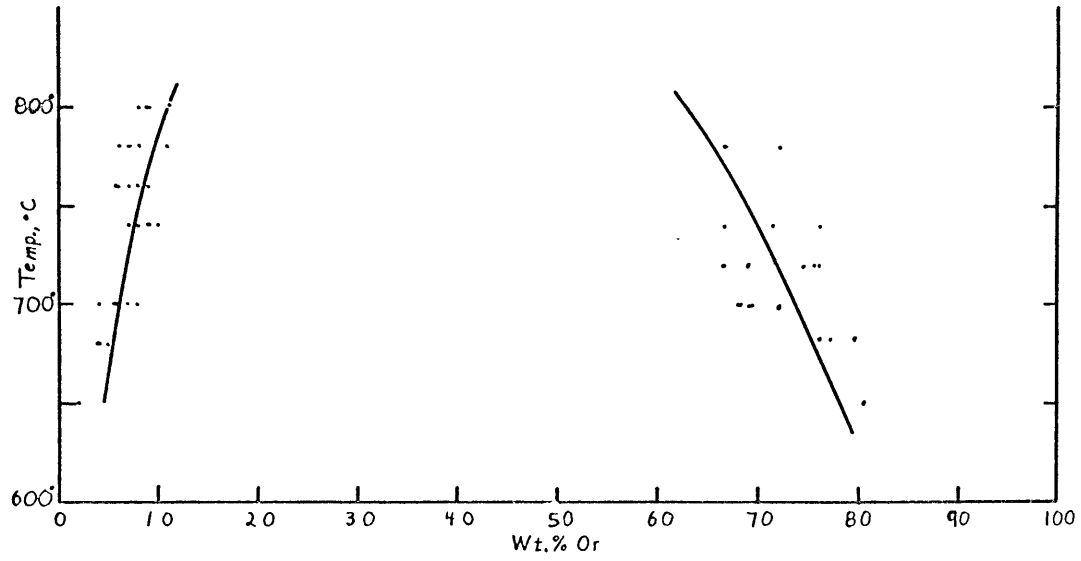

Figure 8. Or. Content of Feldspars in Experiments on Mount Airy.

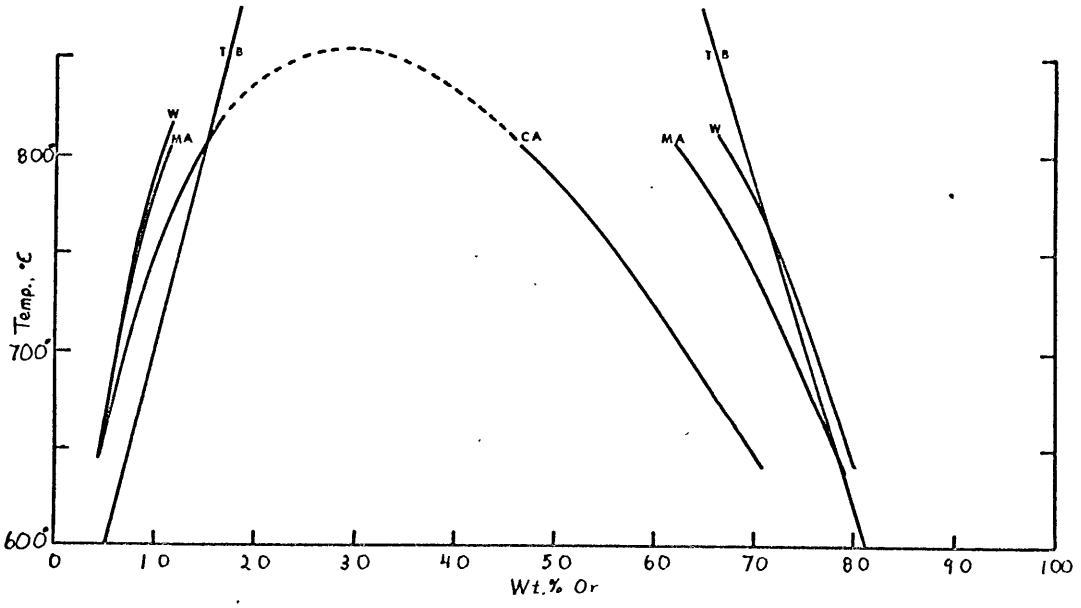

Figure 9. Solvi for various Low Temperature Feldspars.

W Westerly Granite
CA Cape Ann Granite
MA Mount Airy leucogranodiorite
TB Orthoclase cryptoperthite solvus of Tuttle and Bowen, 1958.

For comparison, the top of the microcline-low albite solvus of Bachinski and Orville, 1968, at one atmosphere is at Or_{30}, and 850°C.

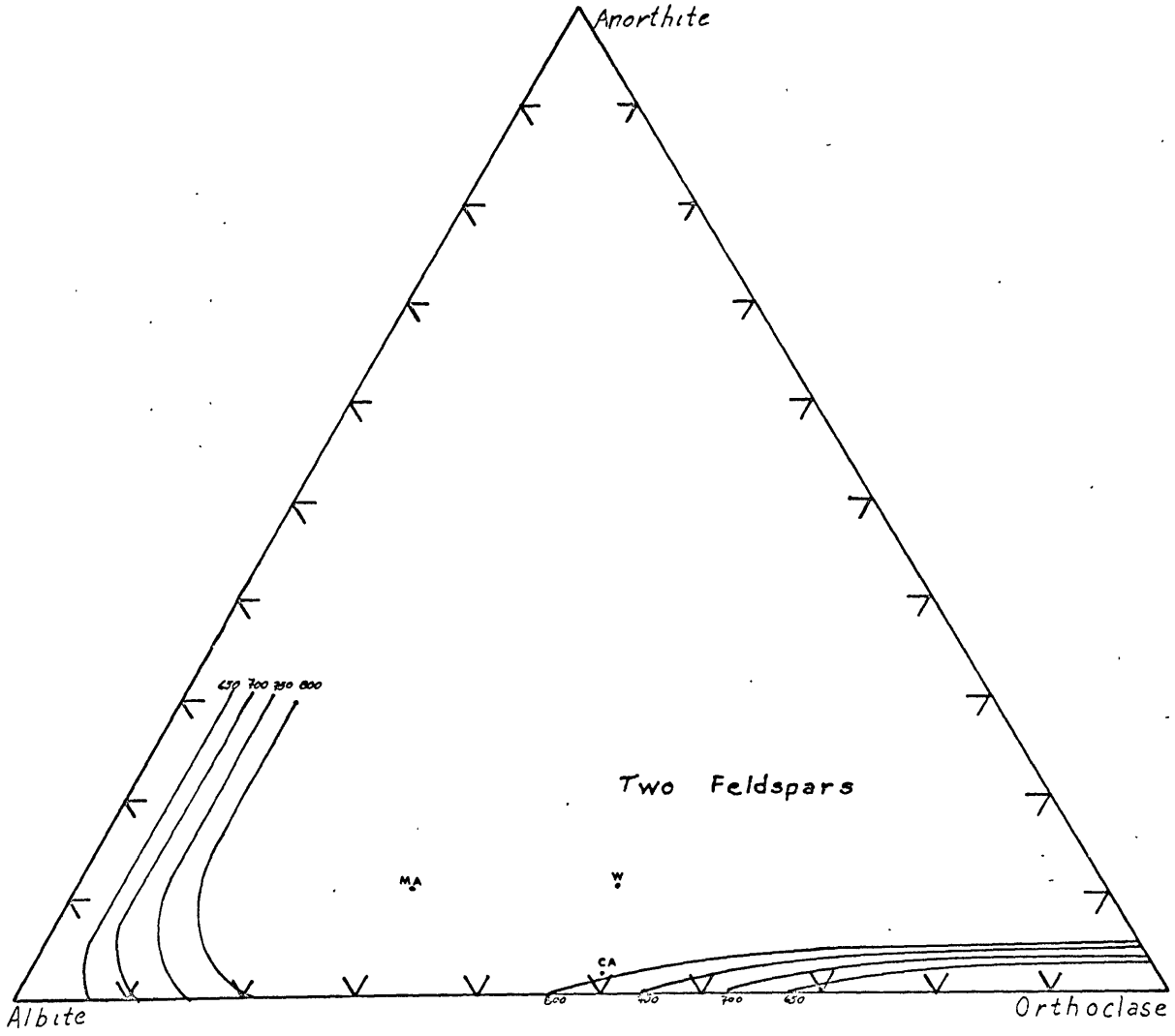
Anorthite
Albite
Orthoclase
Two Feldspars
450 700 750 800
MA
W
CA
600
750
700
650

solvus. If the Cape Ann solvus as drawn is extrapolated graphically, the maximum is in the neighborhood of 850°C or a little higher, and 30% Or. This is in good agreement with the one atmosphere maximum for the metastable microcline-low albite solvus determined by Bachinski and Orville (1968) (Figure 9). The compositions for the Mount Airy and Westerly fall progressively further outside, probably being indicative of the increasing affect of calcium content. When compared with the solvus for orthoclase cryptoperthite given by Tuttle and Bowen (1958) these compositions tend to fall within their solvus. From these three series, a semi-schematic ternary solvus may be drawn for these feldspars (Figure 10).

STRUCTURAL STATE OF THE FELDSPARS

It was not possible to determine cell dimensions for the feldspars from these experiments due to the poor quality of the X-ray patterns of altered material and the interference of other crystalline phases. Therefore, the three peak analysis of Wright (1968) was used to obtain semi-quantitative knowledge of the structural state of the feldspars. All scans were made at $\frac{1}{2}°2\theta$ per minute using spinel as an internal standard, and the 060 and $\bar{2}04$ reflections plotted as in Figure 10. The position on this plot may be cross checked with the $\bar{2}01$ reflection using Figure 3 of Wright (1968), and those that are not consistant with these three reflections are termed 'anomalous' by Wright. It is not known if the

TABLE 19.

SELECTED REFLECTIONS OF FELDSPARS FROM VARIOUS EXPERIMENTS

Run No.	Temp. (°C)	Wt% H_2O	$2\theta^*_{hkl}$ Potassium Rich Feld.			$2\theta^*_{hkl}$ Sodium Rich Feld.		
			$\bar{2}04$	060	$\bar{2}01$	$\bar{2}04$	060	$\bar{2}01$
Q	---	---	50.565	41.815	-----	51.115	42.490	22.04
QB 1	650	10	50.570	41.835	21.20	51.120	42.440	22.03
			50.875	41.625				
QB 3	650	10	50.607	41.860	21.21	51.090	42.452	22.01
			50.875	41.625				
Q 31	680	1	50.590	41.830	21.18	51.110	42.480	22.03
Q 34	680	10	50.546	41.870	21.19	51.068	42.417	22.03
QP 1	760	1	50.663	41.755	21.39	51.025	42.428	22.00
QP 3	760	3	50.63	41.740	21.39	51.070	42.390	21.95
Q 26	800	1	50.608	41.672	21.42	51.108	42.461	21.89
			50,948	41.792				
MA 0	---	--	50.624	41.786	-----	51.245	42.437	22.01
MA 31	680	1	50.722	41.769	21.14	51.295	42.439	21.98
MAR 34-1	680	10	50.768	41.752	21.13	51.389	42.445	21.97
MA 37	760	3	50.688	41.536	-----	51.379	42.403	-----

TABLE 19. (Cont.)

Run No.	Temp. (°C)	Wt% H_2O	$2\theta^*_{hkl}$ Potassium Rich Feld.			$2\theta^*_{hkl}$ Sodium Rich Feld.		
			$\bar{2}04$	060	$\bar{2}01$	$\bar{2}04$	060	$\bar{2}01$
W O	---	--	50.687	41.758	20.998	51.317	42.468	22.038
W 46	800	3	50.608	41.682	21.230	51.50	42.57	21.950
			50.888	41.532				

* All 2θ measured using $Cu_{K_{\alpha 1}}$ radiation with spinel as an internal standard. Numbers W O, Q O, and MA O refer to the starting materials.

anomalous nature affects the determination of structural state.

Figures 12 a-d show the results for the Cape Ann at 650°, 680°, 760°, and 800°C. At 650°C most of the feldspar is in the microcline-low albite state, but there is a weak set of peaks corresponding to sanidine. The source of this is not certain, but it might be due to melting along some grain boundaries and immediate recrystallization in the high form (See Goldsmith and Laves, 1964a). In any case, by 680°C there is no trace of the sanidine and only the microcline and low albite are seen, the microcline having become somewhat richer in albite. By 760°C, the potassium feldspar peaks have become very broad and poorly defined. It was not clear whether a feldspar intermediate between microcline and orthoclase was forming, or whether a mixture of the two was present, but no trace of sanidine was seen. At 800°C, more sanidine appears to have formed at the expense of the microcline. Throughout, albite remained as low albite.

The original Mount Airy feldspars plotted between the microcline and orthoclase series, and both appeared to be somewhat 'anomalous' according to Wright's criteria. Upon heating they moved toward the orthoclase series but the plagioclase became increasingly anomalous (Figures 13 a-b).

The Westerly also appeared somewhat anomalous. The original potassium feldspar was intermediate between microcline and orthoclase, but upon heating moved toward orthoclase. At 800°C, (Figure 14) two potassium feldspars were present,

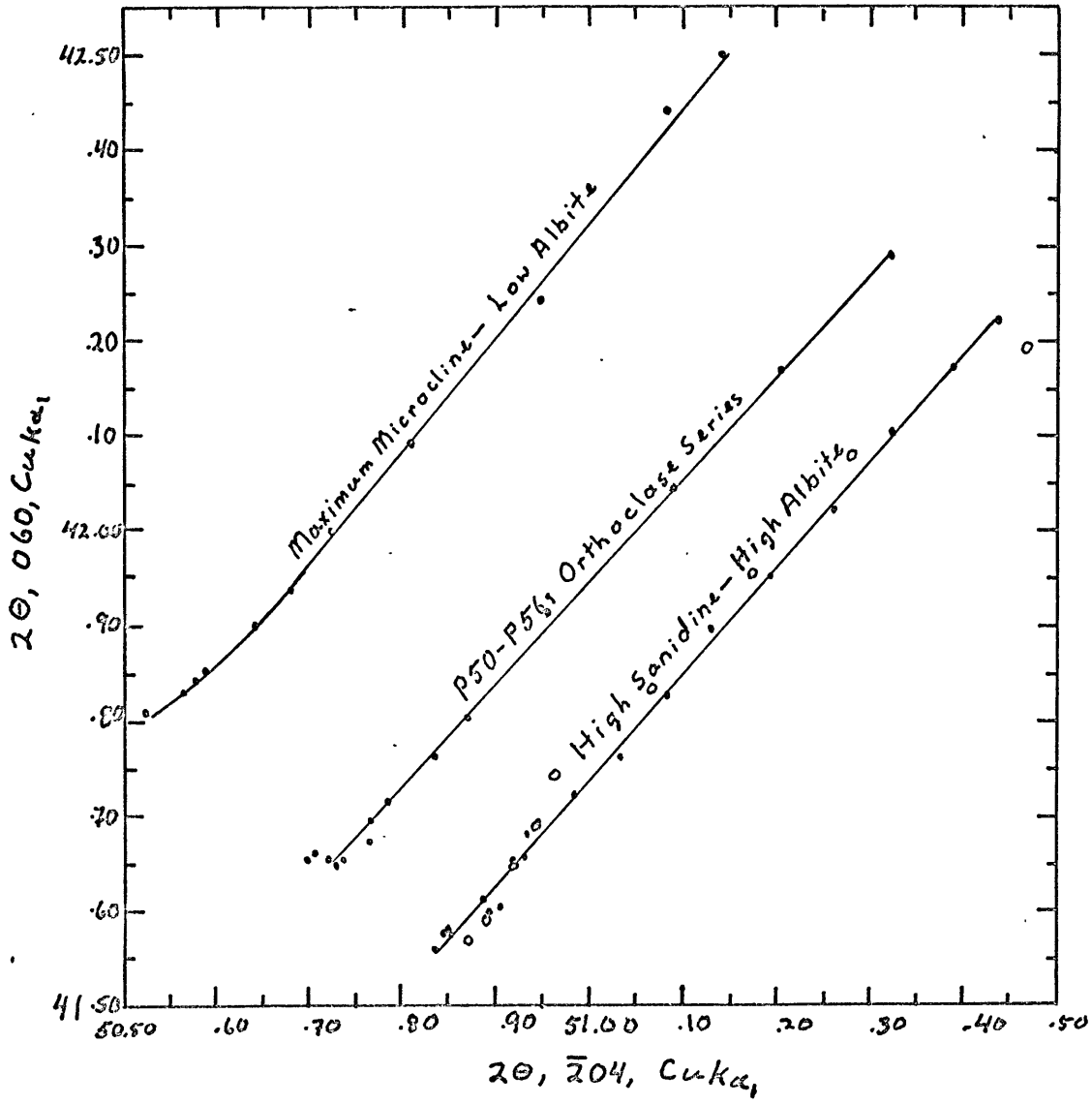

Figure 11. 060 vs. $\bar{2}$04 Diagram from Synthetic Feldspars.

After Wright, 1968. All values using $Cu_{k\alpha 1}$ radiation.

Maximum Microcline-Low Albite	Orville, 1967
P50-P56, Orthoclase Sieres, High Sanidine-High Albite	Wright and Stewart, 1968
(Closed dots)	Orville, 1967
(Open Circles)	Donnay and Donnay, 1952

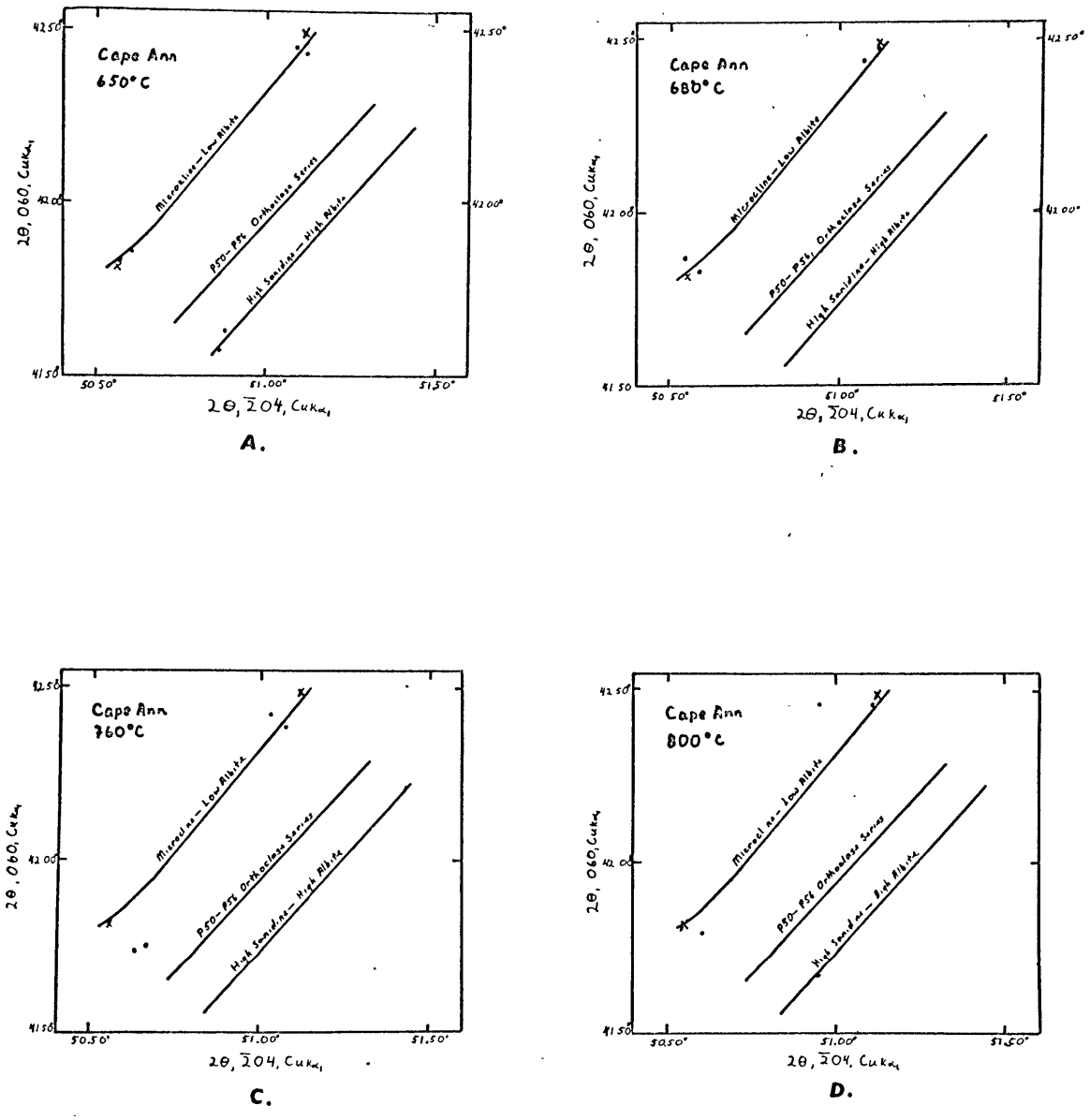

Figure 12.- 060 vs. $\bar{2}$04 Diagram for Feldspars in Experiments on Cape Ann.

'X' represents the starting material. The trends of the different series are determined from the data shown in Figure 11.

All 2θ values measured with $Cu_{K\alpha 1}$ radiation.

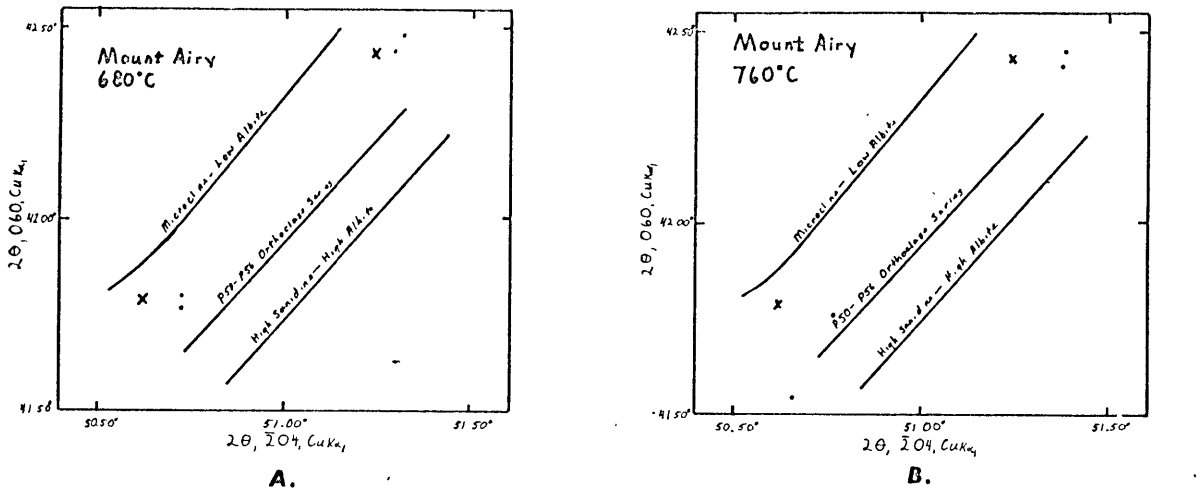

Figure 13. 060 Vs. $\bar{2}04$ Diagram for Feldspars in Experiments on Mount Airy.

All 2θ values measured using $Cu_{k\alpha_1}$ radiation.

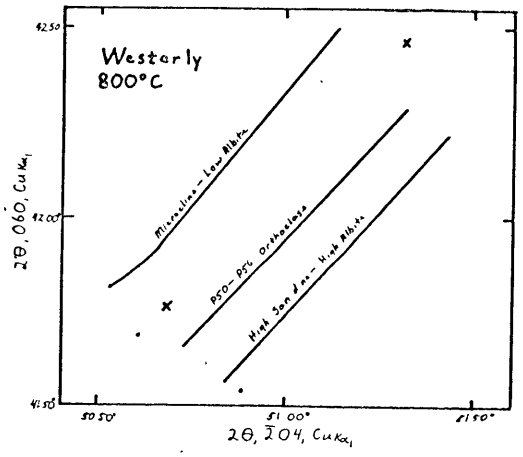

Figure 14. 060 Vs. $\bar{2}04$ Diagram for Feldspars in Experiments on Westerly.

All 2θ values measured using $Cu_{k\alpha_1}$ radiation.

one near the sanidine series, and the other near the orthoclase series. Both were 'anomalous', however, and the plagioclase also appeared to be at the end of the synthetic series and thus 'anomalous'!

The persistance of low albite in the Cape Ann is surprising in light of the thermodynamic data of Holm and Kleppa (1968) on high and low albite, which places the transition at somewhere around 670°C at one atmosphere pressure. It is likely that the low albite seen here is metastable, at least in the high temperature experiments, with respect to high albite.

The early appearance of traces of sanidine is not completely understood, but it disappears when melt forms and may have been metastable. Between 760° and 800°C it appears to become stable. It is unclear whether a truly intermediate feldspar was formed.

Due to the 'anomalous' nature of most of the Mount Airy and Westerly samples, it is not known if the structural state determinations are valid. It appears that they are moving toward the orthoclase series, and then at temperatures similar to those for the Cape Ann, sanidine forms. It is possible that the anorthite content of these feldspars may have an important roll in the 'anomalous' behavior, as may the presence of excess aluminum in the system. The last is especially true in the Mount Airy.

The reactions between the various polymorphs of potassium feldspars have been the source of a great deal of laboratory and field study. Goldsmith and Laves (1954, a, b) suc-

ceeded in making a feldspar that appeared to be orthoclase by heating microcline at 1050°C for short periods of time, and what appeared to be sanidine by heating at 525°C for longer periods of time. This they attributed to metastability. This interpretation, in light of the appearance and disappearance of sanidine in these experiments, seems plausable. Wones and Appleman (1963) found the microcline-sanidine transition in the iron feldspar, $KFeSi_3O_8$, to be reversable about a temperature of 704±6°C at two kilobars. By analogy they suggest that the aluminum feldspars may also have several distinct stable polymorphs. MacKenzie (1954, 1957) and Ferguson (1960) have suggested that orthoclase is a distinct polymorph, and in a number of field occurrences where the heating times have probably been long by laboratory standards the transition seen is from microcline to orthoclase. Wones et.al. (1967) have described an occurrence of coexisting orthoclase and microcline in altered volcanic rocks with no indication of an intermediate phase. Steiger and Hart (1967) have studied the microcline-orthoclase transition in a number of sections across a contact aureole. The suggested transition temperature for this occurrence would be in the range of 400-500°C. Wright (1967) has studied the feldspars from this same area optically and chemically and has found just microcline and orthoclase with no intermediate states.

In connection with the present study, if the microcline - orthoclase transition is between 300 and 500°C, as it is generally thought to be, then much of the microcline

seen in these experiments may be metastable with respect to orthoclase. Considering the persistence of low albite beyond its supposed stability field this is very possible. If the transition to sanidine does not occur until the high 700°'s, then this would explain why the majority of feldspars found in all contact regions are only microcline and orthoclase, and sanidine is generally restricted to volcanics and synthetic feldspars. From the persistence of sanidine in synthetic experiments, the transition process from sanidine to orthoclase must be very slow, or else there is a serious nucleation problem. Both may be the case.

WATER CONTENT OF SILICATE MELTS

A significant problem in igneous petrology is the water content of silicate melts. Different methods for determining water content have been tried which include weight loss on ignition (Tuttle and Bowen, 1958; Goranson, 1936, 1938); analysis of gas phase liberated on ignition (Kennedy et. al., 1962); disappearance of crystalline material with increasing water content (Yoder and Stewart, reported in Burnham and Jahns, 1962); and appearance of a vapor phase with increasing water content (Burnham and Jahns, 1962). A theoretical discussion of water activity in silicate melts based on a quasi-crystalline model has been given by Shaw (1964). From the early work of Goranson (1936, 1938) through latter work the weight percent of water in silicate melts of granitic composition appears to be about 6% at 2kb P_{H_2O}. This however does not vary significantly with the chemical composition of the crystalline silicate phases. The results on the system albite-water, orthoclase-water, and silica-water all give similar water contents in weight percent at constant temperature and pressure (Gorenson, 1936, 1938; Kennedy et. al., 1962; Burnham and Jahns, 1962). Shaw (1964) has shown that except for the data of Kennedy et. al. (1962) a regular solution approximation fits the data for most systems.

WEIGHT FRACTION OF WATER IN THE LIQUID PHASE

In this study, the weight fractions of water in the liquids have been calculated as previously described from modal analyses of the charge and have been tabulated (Table 20).

Graphs of Wt% H_2O vs. V%L and Wt% H_2O vs V%L ρ_L/ρ_{ch} have been prepared (Figures 15-17). On the density corrected graphs the slope of the curve should be $Y^L_{H_2O}$. Short lines have been drawn to show the calculated slope for the curve at different points in the undersaturated region.

From this analysis the content of water in the liquid can be estimated. $Y^L_{H_2O}$ of the saturated liquid can be estimated from runs near the break in slope corresponding to the appearance of a vapor phase (Figures 15-17). This data also correlates with runs in which a vapor phase was present.

MOLE FRACTIONS AND FUGACITY OF WATER IN LIQUID PHASE

Further analysis of the water contents of these melts requires conversion of weight fractions to mole fractions. For this purpose a molecular weight was determined for the anhydrous melt by assuming a composition near the middle of the $KAlSi_3O_8$-$NaAlSi_3O_8$-SiO_2 system, composed of 33.3 wt% of each of the components. Admittedly, this is an oversimplification, but the increase in accuracy obtained by choosing anhydrous compositions near their probable composition

TABLE 20.

WATER CONTENT OF SILICATE MELTS

AND MAJOR PHASES

Run No.	Temp. (°C)	Wt.% H_2O	Vol.% Glass	$\frac{\rho_L}{\rho_{Ch}}$ XVol%	$Y^L_{H_2O}$ x100	Major Phases
WR 19-1	700	1.00	--	----	------	Or,Pl,Q,V,(L)
W 20	700	2.04	--	----	------	Or,Pl,Q,V,(L)
W 21	700	2.95	--	----	------	Or,Pl,Q,V,(L)
W 22	700	5.00	--	----	------	Or,Pl,Q,V,(L)
W 23	700	9.40	--	----	------	Or,Pl,Q,V,(L)
W 24	720	1.04	--	----	------	Or,Pl,Q,L,V?
W 25	720	1.83	--	----	------	Or,Pl,Q,L,V?
W 26	720	3.02	--	----	------	Or,Pl,Q,L,V
WR 27-1	720	4.99	45	41.5	(12.02)	Or,Pl,Q,L,V
W 28	720	10.19	58	55.3	(18.43)	Or,Pl,Q,L,V
W 49	740	0.99	--	----	------	Or,Pl,Q,L
W 50	740	1.99	--	----	------	Or,Pl,Q,L
W 51	740	2.97	--	----	------	Or,Pl,Q,L,V?
W 52	740	4.99	--	----	------	Or,Pl,Q,L,V

TABLE 20. (Cont.)

Run No.	Temp. (°C)	Wt.% H_2O	Vol.% Glass	$\frac{\rho_L}{\rho_{Ch}}$ XVol%	$Y^L_{H_2O}$x100	Major Phases
W 53	740	9.93	70	66.7	(14.89)	Or,Q,L,V,Pl?
W 34	760	1.00	20	17.9	5.57	Or,Pl,Q,L
W 35	760	1.93	37	33.4	5.78	Or,Pl,Q,L
W 36	760	2.94	52.5	47.7	6.16	Or,Pl,Q,L
WR 37-2	760	5.00	77	71.1	(7.03)	Or,L,V?
W 38	760	10.85	81	77.2	(14.05)	L,V,Or?
WR 39-1	780	1.00	21	18.9	5.29	Or,Pl,Q,L
W 40	780	1.98	41.5	37.5	5.28	Or,Pl,Q,L
W 41	780	3.00	61	55.4	5.42	Or,Pl,Q,L
W 42	780	5.12	82	75.7	6.76	Or,L
W 43	780	9.89	90	85.8	(11.53)	L,V
W 44	800	1.00	38.5	34.6	2.89	Or,Pl,Q,L
W 45	800	1.88	62	56.0	3.36	Or,Pl,Q,L
W 46	800	3.07	82	74.5	4.12	Or,Pl,Q,L
W 47	800	4.97	91	84.0	5.91	L
WR 48-1	800	9.94	97	92.4	(10.76)	L,V

TABLE 20. (Cont.)

Run No.	Temp. (°C)	Wt.% H_2O	Vol.% Glass	$\frac{\rho_L}{\rho_{Ch}}$ XVol%	$Y^L_{H_2O}$x100	Major Phases
QR 1-1	700	1.00	5	4.49	(22.27)	Q,Or,Pl,L,V
Q 2	700	1.77	16	14.4	(12.29)	Q,Or,Pl,L,V
Q 3	700	2.85	26	23.6	(12.07)	Q,Or,Pl,L,V
Q 4	700	5.65	56	51.7	(10.93)	Q,Or,Pl,L,V
Q 5	700	11.91	67	63.9	(18.64)	Q,Or,Pl,L,V
Q 6	720	0.89	13	11.7	(7.61)	Q,Or,Pl,L,V?
Q 7	720	1.94	26.4	23.8	(8.15)	Q,Or,Pl,L,V?
Q 8	720	2.98	42	38.1	(7.82)	Q,Or,Pl,L,V?
Q 9	720	4.86	71	65.5	(7.42)	Q,Or,Pl,L,V?
Q 10	720	9.97	95	90.5	(11.02)	Q,L,V,Or?
Q 11	740	1.02	19	17.1	5.85	Q,Or,Pl,L
QR 12-1	740	2.00	37	33.4	5.90	Q,Or,Pl,L
Q 13	740	2.95	56.7	51.5	5.77	Q,Or,Pl,L
Q 14	740	4.94	82	75.7	6.52	Q,Or,Pl,L
QR 15-1	740	10.07	96	91.5	(11.00)	L,V,Q
QR 16-1	760	1.00	20	18.0	5.67	Q,Or,Pl,L

TABLE 20. (Cont.)

Run No.	Temp. (°C)	Wt.% H_2O	Vol.% Glass	$\frac{\rho_L}{\rho_{Ch}}$ XVol%	$Y^L_{H_2O}$x100	Major Phases
Q 17	760	1.97	42	37.9	5.28	Q,Or,Pl,L
Q 18	760	2.97	64	58.1	5.08	Q,L,Or,Pl?
QR 19-1	760	5.01	85	78.5	6.38	Q,L
Q 20	760	9.72	96	91.5	(10.62)	L,V
Q 21	780	1.00	26	23.3	4.29	Q,Or,Pl,L
Q 22	780	2.00	45	40.6	4.93	Q,Or,Pl,L
Q 23	780	2.92	70	63.6	4.62	Q,Or,L,Pl?
Q 24	780	4.96	89	82.1	6.04	Q,L
QR 25-1	780	9.91	97	92.4	(10.73)	L,V
Q 26	800	0.99	33	29.6	3.34	Q,Or,Pl,L
Q 27	800	1.99	50	44.9	4.43	Q,Or,Pl,L
Q 28	800	2.99	76	69.0	4.33	Q,L,Or?
Q 29	800	4.84	92	84.9	5.70	L
Q 30	800	10.00	99	94.3	(10.60)	L,V
MA 1	700	0.81	5	4.5	(18.04)	Pl,Or,Q,L,V
MA 2	700	1.76	10	9.0	(19.56)	Pl,Or,Q,L,V

TABLE 20. (Cont.)

Run No.	Temp. (°C)	Wt.% H_2O	Vol.% Glass	$\frac{\rho_L}{\rho_{Ch}}$ XVol%	$Y^L_{H_2O}$x100	Major Phases
MA 3	700	3.24	20	18.2	(17.80)	Pl,Or,Q,L,V
MA 4	700	5.02	29	26.8	(18.73)	Pl,Or,Q,L,V
MA 5	700	9.37	38	36.2	(25.88)	Pl,Or,Q,L,V
MA 6	720	0.99	12	10.8	(9.17)	Pl,Or,Q,L,V
MAR 7-2	720	1.97	22	19.9	(9.90)	Pl,Or,Q,L,V
MA 8	720	3.04	36	32.7	(9.30)	Pl,Or,Q,L,V
MA 9	720	4.96	60	55.4	(8.95)	Pl,Or,Q,L,V
MA 10	720	9.84	70	66.7	(14.75)	Ql,Q,L,V,Or?
MAR 11-1	740	0.94	17	15.3	6.14	Pl,Or,Q,L
MA 12	740	1.97	32	28.9	6.82	Pl,Or,Q,L
MA 13	740	2.98	48	43.6	6.83	Pl,Or,Q,L
MA 14	740	4.94	62	57.2	(8.93)	Pl,Q,L,V
MA 15	740	9.74	78	74.3	(13.11)	Pl,Q,L,V
MA 35	760	1.00	20	18.0	5.56	Pl,Or,Q,L
MA 36	760	2.01	49	44.2	4.55	Pl,Or,Q,L
MA 37	760	2.99	65	59.0	5.07	Pl,Q,L
MA 38	760	4.99	76	70.1	(7.12)	Pl,Q,L,V?

TABLE 20. (Cont.)

Run No.	Temp. (°C)	Wt.% H_2O	Vol.% Glass	$\frac{\rho_L}{\rho_{Ch}}$ XVol%	$Y^L_{H_2O}$x100	Major Phases
MA 39	760	9.89	84	80.1	(12.35)	Pl,Q,L,V
MA 21	780	0.98	23	20.7	4.73	Pl,Or,Q,L
MA 22	780	1.99	50	45.2	4.40	Pl,Q,L,Or?
MA 23	780	2.99	67	60.8	4.92	Pl,Q,L
MA 24	780	4.94	83	76.7	6.44	Pl,Q,L
MA 25	780	9.51	90	85.8	(10.08)	Pl,Q,L,V
MA 26	800	0.99	27	24.2	4.09	Pl,Or,Q,L
MA 27	800	1.99	55	50.8	3.92	Pl,Q,L
MA 28	800	3.00	73	66.28	4.52	Pl,Q,L
MA 29	800	4.96	89	82.15	6.04	Pl,L
MA 30	800	9.97	95	90.5	(11.02)	L,V

All $Y^L_{H_2O}$ in parentheses represent runs in which it appears as if a vapor phase was present, so that the value obtained is meaningless as far as the silicate melt is concerned.

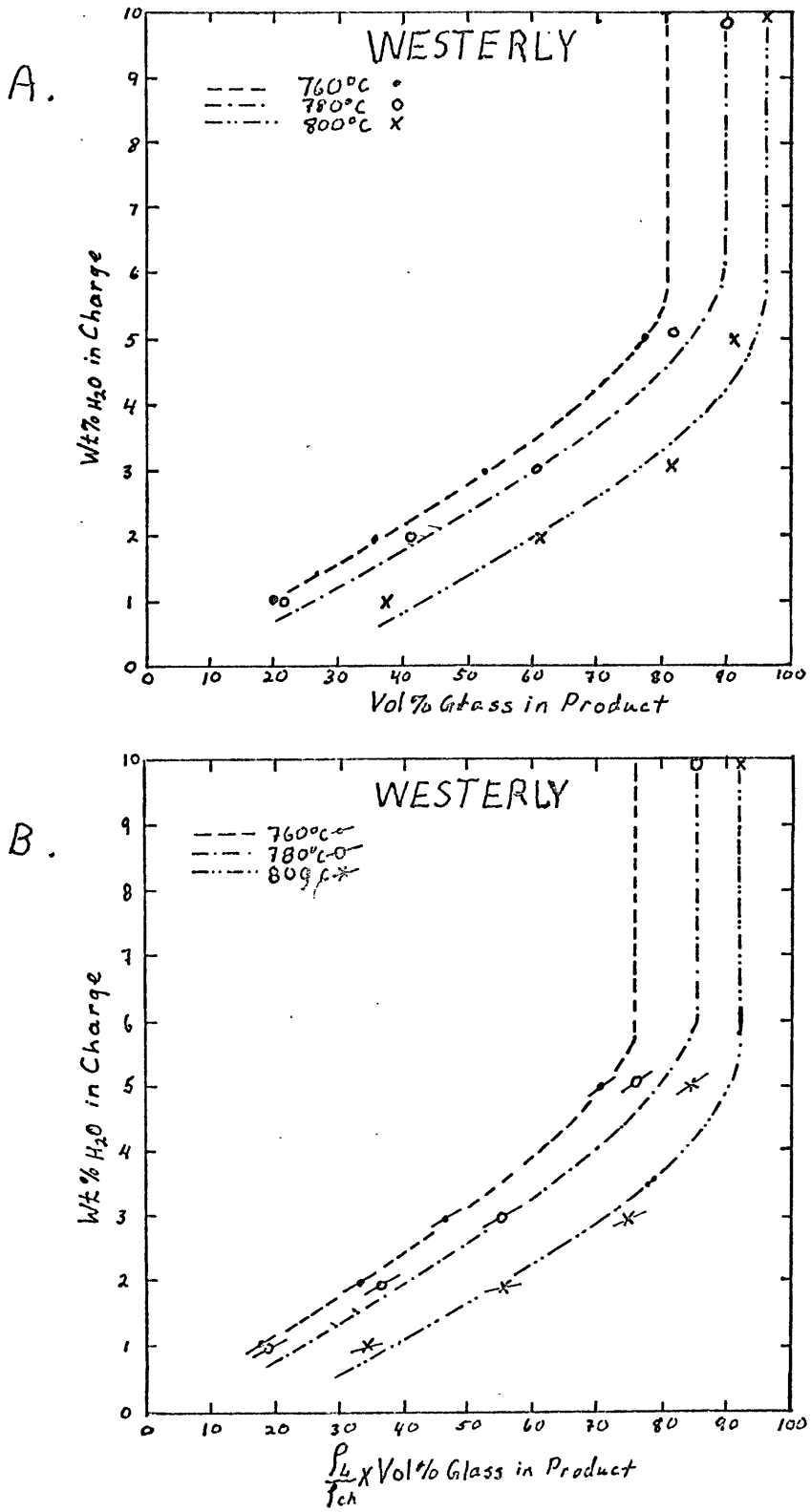

Figure 15. Variation of Glass Content with Original Water Content in Westerly.

Diagram B is a density corrected diagram. The short lines through the symboles represent calculated slopes.

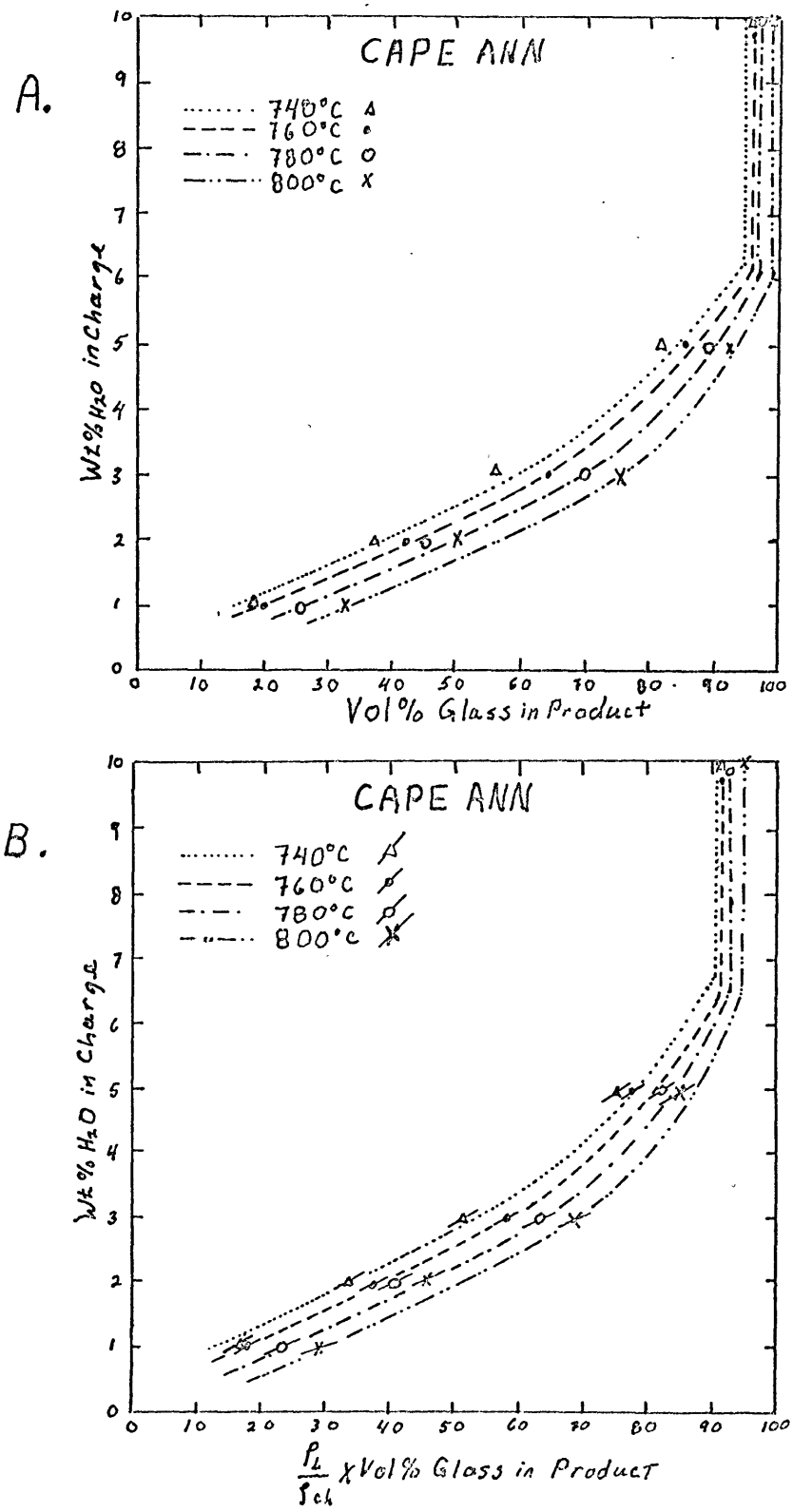

Figure 16. Variation of Glass Content with Original Water Content in Cape Ann.

Diagram B is a density corrected diagram. The short lines through the symboles represent calculated slopes.

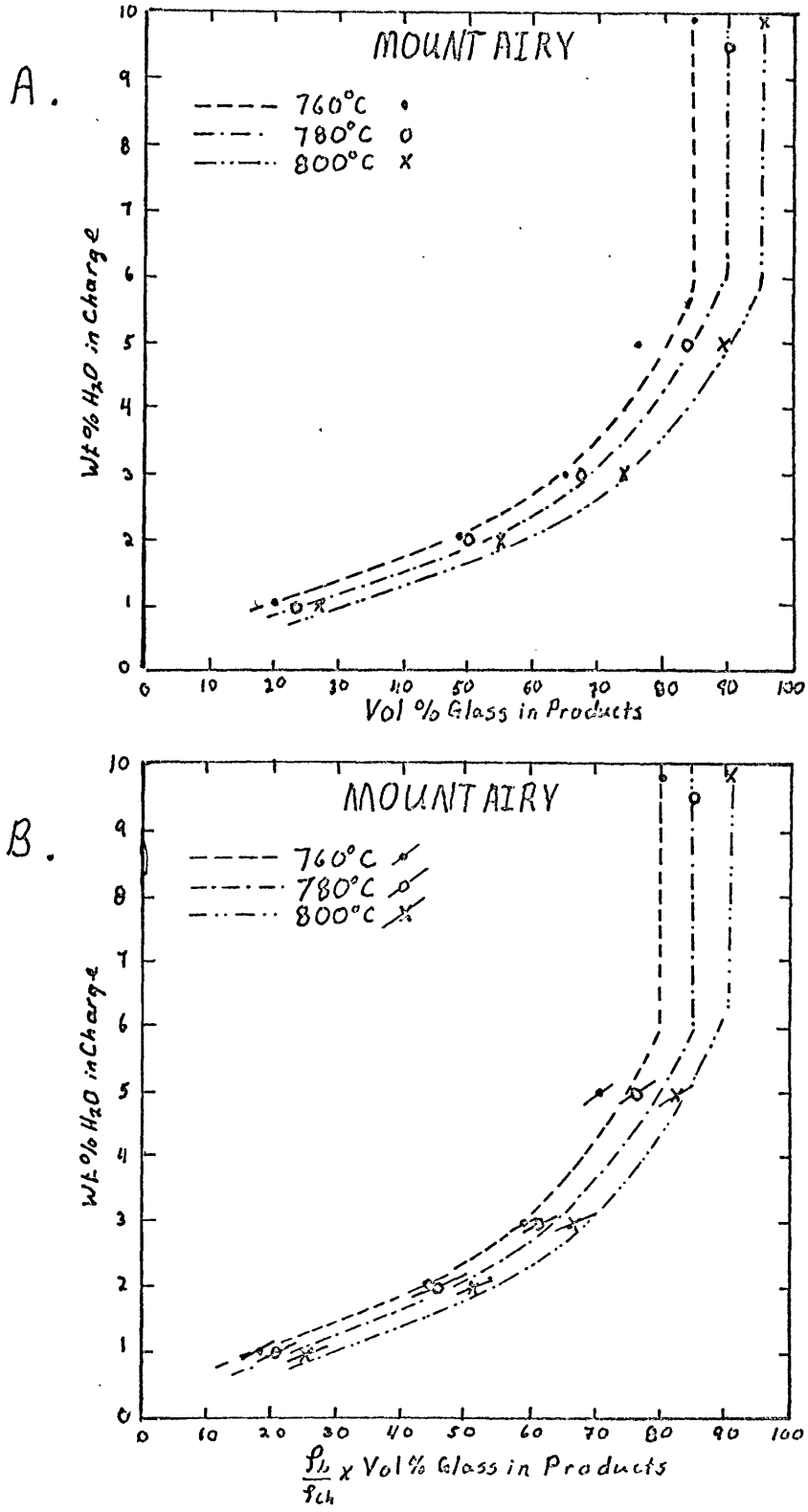

Figure 17. Variation of Glass Content with Original Water Content in Mount Airy.

Diagram B is a density corrected diagram. The short lines through the symboles represent calculated slopes.

for each association does not seem to justify the calculations. Using a molecular weight for the anhydrous melt obtained from this composition (124.735), mole fractions, $X^{L}_{H_2O}$, have been calculated and are tabulated. (Table 22)

Considering the chemical potential of water in a vapor phase in terms of fugacities we may write:

$$u_{H_2O} = u_o + RT \ln f_{H_2O}$$

where f_{H_2O} is the fugacity of H_2O in the vapor phase at this pressure and temperature. For water in the liquid phase we may write the chemical potential in terms of activities:

$$u_{H_2O} = u^* + RT \ln a_{H_2O}$$

where a_{H_2O} is the activity of water in the melt at this pressure and temperature. Equating these two for the coexistence of a liquid and an aqueous vapor phase and rearranging terms, we can arrive at the equation:

$$\frac{f_{H_2O}}{a_{H_2O}} = e^{\frac{(u^*-u_o)}{RT}}$$

The right side of this expression is a function of total pressure and temperature. The left side may now be expressed in terms of $X^{L}_{H_2O}$ and f_{H_2O} by substituting an expression for activity in terms of mole fraction. A number of different formulations could be presented, such as that used by Shaw for the activity of water in silica melts, (Shaw, 1964) but

lacking sufficient data to determine coefficients for such formulations a simpler molecular model has been employed. This leads to the expression:

$$a_{H_2O} = \alpha_{H_2O} X^{L}_{H_2O}$$

where α_{H_2O} is an activity coefficient and is assumed to be only a function of pressure and temperature for this analysis. Consequently:

$$\frac{f_{H_2O}}{X^{L}_{H_2O}} = \alpha_{H_2O} e^{\frac{(u^*-u_o)}{RT}} = C(p,t)$$

At different temperatures we can estimate the $X^{L}_{H_2O}$ in the saturated liquid, and in the saturated case we know that $P_{H_2O} = P_{Tot}$, if there are no other species of consequence in the vapor phase. Using these numbers with fugacity coefficients calculated from the data of Sharp (1962), we can calculate the left hand side of the equation for that temperature and pressure. Using this value of C(p,t), we can then take the mole fractions determined for the undersaturated cases and calculate approximate f_{H_2O} in equilibrium with the melt. The fugacity coefficients used were calculated using the approach outlined by Shaw and Wones (1964). These are tabulated in Table 21 and plotted versus temperature for various pressures on Figure 18.

The C(p,t) have been estimated and the resulting f_{H_2O} values are tabulated in Table 22, for all series of runs where substantial undersaturation had been believed to occur.

TABLE 21.

FUGACITY COEFFICIENTS OF WATER

Temp. (°C)	Pressure (Bars) 500	1000	2000
200	0.038	0.024	0.020
300	0.174	0.111	0.090
400	0.411	0.264	
500	0.651	0.462	0.362
600	0.784	0.635	0.524
700	0.864	0.763	0.670
800	0.910	0.850	0.783
900	0.943	0.904	0.879
1000	0.969	0.950	0.944

Calculated from the data of Sharp (1962) by the method given by Shaw and Wones (1964).

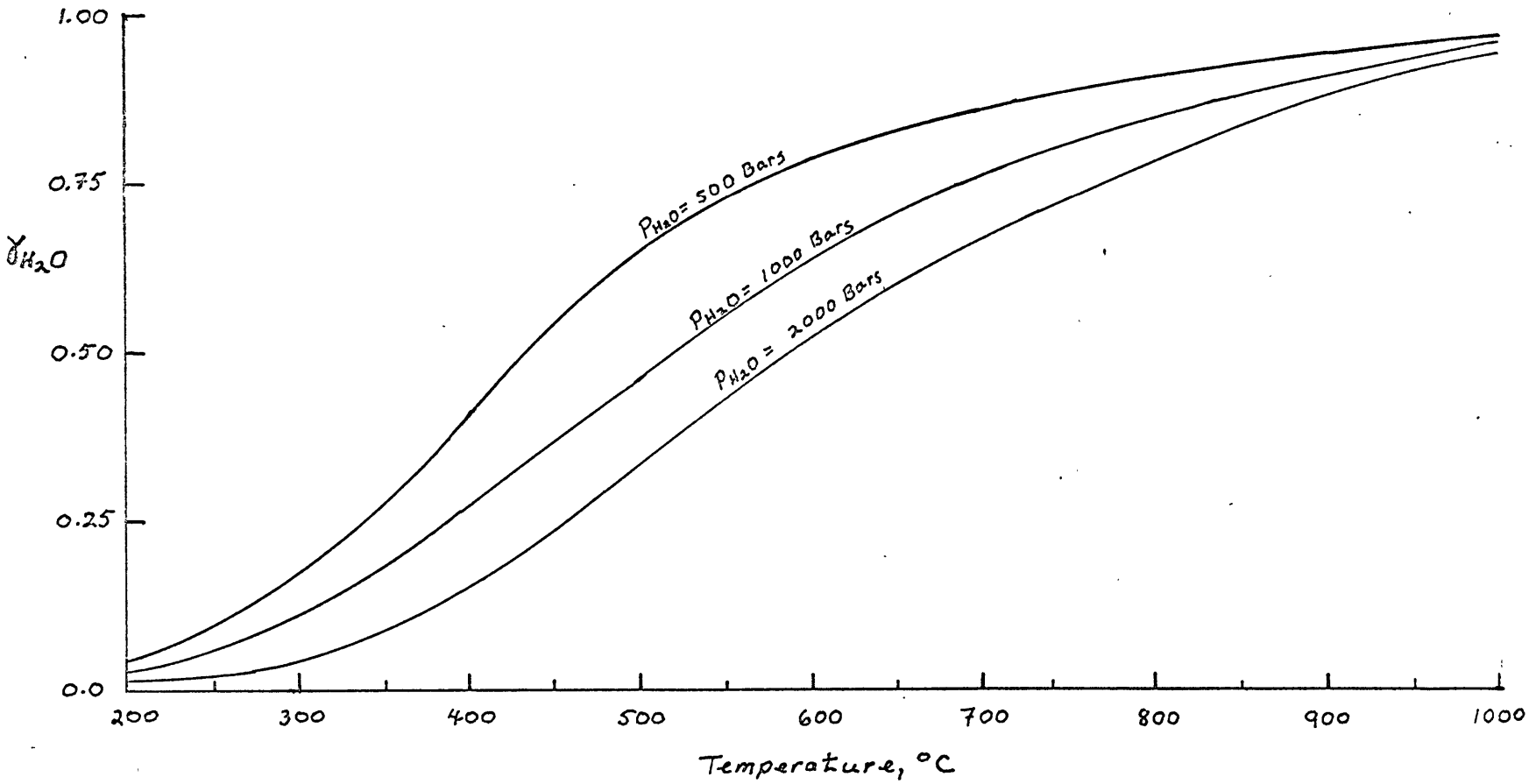

Figure 18. Fugacity Coefficients of Water Vs. Temperature for 500, 1000, and 2000Bars Pressure.

TABLE 22.

FUGACITY OF WATER IN EXPERIMENTS

Run No.	Temp. (^{o}C)	Wt%$_{H_2O}$	$X^{L}_{H_2O}$x100	C(Bars/Mole%)	f_{H_2O}(bars)
W 34	760	1.00	29.02	46.25-41.11	1267
W 35	760	1.93	28.83	46.25-41.11	1259
W 36	760	2.94	31.27	46.25-41.11	1366
WR 37-2	760	5.00	-----	46.25-41.11	1480*
W 38	760	10.85	-----	46.25-41.11	1480*
WR 39-1	780	1.00	27.90	48.94-42.78	1268
W 40	780	1.98	27.86	48.94-42.78	1264
W 41	780	3.00	28.00	48.94-42.78	1274
W 42	780	5.12	33.44	48.94-42.78	1485
W 43	780	9.89	-----	48.94-42.78	1540*
W 44	800	1.00	17.10	48.94-43.50	790
W 45	800	1.88	19.42	48.94-43.50	926
W 46	800	3.07	22.95	48.94-43.50	1070
WR 48-1	800	9.94	-----	48.94-43.50	1566*
Q 11	740	1.02	30.10	45.00-40.00	1280
QR 12-1	740	2.00	30.29	45.00-40.00	1277
Q 13	740	2.95	29.79	45.00-40.00	1266
Q 14	740	4.94	32.58	45.00-40.00	1380
QR 15-1	740	10.07	-----	45.00-40.00	1440*
QR 16-1	760	1.00	29.41	46.25-41.11	1285
Q 17	760	1.97	27.86	46.25-41.11	1217
Q 18	760	2.97	27.05	46.25-41.11	1181
QR 19-1	760	5.01	32.08	46.25-41.11	1398
Q 20	760	9.72	-----	46.25-41.11	1480*

TABLE 22. (Cont.)

Run No.	Temp. (°C)	Wt% H_2O	$X^L_{H_2O}$x100	C(Bars/Mole%)	f_{H_2O}(Bars)
Q 21	780	1.00	23.70	48.13-42.78	1077
Q 22	780	2.00	26.44	48.13-42.78	1202
Q 23	780	2.92	25.13	48.13-42.78	1132
Q 24	780	4.96	30.82	48.13-42.78	1401
QR 25-1	780	9.91	-----	48.13-42.78	1540*
Q 26	800	0.99	19.32	48.94-43.50	893
Q 27	800	1.99	24.31	48.94-43.50	1123
Q 28	800	2.99	23.88	48.94-43.50	1104
Q 29	800	4.84	29.52	48.94-43.50	1364
Q 30	800	10.00	-----	48.94-43.50	1566*
MAR 11-1	740	0.94	31.19	45.00-40.00	1325
MA 12	740	1.97	33.67	45.00-40.00	1373
MA 13	740	2.98	33.68	45.00-40.00	1373
MA 14	740	4.94	-----	45.00-40.00	1440*
MA 15	740	974	-----	45.00-40.00	1440*
MA 35	760	1.00	28.98	46.25-41.11	1265
MA 36	760	2.01	25.23	46.25-41.11	1101
MA 37	760	2.99	27.01	46.25-41.11	1179
MA 38	760	4.99	-----	46.25-41.11	1480*
MA 39	760	9.89	-----	46.25-41.11	1480*
MA 21	780	0.98	25.60	48.13-42.78	1163
MA 22	780	1.99	24.18	48.13-42.78	1098
MA 23	780	2.99	26.59	48.13-42.78	1209
MA 24	780	4.94	32.40	48.13-42.78	1209
MA 25	780	9.51	-----	48.13-42.78	1540

TABLE 22. (Cont.)

Run No.	Temp. (^{o}C)	Wt%$_{H_2O}$	$X^{L}_{H_2O}$x100	C(Bars/Mole%)	f_{H_2O}(Bars)
MA 26	800	0.99	22.81	48.94-43.50	1054
MA 27	800	1.99	22.04	48.94-43.50	1019
MA 28	800	3.00	24.70	48.94-43.50	1142
MA 29	800	4.96	30.82	48.94-43.50	1425
MA 30	800	9.97	-----	48.94-43.50	1566*

* These are the fugacities of the saturated runs and are simply the fugacity of water at two kilobars and that temperature. From the C determined from these runs, the fugacities is the series directly above it in this table are calculated.

In general the original estimates of volume percent of glass formed will tend to be too low. In runs with little melting glass rims are not easily seen. In higher temperature runs a small amount of birefringent material embedded in glass leads to an overestimation of the amount of crystalline material present. As a result the final fugacities calculated will probably be maximum values. Keeping this in mind we can see that at 760°C the water fugacity is lowered to around 1250 bars, 780°C, to about 1100 bars, and at 800°C to about 825 bars. This final fugacity is slightly less than that which is in equilibrium with a pure vapor phase at a total pressure of one kilobar at this temperature. At this temperature undersatuartion has lowered the fugacity an amount equivalent to decreasing the total pressure on the saturated melt by one kilobar. Here it can be seen that by increasing the total pressure by one kilobar while holding the P_{H_2O} relatively constant, as defined by the relationship: $P_{H_2O} = \gamma_{H_2O} f_{H_2O}$, has increased the temperature at which feldspar and quartz are in equilibrium with a liquid by some 100°C.

VARIATION IN ANHYDROUS COMPOSITION OF SILICATE MELTS

WITHIN THE SYSTEM $CaAl_2Si_2O_8$-$NaAlSi_3O_8$-$KAlSi_3O_8$-SiO_2

The saturated relationships of the major phases may best be represented within the quaternary system $NaAlSi_3O_8$-$KAlSi_3O_8$-$CaAl_2Si_2O_8$-SiO_2, projecting from water. Within this system, the first melt will form on the $NaAlSi_3O_8$-$KAlSi_3O_8$-SiO_2 base at the cotectic, or eutectic, determined for this subsystem by Tuttle and Bowen (1958). At this temperature, a four phase region will be formed within this system between plagioclase-orthoclase-quartz- and liquid. As the temperature rises, under equilibrium conditions, the four phase volume will migrate 'upward' into the quaternary system. The liquid in equilibrium with the three other crystalline phases will migrate along a low melting channel in the quaternary system (Figure 19). At this time the base of the liquid field is determined by the isotherms in the Ab-Or-Q subsystem. From there it will extend upward along the low melting channel, forming a liquid region shaped like a thorn (Figure 19). As the tip of this 'thorn' migrates upward, it pierces planes of increasing anorthite content. These 'piercing points' have been determined for several An contents by James (1968) at one kilobar water pressure. These are shown on Figure 20 projected onto the Ab-Or-Q base. As can be seen, increasing anorthite contents up to about 10% move the piercing point towards more quartz and orthoclase rich composi-

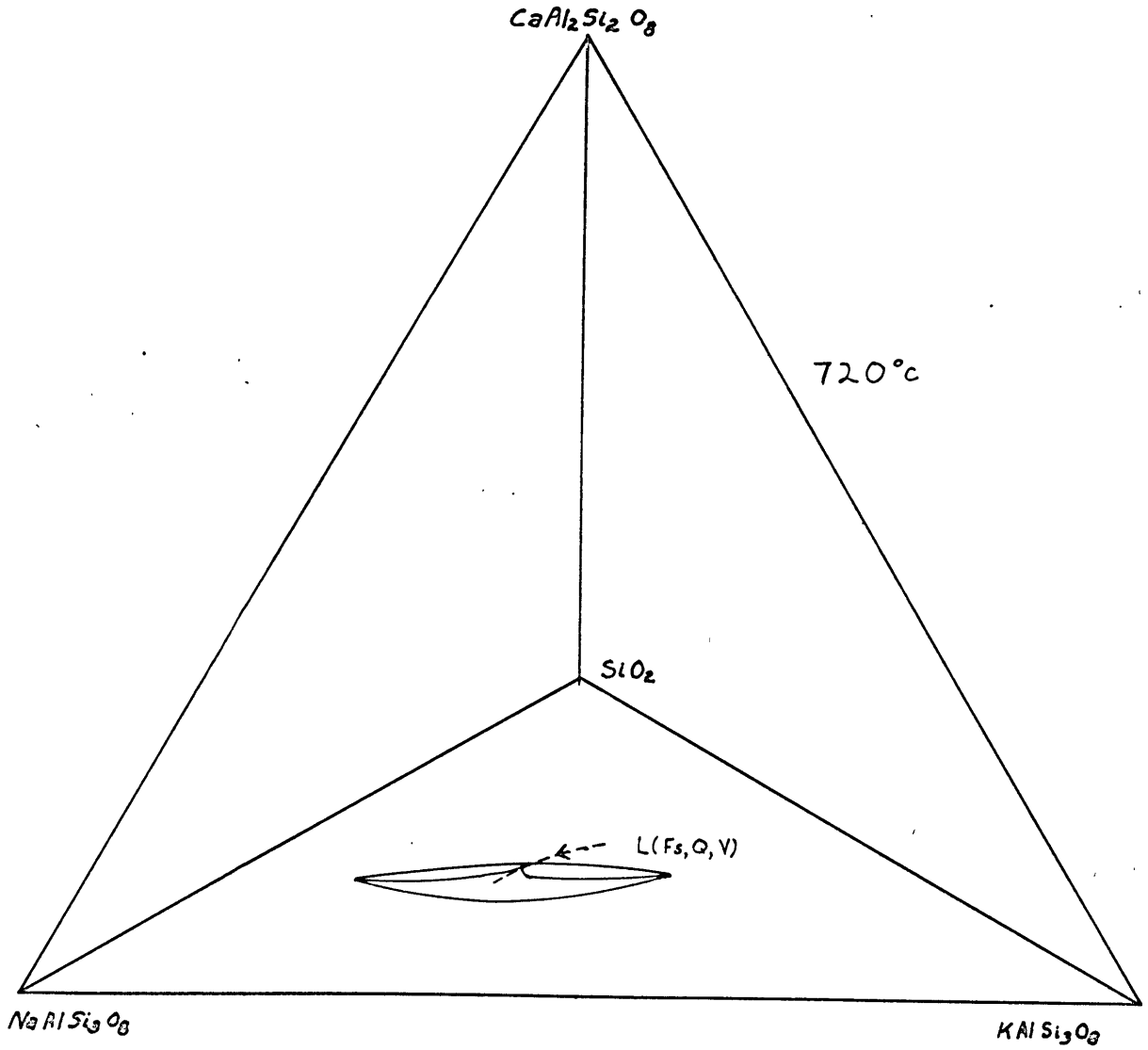
$CaAl_2Si_2O_8$
720°c
SiO_2
L(Fs, Q, V)
$NaAlSi_3O_8$
$KAlSi_3O_8$

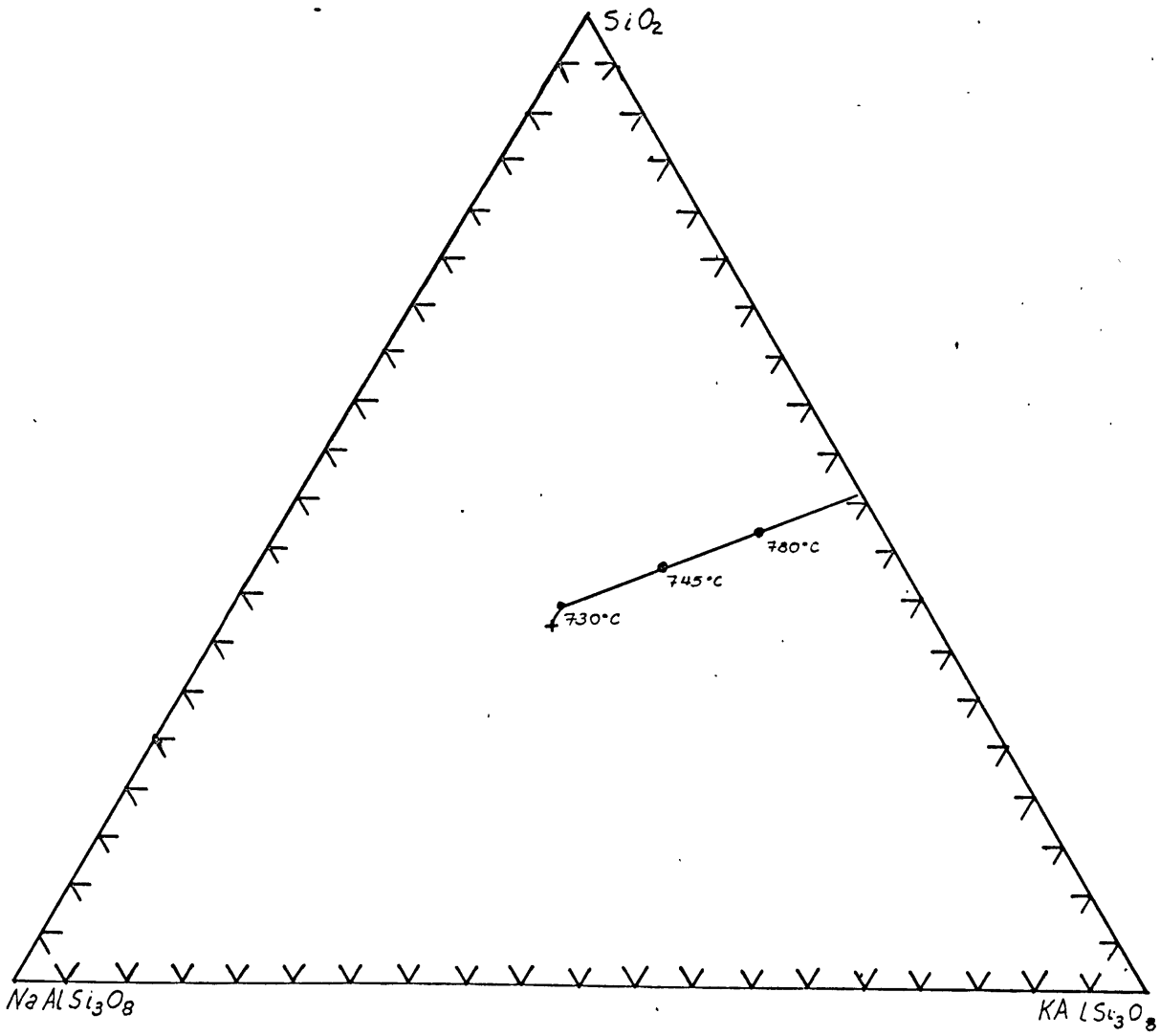
SiO_2
780°C
745°C
730°C
$NaAlSi_3O_8$
$KAlSi_3O_8$

tions. By the time the point of the 'thorn' has reached the An-Or-Q sideline the four phase volume has degenerated to the An-Or-Q plane and disappeared. For any composition within the quaternary system, as long as the composition lies within the four phase region the liquid in equilibrium with the crystalline phases will migrate along this low temperature valley, but when the composition passes out of the four phase region, the liquid will tend to move in the general direction of the bulk composition.

For saturated relationships the compositions used in these experiments may be represented in a ternary system by projecting from quartz onto the An-Ab-Or face. This has been done for temperatures up to 760°C when all three compositions have passed out of the four phase region within the quaternary system (Figure 21, a-e). The compositions lying below the saturation surface pass out of the five phase assemblage Plag-Or-Q-Liquid-Vapor before the saturated compositions do.

To represent these undersaturated relationships, we go to the system Ab-Or-Q-H O. The anhydrous compositions plot within the Ab-Or-Q subsystem as shown in Figure 22. Now we may draw sections through the quaternary system along the sections A-E and C-D. For the section C-D we will project the liquid and crystalline phases onto the section from a point located an infinite distance to the left along the line A-B. This type of projection has the advantage that water contents of the liquid phases may be plotted

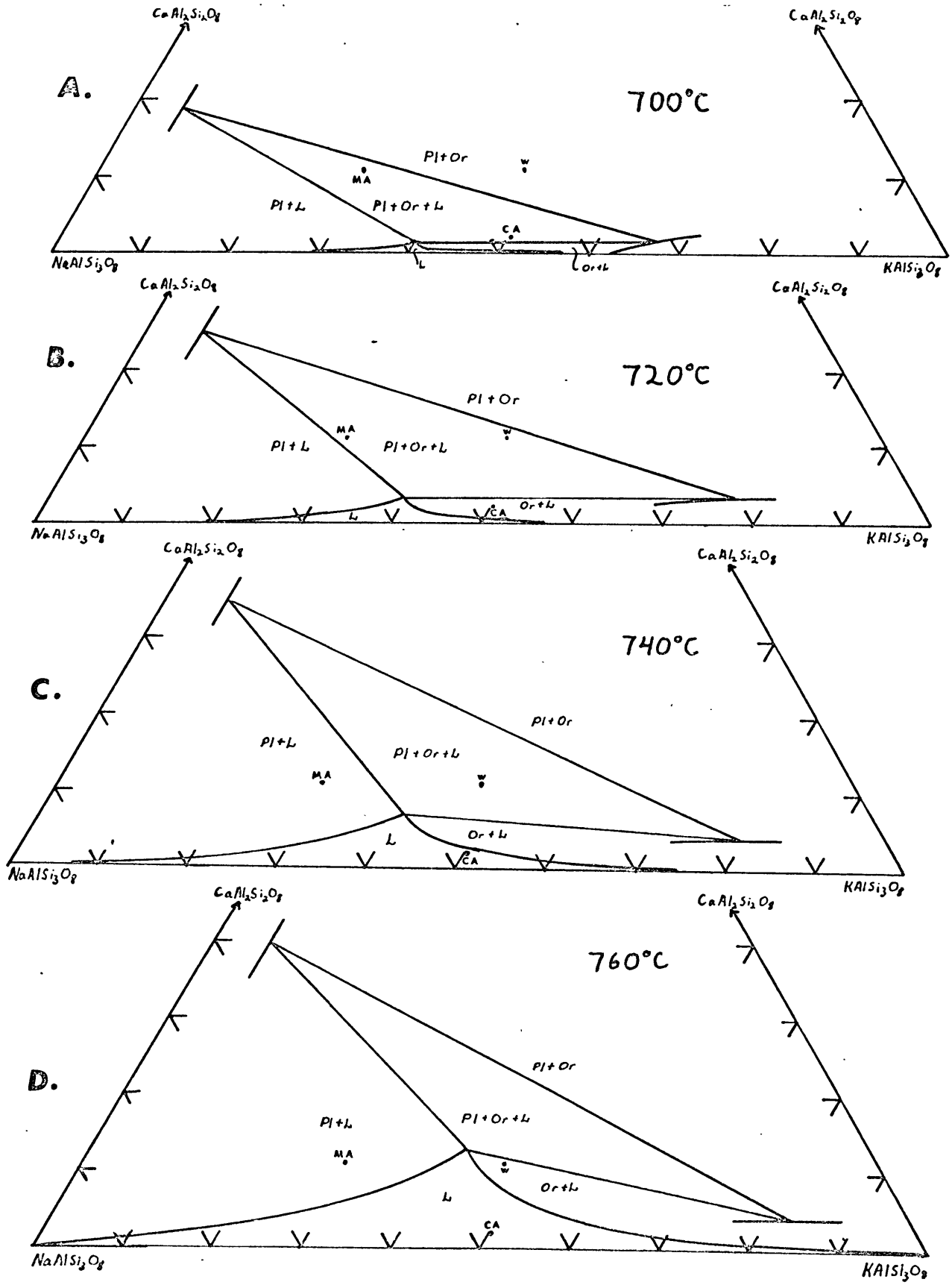
A.
700°C
Pl+Or
MA
W
Pl+L
Pl+Or+L
CA
L
Or+L
B.
720°C
Pl+Or
MA
W
Pl+L
Pl+Or+L
L
CA
Or+L
C.
740°C
Pl+Or
Pl+L
Pl+Or+L
MA
W
L
Or+L
CA
D.
760°C
Pl+Or
Pl+L
Pl+Or+L
MA
W
L
Or+L
CA

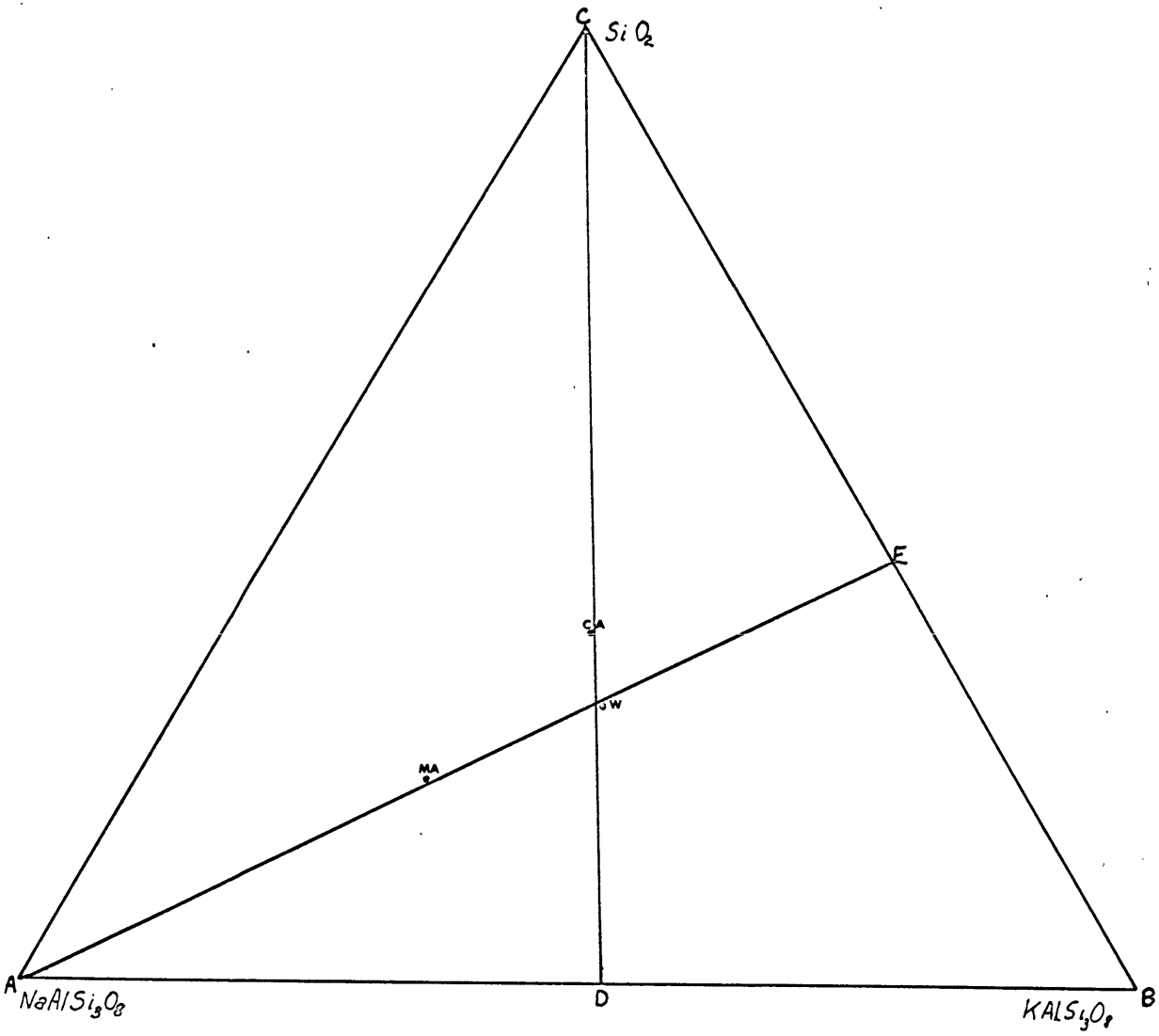
C
SiO_2
E
A
$NaAlSi_3O_8$
D
B
$KALSi_3O_8$

directly without distortion. Also, all phases will be projected parallel to the base A-B. From these diagrams, (Figure 23 a-d) the approximate projection of the composition of the liquid in equilibrium with feldspar and quartz can be determined at different temperatures. This projection determines the quartz content of this liquid . For the section A-E, we may project onto the section from quartz. Since the compositions of the samples lie on the plane, the water content of the runs may be plotted directly without distortion, however water contents of liquids lying far from the plane will appear too high. This distortion will not be greater than 0.1 wt% H_2O unless the liquid composition is more than 10 Wt% from the plane of projection. From these diagrams (Figure 24) approximate projections for the liquid in equilibrium with feldspar and quartz may again be found at different temperatures and this will determine its position to be along a ray from quartz to the composition in the projection. The combination of these two projections thus determines the approximate composition of the liquid in the undersaturated region in equilibrium with feldspar and quartz. These compositions have been plotted on the anhydrous base for temperatures of 760, 780, and 800°C (Figure 25). As can be seen, there is a definite trend toward the orthoclase end of the diagram. Also plotted is an approximation to the path of the liquid in the absence of anorthite (line A-C^1).

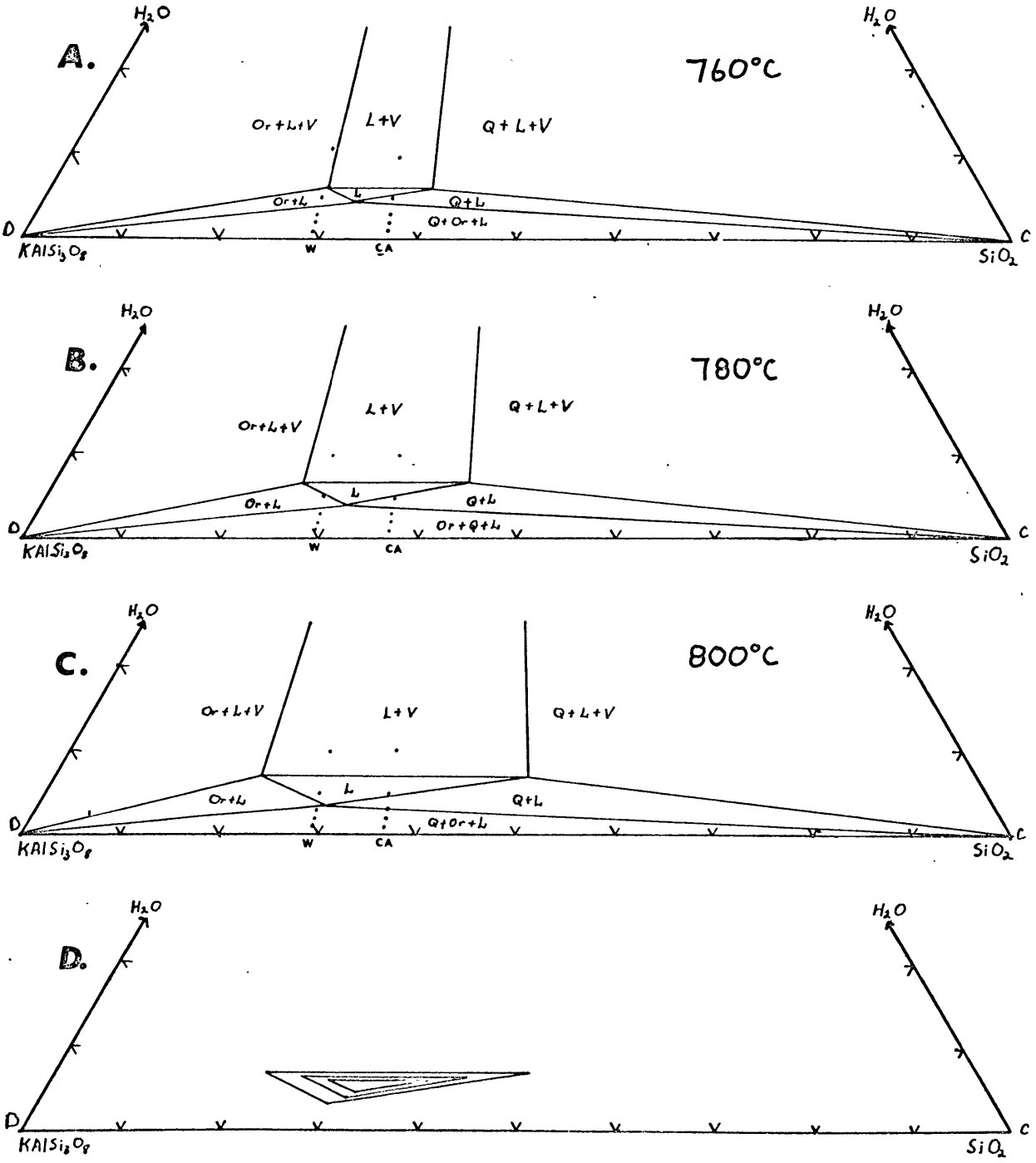

Figure 23. Section C-D-H_2O in the system $KAlSi_3O_8$-$NaAlSi_3O_8$-SiO_2-H_2O.

Projections onto section as described in Text. Figure D is a polythermal representation of the liquid fields shown in A-C.

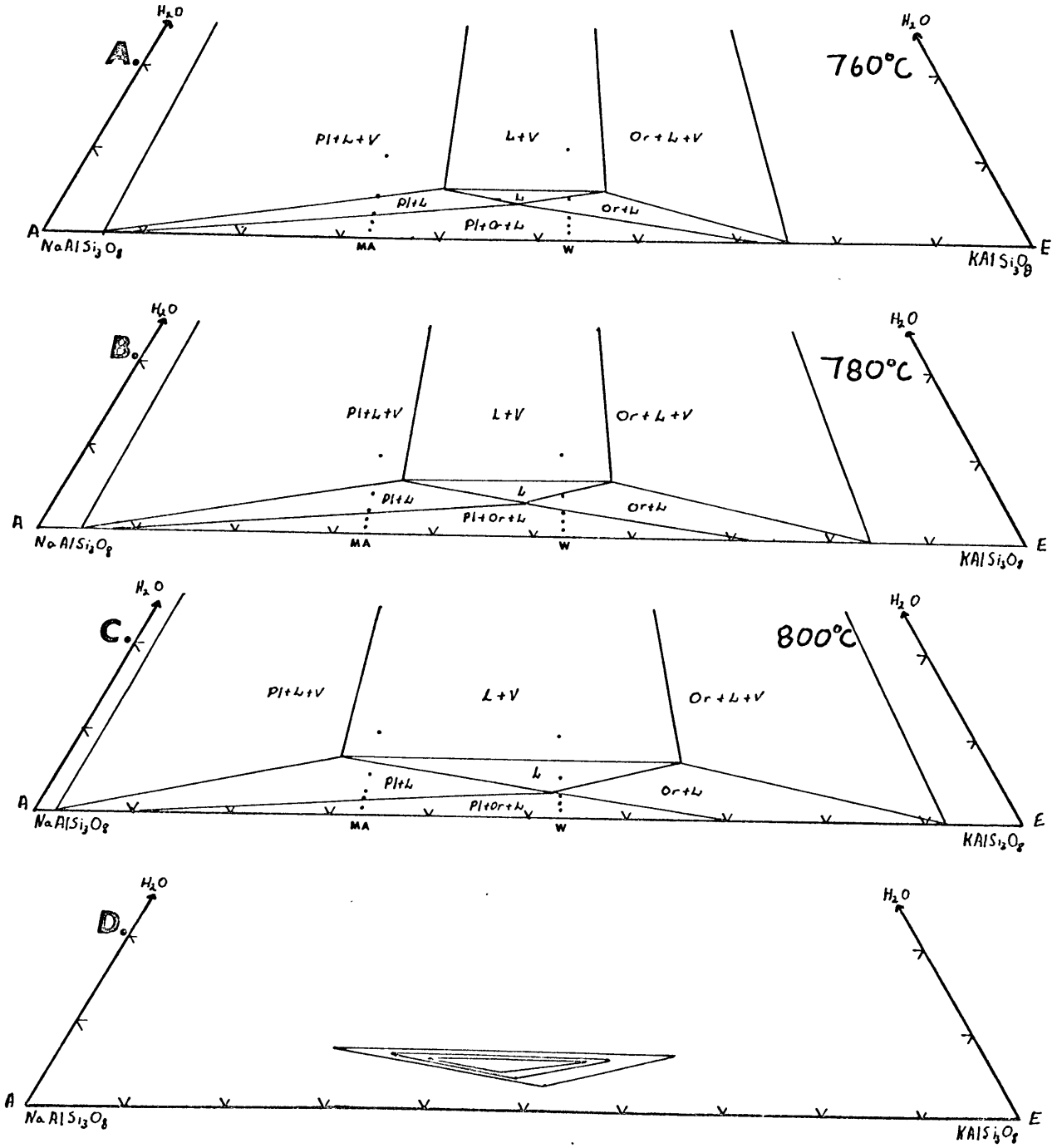

Figure 24. Section A--E--H_2O in the System $KAlSi_3O_8$--$NaAlSi_3O_8$--SiO_2--H_2O.

Projection onto section as described in text. Figure D is a polythermal representation of the liquid fields shown in A-C

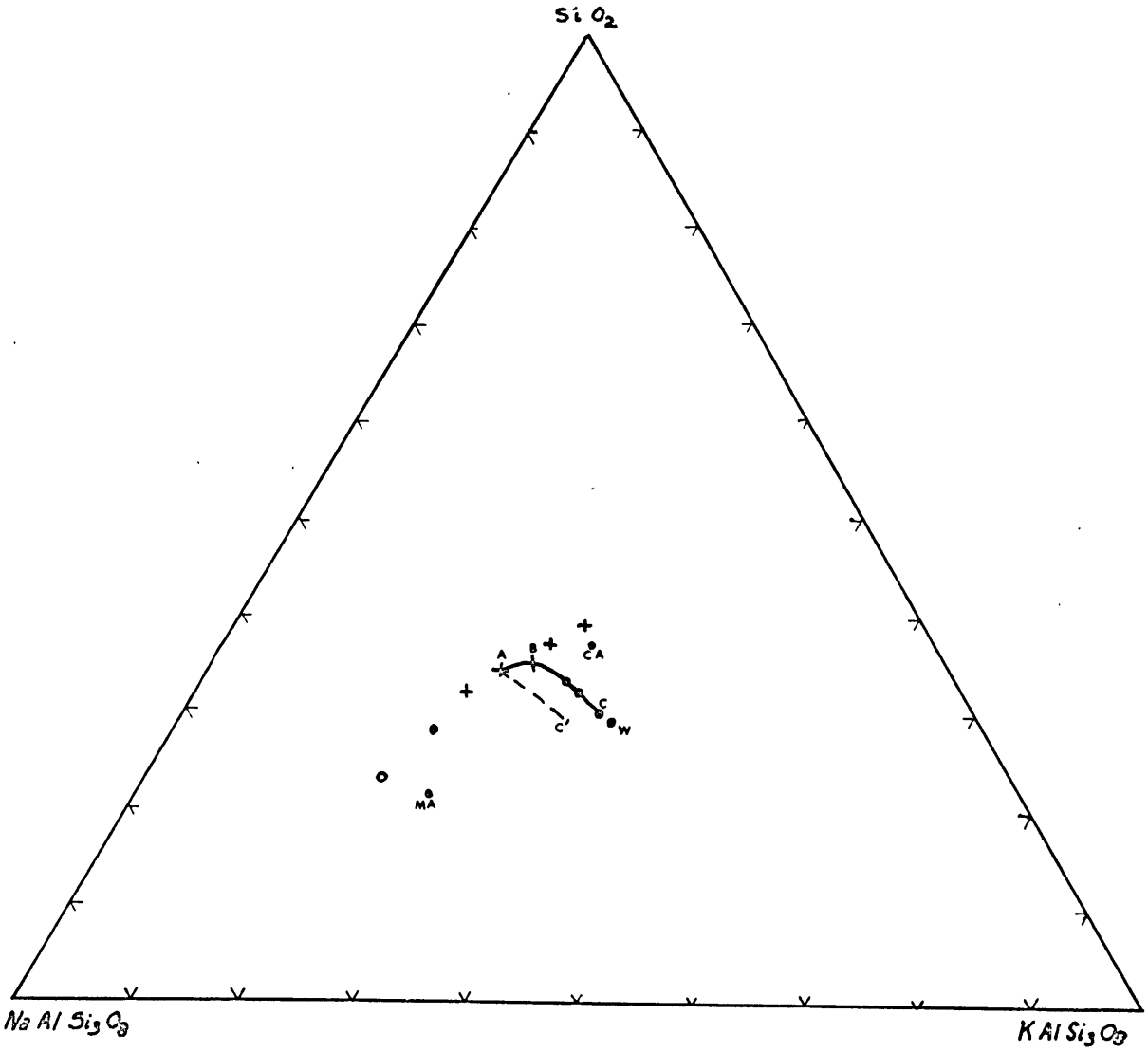
Si O2
Na Al Si3 O8
K Al Si3 O8
A
B
C
C'
CA
W
MA

COMPARISON WITH EXPERIMENTAL WORK

The solidus temperatures in the system studied here are in good agreement with those given by Tuttle and Bowen (1958) on the system Ab-Or-Q-H_2O. However, the different granites do not appear to begin melting at the same temperature as stated by them. Instead, the Westerly melts some 20 to 30°C higher than the minimum in the system. This melting trend is in good agreement with the position of the various compositions in the system Ab-An-Or-Q-H_2O. As has been shown in the previous section, the solidus relationships can be described by projection onto the system Ab-Or-An and are consistent with this system.

The liquidus temperatures are somewhat higher than shown by the liquidus diagram for the Ab-Or-Q-H_2O system. This may be due to the affect of anorthite component in the system. The only other difference between the synthetic and natural experiments is the persistence of two partially ordered feldspars in the natural runs, and this would not be expected to raise the liquidus temperatures unless the more ordered feldspar were the phase with the lower free energy.

The undersaturated liquid points appear to extrapolate back to a point at about 740°C some distance to the right of the minimum in the system Ab-Or-Q-H_2O as determined by Tuttle and Bowen. This shift is caused by the movement seen in the Ab-An-Or-Q-H_2O system between 700 and 740°C along

the low temperature trough. Thus, the overall shift in the composition of the liquid in equilibrium with feldspar and quartz is made up of two parts, first a shift slightly toward quartz and orthoclase caused by the affect of anorthite (A to B, Figure 25), and then a shift away from the quartz toward orthoclase caused by undersaturation (B to C, Figure 25). The shift caused by anorthite roughly parallels the data of James (1968) at one kilobar water pressure, and is similar to the trend seen in experiments on obsidians by von Platen (1965). The latter shift attributed to undersaturation has quite a different trend, moving away from quartz and towards orthoclase. Since all compositions had moved out of the five phase volume by this temperature there should have been little shift in liquid composition caused by anorthite at higher temperatures, and almost all of the movement seen should be caused by undersaturation.

It is thus necessary to divide the original shift in the cotectic point with water pressure into two parts, one caused by the increase in pressure, and one caused by water as a component in the melt. The estimation of water fugacity gives a fugacity at 800°C for most undersaturated runs of about 800 to 900 bars. This is about the fugacity above a saturated melt at one kilobar P_{H_2O}. Thus, the increase in pressure of from one to two kilobars has shifted the composition of the liquid in equilibrium with feldspar and quartz from that determined by Tuttle and Bowen to the point determined at 800°C in the present study. This

change due to an increase in pressure is roughly away from quartz. This is in good agreement with data on the sidelines of Luth (1967). Luth found that an increase of several kilobars total pressure tended to decrease the quartz content of the eutectic in the dry systems orthoclase-quartz and albite-quartz, the affect being more pronounced in the orthoclase-quartz system.

If we consider the molar volumes of quartz, orthoclase, and albite corrected to these temperatures and pressures (Table 23) we see that the molar volumes of the feldspars are considerably larger than quartz. Therefore;

$$\frac{\partial G_{Or}}{\partial P} \cong \frac{\partial G_{Ab}}{\partial P} >> \frac{\partial G_{Q}}{\partial P}$$

and consequently the free energy of feldspar rises faster than for quartz with increasing pressure, and the composition of the liquid will become richer in feldspar. In truth, the molar volume of the liquid must also be considered and it will vary with varying composition, but this rationalization in terms of crystalline phases is an indicator.

This leaves a shift caused by water as a component that is dominantly an increase in the content of albite in the melt. This is probably caused by increased hydrolization of sodium by water and its subsequent solution in the water rich melt.

Thus, by considering the two effects of water separately, two different possible trends can be seen for changing composition with pressure. In most natural situations the trend will probably lie in between these two extremes.

TABLE 23.

MOLAR VOLUMES OF QUARTZ, ORTHOCLASE, AND ALBITE

	25°C, 1 At.	700°C, 2000 At.
Quartz	22.690 g/cc	23.62 g/cc*
Orthoclase	108.69 g/cc	110.2 g/cc
Albite	I00.21 g/cc	101.9 g/cc

Volumes at 25° and 1 atmosphere from Clark, 1966. Volumes at higher temperature and pressure calculated from thermal expansion and complressability data from same source.

* This figure includes the change in volume due to the α-β quartz transition.

COMPARISON WITH GRANITIC COMPOSITIONS

Figure 26 a-b show the normative distribution of 507 granites and 97 aplites as listed in the tables of Washington (1917), and presented by Luth, Jahns, and Tuttle (1964). As can be seen, the trend of granitic compositions lies to the orthoclase side of the cotectic and eutectic compositions in the saturated system Ab-Or-Q-H O. This trend is approximately what would be expected from partial melting or differentiation under conditions in which the liquid is undersaturated with respect to water. That is, the fugacity of water in equilibrium with the melt would have been less than that of a pure water phase at a pressure equal to the lithostatic pressure:

$$f_{H_2O} < \gamma_{H_2O} P_{Tot}$$

This trend would then be indicative that conditions of water undersaturation are important in the origin and crystallization of granitic melts.

The aplite compositions (Figure 26 b) show less tendency to lie out of the polybaric valley. This would be consistent with their being late state liquids from a crystallizing body since near the end of crystallization the liquid will become more nearly saturated with respect to water. Similarly, the composition of a number of pegmatites (Figure 26 c) plot above the polythermal valley and are consistent with a water rich residue showing the effects of vapor transport (Luth, Jahns, Tuttle, 1964).

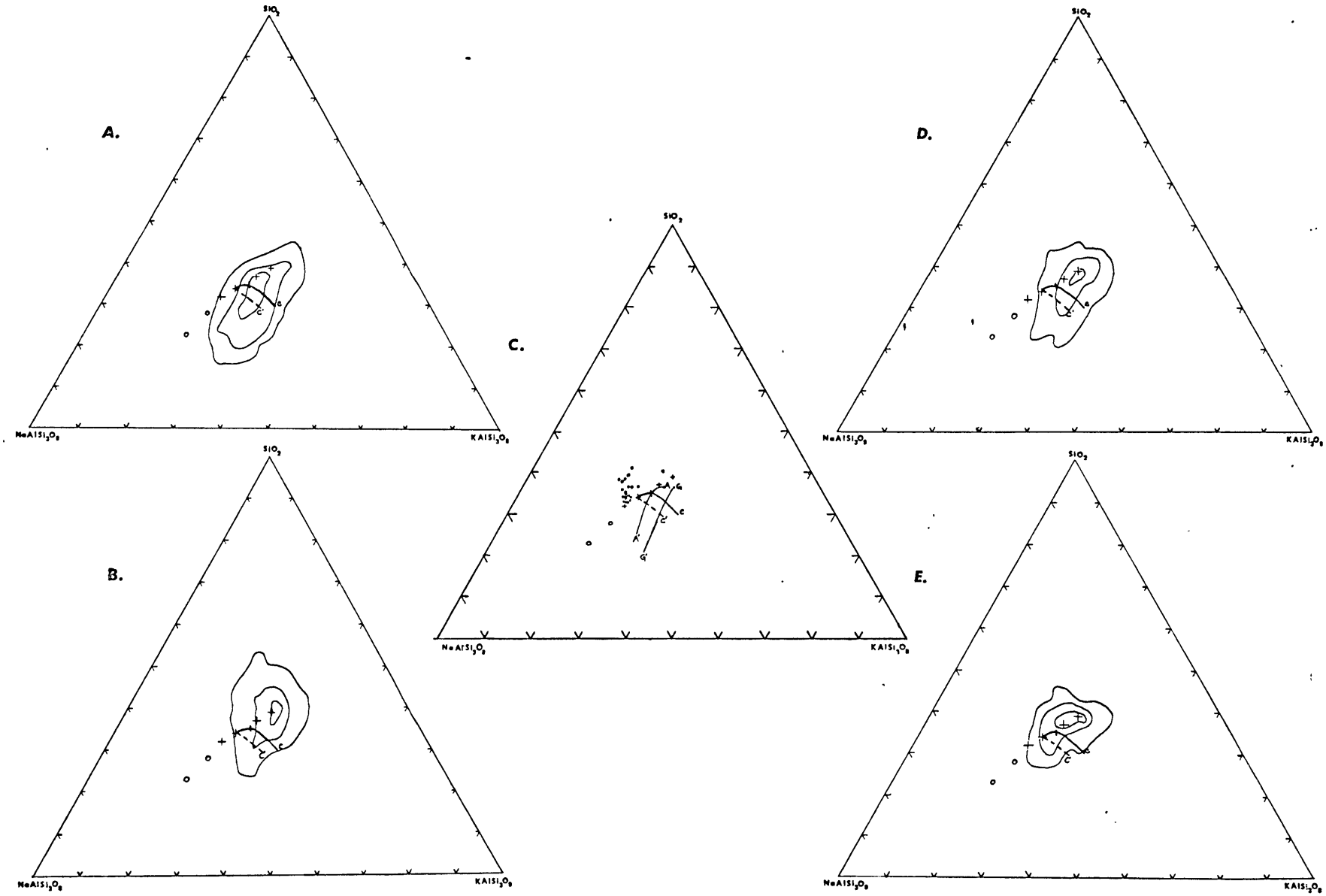
A.
B.
C.
D.
E.
SiO2
NaAlSi3O8
KAlSi3O8

If we further break the granitic compositions down and look at the peralkaline and peraluminous compositions given by Washington we obtain distribution diagrams shown in Figure 26, D-E. As can be seen, the peralkaline compositions have a very strong orientation intersecting the polybaric saturated minimum at low water pressures and extending to the orthoclase rich side of that minimum valley at higher pressures. This is in very good agreement with what would be expected under the effects of undersaturation and suggests that partial differentiation or partial melting under conditions of undersaturation may be typical in the origin of peralkaline granitic melts. The trend in the peraluminous compositions is much less strong. It may be that the excess aluminum may also have some affect on the minimum melt in the granite system. In general peraluminous granitic rocks are more rich in calcium than are peralkaline rocks, and perhaps an increase in calcium may help shift the minimum towards quartz and orthoclase and may also contribute to the final composition. In considering this affect the movement of the eutectic in the system An-Or-Q-H_2O with increasing P_{H_2O} is of importance since if it moved toward quartz the low temperature valley in the system An-Ab-Or-Q would migrate towards quartz on the An-Or-Q end thus rotating the low melting channel and shifting compositions along it toward more quartz rich compositions. A shift toward orthoclase would have the opposite effect on composition along this channel.

APPLICATION TO SPECIFIC GRANITES

WESTERLY GRANITE

The compositions of the Westerly determined from modal analyses by Chayes (1952), as plotted in the system Ab-Or-Q, is what would be expected from a melt last in equilibrium with crystalline material under a total pressure of several kilobars and a water pressure of one to two kilobars. If calcium has had some effect, the water pressure may have been somewhat higher. The Westerly occurs as fairly uniform, fine to medium grained southerly dipping dikes cutting igneous and metamorphic rocks (Feiniger, 1965). Significant amounts of pegmatitic material is commonly associated with these dikes. Further west in Connecticut there are significant migmatite terrains which commonly lie above the second sillimanite isograd (Lundgren, 1966). If the thermal metamorphism increasing to the south east in this area is related to the thermal events that formed the Westerly and related rocks, then there must have been fairly high temperatures developed in the basement rocks to the south and east of Rhode Island and Connecticut. The development of such high temperatures might be accompanied by partial melting of water poor material to form undersaturated magmas. These could then be emplaced and crystallized further up in the crust. Thus, the Westerly dikes may represent a fairly rapid crystallization of a melt separated from a magma chamber

or source at three to four kilobars and water pressure less than total pressure. Upon intrusion into the upper crust it would then have been near saturation depending on original water content and depth of intrusion. These conditions agree well with the estimates of water fugacity obtained from the biotites and the common occurrences of pegmatitic material. The stability of muscovite and quartz under these conditions is questionable.

CAPE ANN AND RELATED ALKALIC ROCKS

The origin of the Cape Ann cannot be considered without considering the relationships with other alkalic granitic and syenitic rocks. A good description of these igneous associations is given by Toulmin (1964). The Cape Ann is closely associated spacially with syenitic rocks, as well as being closely adjacent to other alkalic rocks such as the Peabody Granite and Quincy Granite. These rocks are of such close association and have such related chemistry that a common source is likely. If the composition of the Cape Ann, Peabody, and Beverly Syenite given by Toulmin are plotted on the anhydrous system Ab-Or-Q, it may be seen (Figure 27) that these three fall practically on a straight line. The Cape Ann plots near the saturated polythermal minimum at close to P_{H_2O} = 1 kilobar. The Peabody on the other hand plots far to the right of the polybaric minimum valley, perhaps being formed in processes involving undersaturation

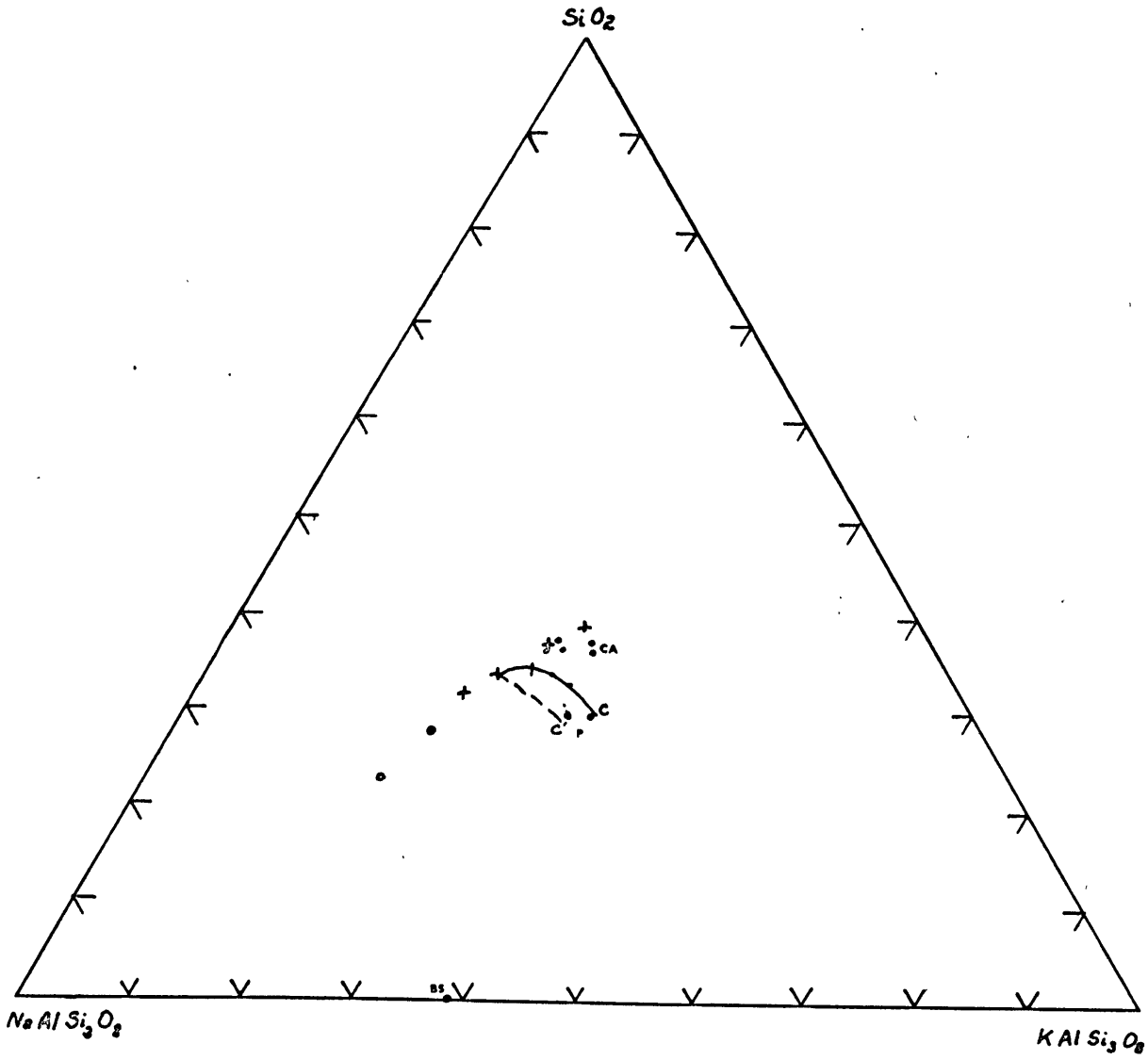
Si O2
CA
C
C'
P
BS
Na Al Si3 O8
K Al Si3 O8

at high load pressures. The line joining these two compositions and passing through the syenite composition is roughly parallel to the shift in the minimum liquid composition caused by an increase in total pressure, holding fugacity of water constant at about that in equilibrium with one kilobar P_{H_2O}.

It may be that if a melt of the bulk composition of the Peabody was emplaced high in the crust, followed by crystallization of feldspathic material to reequilibrate the composition of the melt with its new environment. If sufficient water were present, or if sufficient convection due to volcanism or some other cause were present to cause concentration of crystallizing material then syenitic material might be formed about the main body. If there were sufficient volcanism, excess volatiles, formed when the magma was emplaced at pressures less than that in equilibrium with its water content, would be liberated. Otherwise there might be large amounts of pegmatitic material formed upon late stage crystallization. In this manner, a body similar to the Cape Ann with associated syenitic bodies might be formed from a magma of composition of the Peabody by injection at low pressure and subsequent concentration of crystallized material. A body emplaced at a greater depth, or one which underwent more quiescent crystallization might give a body less rich in quartz and more similar to the Peabody. Upon late stage crystallization, water will be concentrated and during late stage pegmatitic material may be

formed if vesiculation during crystallization is faster than diffusion.

In considering the formation of the Cape Ann Granite and related amphibole bearing rocks, the stability of the amphibole in the presence of feldspars and quartz is of fundamental importance.

Consider the affect of the previously described reactions on the crystallization and subsequent reactions in the Cape Ann granite. During late crystallization a perthite, containing about 50% orthoclase was present along with quartz, pyroxene, some biotite and a finite amount of anorthite in the feldspar. Due to the shape of the solvus and the high insolubility of anorthite in alkali feldspar of this composition the activity of anorthite will be relatively high. Due to the decreased activity of potassium feldspar an amphibole might crystallize even though it was not stable with respect to pure sanidine. Then, after final crystallization at a lower temperature the feldspar began to exsolve to form an orthoclase rich phase. As it did so, the activity of sanidine was increased to the point where the amphibole would be unstable with respect to the last reaction. It would then react to form pyroxene and sheaves of biotite, along with some anorthite that would be absorbed in the plagioclase. If the amphibole contained a finite riebeckite or arfvedsonite component, then the point might come when it could no longer hold all of the sodium amphibole in solid solution and it would exsolve blue stringers of

sodium amphibole. The pyroxene might also go to a sodium rich amphibole with alteration, thus giving the two varieties of blue amphibole, the sheaved amphibole, and the badly reacted texture of the amphibole seen in a number of Cape Ann samples.

MOUNT AIRY LEUCOGRANODIORITE

From the petrology described by Dietrich and the results of these experiments it appears as if biotite and perhaps some magnetite were the dominant early mafic minerals. Some of the muscovite, and perhaps some of the epidote may have been primary in origin as long as the water pressure was high. The plagioclase represented by the cores of An_{24} were probably some of the first crystalline material to form. The crystallization of plagioclase must have been complex from the complex zoning present, but was dominantly a trend toward lower anorthite component down to about An_{12}. Later, crystallization of poikilitic orthoclase along with minor amounts of quartz took place. Much of the coarse aggregates of pure quartz crystals probably represent very late crystallization. The small amounts of perthite and rims of about An_5 about the contact of some microcline crystals probably represents exsolution at subsolidus temperatures.

Although few analyses are available to estimate the bulk composition of the Mount Airy body, the compositions used

here lie close to the minimum in the saturated system at between five and ten kilobars. Thus, it may have been formed under conditions of high pressure and high water fugacity. The structural environment and high internal stress in the Mount Airy (Dietrich, 1961) along with the mineral assemblages may indicate that it was also emplaced under fairly high pressures.

There has been considerable reaction between the granite and included xenoliths. There are also a number of flow features and good foliation in the biotite about xenoliths suggesting a fairly fluid magma. There have been small amounts of aplitic material found in one of the larger quarries, but on the whole there does not appear to be large amounts of late stage water rich crystallization which would be expected if the original magma were nearly saturated. It is therefore not clear what the fugacity of water might have been in this magma except from the questionable stability of epidote and muscovite, and the approximate composition of the analyses on the Ab-Or-Q diagram. If analyses were available on the biotite then some approximation might be made for water fugacity from that calculation.

Two other matters of importance must be considered in the crystallization history of the Mount Airy. First, Dietrich states that the Mount Airy body is outlined by a very strong negative Bougher anomaly. This probably indicates that this granitic body has deep roots and what is now seen on the surface may be only a small part of the total body,

and samples taken from the upper layers may not be characteristic. Secondly, the abundance of aluminum necessitates the consideration of excess aluminum in granitic melts and affects on liquid composition caused by such variations. However, the very low solubility of aluminum in granitic melts at low pressures (Schairer and Bowen, 1955, 1956) suggests that little change would be expected in temperatures around the early melting in the granite system.

Thus, although the Mount Airy appears to be consistant with an origin involving high pressure and high water fugacity, no good restraints can be placed on these conditions at this time.

SUGGESTIONS FOR FUTURE WORK

It appears that the melting relationships of granitic rocks can be modeled in the system $CaAl_2Si_2O_8$-$NaAlSi_3O_8$-$KAlSi_3O_8$-SiO_2-H_2O if the undersaturated region is included. As a result of the necessity of considering the effects of water as a component and water as a pressure medium separately, more synthetic work on the undersaturated region is needed. Recent work by Luth (1967) and Kushiro (1968) represents a significant start.

If good synthetic data were available on the liquid compositions in the undersaturated region, as well as more information on the effect of anorthite, then quantitative determinations of melting conditions might be made from the bulk compositions of granitic rocks. This coupled with evidence from accesory minerals would help to determine pressure, temperature, f_{O_2}, and f_{H_2O} in melting and crystallization.

Meanwhile, qualitative suggestions can be made for specific granites from the trend of the liquid in the undersaturated region seen here.

In future study of granitic suites it might be expected that different fractionation trends might be discerned according to the conditions of pressure and f_{H_2O}. Such trends would help to explain compositional variations seen in rocks of apparent common origin. This might also help correlate distinct methods of formation of different general types of granite rocks.

ACKNOWLEDGEMENTS

The author wishes to express his deep gratitude to Dr. William C. Luth who suggested and directed the original experimental phase of this study. His inspiration and guidance, along with many helpful suggestions were of invaluable assistance in formulating and performing this study.

Many of the observations and the preparations of the study were done under the excellent guidance of Dr. David R. Wones for whose inspiration and very constructive suggestions and criticism the author is deeply indebted.

Thanks are also due to Karen Barker who typed the final copy, and to Alicia Compere for help in preparation of diagrams. Many helpful discussions have also occurred with Phillip Fenn, Joe Chernosky, Yves Pelletier, Razel Wittels, and Betty Recks for which the author is grateful.

Expenses during the early stage of this work were defrayed by NSF Grant Number GP5054 under W. C. Luth, and during the latter stages by NSF Grant Number GA1109 under D. R. Wones. It was completed while the author was under a First Year Fellowship from the National Science Foundation.

BIBLIOGRAPHY

Bachinski, Sharon W., Orville, P. M., 1968, Experimental Determination of the Microcline-Low Albite Solvus and Interpretation of the Crystallization History of Perthites (Abs): Geol. Soc. of Amer., Program with Abstracts, 1968 Annual Meetings, Mexico City, Mexico, p. 15.

Burnham, C. W., Jahns, R. H., 1962, A method for determining the solubility of water in silicate melts: Amer. Jour. Sci., v. 260, p. 721-745.

Chayes, F., 1950, Composition of the Granites of Westerly and Bradford Rhode Island: Amer. Jour. Sci., v. 248, p. 52-66.

Chayes, F., 1952, The finer-grained calcalkaline granites of New England: Jour. Geol., v. 60, p. 207-254.

Clapp, C. H., 1921, Geology of the igneous rocks of Essex County, Massachusetts: U. S. G. S. Bull. 704, 132p.

Clark, S. P. ed., 1966, Handbook of Physical Constants, revised ed., Geol. Soc. Amer. Mem. 97

Cooke, J. P., Jr., 1867, On cryophyllite, a new mineral species of the mica family, with some associated minerals in the granite of Rockport, Mass.: Amer. Jour. Sci., 2nd Ser., v. 43, p. 217-230.

Crowley, M. S., Roy, R., 1964, Crystalline Solubility in the Muscovite and Phlogopite Groups: Amer. Mineral., v. 49, p. 348-362.

Daly, R. A., Manger, C. F., Clark, S. P., Jr., 1966, 'Density of Rocks' contained in Handbook of Physical Constants, Ed. S. P. Clark, Jr., Geol. Soc. Amer. Mem. 97, p. 19-26.

Dana, Edward S., 1898, A Textbook of Mineralogy, 1st Edition, John Wiley and Sons, Inc., New York, New York, 1898.

Deer, W. A., Howie, R. A., Zussman, J., 1963, Rock Forming Minerals., v. 2, Chain Silicates, Longmans Press, London.

Deer, W. A., Howie, R. A., Zussman, J., 1963, Rock Forming Minerals, v. 4, The Network Silicates, Longmans Press, London.

Dietrich, R. V., 1961, Petrology of the Mount Airy "Granite": Bull. of the Virginia Polytechnic Institute Engineering Station Series No. 144, v. 54, no. 6, 63p.

Donnay, J. D. H., Donnay, G., 1952, The Symmetry Change in the High-temperature Alkali Feldspar Series: Amer. Jour. Sci., Bowen Vol., p. 115-132.

Emerson, B. K., 1917, Geology of Massachusetts and Rhode Island, U.S.G.S. Bulletin 597.

Ernst, W. G., 1962, Synthesis, stability realtionships, and occurrence of riebeckite and riebeckite-arfvedsonite solid solutions: Jour. Geol., v. 70, p. 689-736.

Eugster, H. P., Skippen, G. B., 1967, Igneous and Metamorphic Reactions Involving Gas Equilibrium: Researches in Geochemistry, v. 2, P. H. Abelson, Ed., John Wiley and Sons, Inc., New York, New York, p. 492-520.

Eugster, H. P., Wones, D. R., 1962, Stability of the ferruginous biotite annite: Jour. Petrol., v. 3, p. 82-125.

Evans, B. W., 1965, Applications of a reaction-rule method to the breakdown equilibria of muscovite and muscovite plus quartz: Amer. Jour. Sci., v. 263, p. 647-667.

Fairbairn, H. W., and others, 1951, A cooperative investigation of precision and accuracy in chemical, spectrochemical, and modal analysis of silicate rocks: U.S.G.S. Bull. 980, 71p.

Feininger, Tomas (1965), Bedrock geologic map of the Ashaway Quadrangle, Connecticut-Rhode Island: U.S.G.S. Geol. Quad. Map G.Q.-403, Scale 1:24,000.

Ferguson, R. B., 1960, The low-temperature phases of the alkali feldspars and their origin: Canad. Min., v. 6, p. 415-436.

Fleischer, M., 1965, Summary of new data on rock samples G-1 and W-1: Geochim. et Cosmochim. Acta, v. 29, p. 1263-1283.

Fleischer, M., Stevens, R. E., 1962, Summary of new data on rock samples G-1 and W-1: Geochim. et Cosmochim. Acta, v. 26, p. 525-543.

Foster, M. P., 1950, Interpretation of the composition of trioctahedral micas: U.S.G.S. Prof. Paper, 354-B, p. 11-49.

Fyfe, W. S., 1960, Stability of epidote minerals: Nature, v. 187, p. 497.

Goldsmith, J. R., Laves, F., 1954a, The microcline-sanidine stability relations: Geochim. et Cosmochim. Acta, v. 5, p. 1-19.

Goldsmith, J. R., Laves, F., 1954b, Potassium Feldspars Structuarally Intermediate between Microcline and Sanidine: Geochim. et Cosmochim. Acta, v. 6, p. 104-115.

Goranson, R. W., 1936, Silicate-water systems; the stability of water in albite-melt: Am. Geophys. Union Trans., v. 17, p. 257-259.

Goranson, R. W., 1938, Silicate-water systems; phase equilibria in the $NaAlSi_3O_8$-H_2O and $KAlSi_3O_8$-H_2O systems at high temperatures and pressures: Amer. Jour. Sci., v. 35-A, p. 71-91.

Hall, A. J., 1941, The relation between chemical composition and refractive index in biotites: Amer. Mineral., v. 26, p. 34.

Holdaway, M. J., 1966, Hydrothermal stability of clinozoisite plus quartz: Amer. Jour. Sci., v. 264, p. 643-667.

Holm, J. L., Kleppa, O. J., 1968, Thermodynamics of the disordering process in albite: Amer. Mineral., v. 53, p. 123-133.

James, R. S., 1968, Phase equilibrium studies in the system $NaAlSi_3O_8$-$KAlSi_3O_8$-$CaAl_2Si_2O_8$-SiO_2-H_2O at 1000 bars water vapor pressure: Amer. Geophys. Union Trans. (Abs.)

Kennedy, G. C., Wasserburg, G. J., Heard, H. C., Newton, R. C., 1962, The upper three-phase region in the system SiO_2-H_2O: Amer. Jour. Sci., v. 260, p. 501-521.

Kushiro, I., Yoder, H. S., Jr., Nishikawa, M., 1968, Effects of water on the melting of enstatite: Geol. Soc. Amer. Bull., v. 79, p. 1685-1692.

Lundgren, L. W., 1966, Muscovite reactions and partial melting in South Eastern Connecticut: Jour. Petrol. , v.7, p. 421-453.

Luth, W. C., 1967, The influence of pressure on the composition of eutectic liquids in the binary systems sanidine-silica and albite-silica: Carnegie Inst. Wash. Yr. book, 67, p

Luth, W. C., Jahns, R. H., Tuttle, O. F., 1964, The granite system at pressures of 4 to 10 kilobars: Jour. Geophys. Res., v. 67, p. 759-773.

Luth, W. C., Tuttle, O. F., 1966, The alkali feldspar solvus in the system Na_2O-K_2O-Al_2O_3-SiO_2-H_2O: Amer. Mineral., v. 51, p. 1359-1373.

MacKenzie, W. S., 1954, The orthoclase-microcline inversion: Min. Mag., v. 30, p. 343-366.

MacKenzie, W. S., 1957, The crystalline modifications of $NaAlSi_3O_8$: Amer. Jour. Sci., v. 255, p. 481-516.

Merrin, S., 1960, Synthesis of epidote and its apparent P-T stability curve (Abs.): Geol. Soc. Amer. Prog., 1960 Annual Meeting, p. 161.

Newton, R. C., 1966, Some calc-silicate equilibrium relations: Amer. Jour. Sci., v. 264, p. 204.

Orville, P. M., 1963, Alkali ion exchange between vapor and feldspar phases: Amer. Jour. Sci., v. 261, p. 201-232.

Orville, P. M., 1967, Unit-cell parameters of the microcline-low albite and the sanidine-high albite solid solution series: Amer. Mineral., v. 52, p. 55-86.

Platen, H. von, 1965, Kristallisation Granitischer Schmelzen: Beitr. Miner. U. Petrogr., v. 11, p. 334-381.

Schlecht, W. G., Stevens, R. E., 1951, 'Results of chemical analyses of samples of granite and diabase' contained in A Cooperative Investigation of Precision and Accuracy in Chemical, Spectrochemical, and Modal analysis of Silicate Rocks, Ed., H. W. Fairbairn, U. S. G. S.Bull. 780, p. 7-52.

Schrairer, J. F., Bowen, N. L., 1955, The system K_2O-Al_2O_3-SiO_2: Amer. Jour. Sci., v. 253, p. 681-746.

Schairer, J. F., Bowen, N. L., 1956, The system Na_2O-Al_2O_3-SiO_2: Amer. Jour. Sci., v. 254, p. 129-195.

Sharp, W. E., 1962, The thermodynamic functions for water in the range -10 to 1000°C, and 1 to 250,000 bars: California University Lawrence Radiation Laboratory, Publication Number UCRL-7118, 50p.

Shaw, H. R., 1964, Theoretical stability of H_2O in silicate melts: Quasi-crystalline model: Jour. Geol., v. 72, p. 601-617.

Shaw, H.R., 1967, Hydrogen osmosis in hydrothermal experiments: Researches in Geochemistry, v. 2, P. H. Abelson, Ed., John Wiley and Sons, Inc., New York, New York, p. 521-543.

Shaw, H. R., Wones, D. R., 1964, Fugacity coefficients for hydrogen gas between 0° and 1000°C, for pressures to 3000 atm.: Amer. Jour. Sci., v. 262, p. 918-929.

Steiger, R. H., Hart, S. R., 1967, The microcline-orthoclase transition within a contact annite: Amer. Mineral., v. 52, p. 87-116.

Stevens, R. E., Niles, W. W., 1960, Chemical Analysis of the Granite and Diabase, contained in Second Report on a Cooperative Investigation of the Composition of Two Silicate Rocks: U.S.G.S. Bull 1113, p. 3-43.

Stewart, D. B., 1957, The system $CaAl_2Si_2O_8$-SiO_2-H_2O: C.I.W. Yearbook, v. 56, p. 214-216.

Toulmin, P., 1964, Bedrock geology of the Salem Quadrangle and vicinity Massachusetts: U.S.G.S. Bull. 1163-A, 77p.

Tuttle, O. F., 1949, Two pressure vessels for silicate-water studies: Geol. Soc. Amer. Bull., v. 60, p. 1727-1729.

Tuttle, O. F., Bowen, N. L., 1958, Origin of granite in the light of experimental studies in the system $NaAlSi_3O_8$-$KAlSi_3O_8$-SiO_2-H_2O: Geol. Soc. Amer. Mem. 74.

Velde, B., 1966, Upper stability of muscovite: Amer. Mineral., v. 51, p. 924-929.

Warren, C. H., McKinstry, H. E., 1924, The granites and pegmatites of Cape Ann, Massachusetts: Am. Acad. Arts Sci. Proc., v. 59, p. 315-357.

Washington, H. S., 1898, The petrographic province of Essex County, Massachusetts, Part I: Jour. Geol., v. 6, p. 787-808.

Washington, H. S., 1899, The petrographic province of Essex County, Massachusetts, Part II: Jour. Geol., v. 7, p. 53-64, 105-121, 284-294, 463-482.

Washington, H. S. 1917, Chemical Analysis of Igneous Rocks: U.S.G.S. Prof. Paper 99, 1201 p.

Watson, T. L., 1910, Granites of southeastern Atlantic states: U.S.G.S. Prof. Paper 14, 495p.

Winchell, A. N., Winchell, H., 1951, Elements of optical mineralogy, Part II, discription of minerals, Fourth Ed., John Wiley and Sons, New York, New York.

Wones, D. R., 1963, Physical properties of synthetic biotites on the join phlogopite-annite: Amer. Mineral., v. 48, p. 1300-1321.

Wones, D. R., Appleman, D. F., 1963, Properties of synthetic triclinic $KFeSi_3O_8$, iron microcline, with some observations on the iron-microcline iron-sanidine transition: Jour. Petrol., v. 4, p. 131-137.

Wones, D. R., Eugster, H. P., 1965, Stability of biotite: experiment, theory and application: Amer. Mineral., v. 50, p. 1228-1272.

Wones, D. R., Tatlock, D. B., Linback, Dora Von, 1967, Coexisting orthoclase and microcline in altered volcanic rocks, West Humbolt Range, Pershing County, Nevada: Schweiz. Min. Petr. Mitt., v. 471, p. 169-170.

Wright, T. L., 1964, The alkali feldspar of the Tatoosh Pluton in Mount Rainier National Park: Amer. Mineral., v. 49, p. 715-735.

Wright, T. L., 1967, The microcline-orthoclase transformation in the contact aureole of the Eldora Stock, Colorado: Amer. Mineral., v. 52, p. 117-136.

Wright, T. L., 1968, X-ray and optical study of alkali feldspars; II.An x-ray method for determining the composition and structural state from measurement of 2θ values for these reflections: Amer. Mineral., v. 53, p. 88-104.

Wright, T. L., Stewart, D. B., 1968, X-ray and optical study of alkali feldspars: I. Determination of composition and structural state from refined unit-cell parameters and 2V: Amer. Mineral., v. 53, p. 38-87.

Yoder, H. S., 1967, Albite-anorthite-quartz-water at 5kb: C.I.W. Yearbook, v. 66, p. 477-480.

Yoder, H. S., Eugster, H. P., 1955, Synthetic and natural muscovites: Geochim. et Cosmochim. Acta, v. 8, p. 225-280.

Yoder, H. S., Stewart, D. B., Smith J. R., 1956, Ternary feldspars: C.I.W. Yearbook, v. 55, p. 190-194.

Yoder, H. S., Stewart, D. B., Smith, J. R., 1957, Ternary Feldspars: C.I.W. Yearbook, v. 56, p. 206-214.